

**UNIVERSIDADE FEDERAL DO RIO GRANDE DO SUL
INSTITUTO DE GEOCIÊNCIAS
PROGRAMA DE PÓS-GRADUAÇÃO EM GEOCIÊNCIAS**

**NEOTECTÔNICA E CONTROLE DA SEDIMENTAÇÃO
NA PLANÍCIE COSTEIRA DO RS**

BRUNO SILVA DA FONTOURA

ORIENTADOR: Prof. Dr. Iran Carlos Stalliviere Corrêa

CO-ORIENTADOR: Prof. Dr. Adelar José Strieder (UFPel)

Porto Alegre, 2023.

**UNIVERSIDADE FEDERAL DO RIO GRANDE DO SUL
INSTITUTO DE GEOCIÊNCIAS
PROGRAMA DE PÓS-GRADUAÇÃO EM GEOCIÊNCIAS**

**NEOTECTÔNICA E CONTROLE DA SEDIMENTAÇÃO
NA PLANÍCIE COSTEIRA DO RS**

BRUNO SILVA DA FONTOURA

ORIENTADOR: Prof. Dr. Iran Carlos Stalliviere Corrêa

CO-ORIENTADOR: Prof. Dr. Adélir José Strieder (UFPel)

BANCA EXAMINADORA:

Prof. Dr. Nelson Luiz Sambaqui Gruber, Instituto de Geociências, Universidade Federal do Rio Grande do Sul (UFRGS)

Prof. Dr. Venerando Eustáquio Amaro, Departamento de Engenharia Civil e Ambiental (UFRN)

Prof^a. Dr^a. Ana Carolina Oliveira dos Santos, Campus Caçapava do Sul (UNIPAMPA)

Tese de Doutorado apresentada como requisito parcial para a obtenção do Título de Doutor em Ciências.

Porto Alegre, 2023.

UNIVERSIDADE FEDERAL DO RIO GRANDE DO SUL

Reitor: Carlos André Bulhões Mendes
Vice-Reitor: Patricia Helena Lucas Pranke

INSTITUTO DE GEOCIÊNCIAS

Diretor: Nelson Luiz Sambaqui Gruber
Vice-Diretor: Tatiana Silva da Silva

PROGRAMA DE PÓS-GRADUAÇÃO EM GEOCIÊNCIAS

Coordenadora: Maria de Fátima Saraiva Bitencourt
Vice-Coordenador: Juliano Kühle

CIP - Catalogação na Publicação

Silva da Fontoura, Bruno
NEOTECTÔNICA E CONTROLE DA SEDIMENTAÇÃO NA PLANÍCIE
COSTEIRA DO RS / Bruno Silva da Fontoura. -- 2023.
167 f.

Orientador: Iran Carlos Stalliviere Corrêa.

Coorientador: Adelir José Strieder.

Tese (Doutorado) -- Universidade Federal do Rio Grande do Sul, Instituto de Geociências, Programa de Pós-Graduação em Geociências, Porto Alegre, BR-RS, 2023.

1. Ground Penetrating Radar. 2. Depósitos de minerais pesados. 3. Falha de crescimento listrica. 4. Beach ridges. 5. Subsidência mecânica. I. Stalliviere Corrêa, Iran Carlos, orient. II. Strieder, Adelir José, coorient. III. Título.

“We are like a judge confronted by a defendant who declines to answer, and we must determine the truth from the circumstantial evidence”

(Alfred Wegener)

“Deixe o mundo mudar você e você poderá mudar o mundo”

(Che Guevara)

“Seja resoluto, não tenha medo de sacrifícios e derrube todas as dificuldades para a vitória.”

(Mao Tse Tung)

AGRADECIMENTOS

Gostaria de agradecer, primeiramente, ao Conselho Nacional de Desenvolvimento Científico e Tecnológico (CNPq), o qual financiou a realização deste trabalho.

Um agradecimento indispensável à Universidade Federal do Rio Grande do Sul (UFRGS), ao Instituto de Geociências (IGEO), ao Centro de Estudos de Geologia Costeira e Oceânica (CECO) e ao Programa de Pós-Graduação em Geociências (PPGGEO) por fornecer toda a estrutura necessária para o meu pleno desenvolvimento acadêmico. Foi um sonho realizado estudar nessa instituição, na qual carregarei com muito orgulho durante toda a minha vida profissional!

Agradeço a todos os funcionários e técnicos do PPGGEO, especialmente ao Robertinho da secretária que sempre foi muito solícito e prestativo para resolução de todas as questões institucionais.

Ao meu orientador Prof. Dr. Iran Carlos Stalliviere Corrêa que me acolheu de braços abertos e sempre me ajudou quando precisei, desde questões burocráticas da universidade aos ensinamentos que foram de grande valia para a construção desta tese.

Ao meu coorientador Prof. Dr. Adelir José Strieder pela confiança depositada em mim no desenvolvimento de um projeto que começou lá na graduação e culminou neste trabalho. Sua amizade, conversas, conselhos e orientações foram de suma importância neste processo. A maneira de pensar a Geologia como um todo (fora da caixa) com certeza me fizeram um pesquisador melhor. Muito obrigado Adelir!

Agradeço a todos os professores do IGEO e do CECO, pessoas que eu só conhecia de livros, artigos e tive a oportunidade de aprender de perto com todos eles, em especial aos professores: Prof. Dr. Elírio Ernestino Toldo Jr. pelos conselhos, aos Prof. Dr. Sergio Rebello Dillenburg, Prof. Dr. Eduardo Guimarães Barboza, à Prof^a. Dr^a Maria Luiza da Correa da Camara Rosa e Prof. Dr. Felipe Caron pelos ensinamentos sobre a Evolução Costeira, ao Prof. Dr. Léo Afraneo

Hartmann pelo suporte da confecção de artigos, ao Prof. Dr. Jair Weschenfelder, e ao Prof. Dr. Nelson Luiz Sambaqui Gruber pela amizade e apoio para a execução deste trabalho. Aos funcionários e técnicos do IGEO e do CECO, em particular ao José “Zé” Nunes e ao Gilberto “Giba” dos Santos. Aos colegas que fiz no CECO e, que infelizmente o convívio diário foi interrompido pela pandemia, em especial ao Nicolas, Mariah, Volney, Sushi, Carol, Camila e Ana.

Ao Laboratório de Oceanografia Geológica (LOG) da Universidade Federal do Rio Grande (FURG), em especial ao Prof. Dr. Lauro Júlio Calliari (*in memoriam*), pela amizade, carinho e apoio incondicional durante todos esses anos de trabalho e estudo. Serei eternamente grato Lauro! À Prof^a. Dr^a. Salette Figueiredo pela amizade, conselhos e suporte nas tentativas iniciais na saída de campo da sondagem à percussão, além do colega Rodrigo da mesma forma. Aos professores Prof. Dr. Carlos Tagliani, Prof^a. Dr^a Elaine Goulart, Prof. Dr. João Nicolodi e Prof. Dr. Luis Pedro Almeida pelos ensinamentos. Aos amigos do LOG Lelo, Débora, Natan, Ana, Carol, Gabrielle e Matheus.

Ao Laboratório de Engenharia Costeira (LEC) da FURG que ofereceu todo o suporte na realização da saída de campo da sondagem à percussão, principalmente na figura do Prof. Dr. Jose Antonio Scotti Fontoura (meu pai) que sempre se mostrou incansável ajudando na confecção dos equipamentos, na solução dos problemas, foi companheiro de expedições de campo, fez sugestões sobre a execução dos trabalhos e até pitacos na tese, ou seja, conselhos que só um pai pode dar ainda mais com toda sua experiência acadêmica e de vida. Eu posso dizer com propriedade que meu pai é meu herói! Ao técnico do LEC Marcelo pela amizade e ajuda na produção de alguns equipamentos utilizados. Ao Prof. Dr. Christian Serpa pela amizade, pela ajuda na elaboração de mapas e figuras e pela realização do levantamento geodésico. Ao Pablo “Castilhano” e ao seu Antonio – fundamentais no trabalho de campo.

Ao Prof. Dr. Alexandre Bruch e à Prof^a. Dr^a. Angelica Cirolini da Universidade Federal de Pelotas (UFPel) no apoio ao levantamento com o DRONE e, também, ao Geólogo Paulo Mendes (HIDROSERV) que concedeu o georradar para a realização do trabalho.

Agradeço a minha família, em especial ao meu pai Jose Antonio (já mencionado acima) e a minha mãe Rosa Maria pelo amor e apoio incondicional fazendo o possível e o impossível para viabilizar todos os meus desejos e projetos e, a minha irmã Julia e ao Anderson. A minha vó Luisa (*in memoriam*) que sempre foi uma incentivadora e torcedora do meu sucesso. Aos tios, tias, primos e primas que me acompanham e sempre que possível me ajudam nessa jornada de vida. Salientando que sou imensamente grato aos meus tios Flavio e Berenice e ao meu primo Joãozinho que me acolheram na sua casa por dois anos em Porto Alegre para que eu pudesse cursar o doutorado na sua plenitude. Sem eles seria muito mais difícil.

Finalmente, agradeço a minha companheira Aline que mudou o rumo da minha vida e me fez acreditar que tudo é possível. Passou firme comigo o momento mais conturbado da minha vida. E a minha filha Marine que é a razão da minha vida. Sem ela nada faz sentido!

Obrigado a todos que fizeram parte da minha vida durante esse projeto. Todos vocês são muito importantes!

Valeuuuu!!

RESUMO

A Planície Costeira do Rio Grande do Sul (PCRS) é formada por quatro sistemas deposicionais do tipo laguna/barreira e configura a porção mais superficial e proximal da Bacia de Pelotas. Os estudos sobre a PCRS apontam que, em sua gênese, não ocorreram movimentos tectônicos, isso porque não foram identificados indícios de estruturas tectônicas em grande escala na região. Porém, como demonstra a presente pesquisa de tese, existem falhas de crescimento que controlam a sedimentação e a formação do sistema lagunar holocênico da Barreira IV, indicando a ocorrência daqueles movimentos. O estudo está localizado nas regiões de Mostardas, Tavares, São José do Norte e Rio Grande, no estado do Rio Grande do Sul. Primeiramente, foram analisadas imagens de satélite e fotografias aéreas da região, para investigar a geologia e as características sedimentares, além de saídas de campo para observar as estruturas deformacionais gravitacionais. Ainda, foram efetuados levantamentos com GPR de baixa frequência com antena de 50 MHz (RTA), perpendiculares à linha de costa e às estruturas de interesse, furos de sondagem à percussão, executados para identificar a camada de turfa que aflora na praia no distrito de Bujuru (RS), correlacionando-os aos levantamentos de GPR. A tese busca enfatizar o processo de subsidência mecânica presente na Barreira Pleistocênica III, através de uma escarpa linear com mais de 100 km de extensão, constituída por uma falha de crescimento lítrica que controla a margem noroeste da Lagoa do Peixe. Ademais, visa salientar as evidências de estruturas deformacionais, controlando as feições estratigráficas e geomórficas e a sedimentação holocênica dos cordões litorâneos na região da Quinta – Cassino (RS). Ainda, objetiva identificar armadilhas deformacionais que conduziram à ocorrência dos depósitos de minerais pesados em São José do Norte (RS).

Palavras-chave: Ground Penetrating Radar; Depósitos de minerais pesados; Falha de crescimento lítrica; Beach ridges; Subsidência mecânica.

ABSTRACT

The Coastal Plain of the Rio Grande do Sul (PCRS) is formed by four lagoon/barrier depositional systems and it forms the most superficial and proximal portion of the Pelotas Basin. Studies on the PCRS indicate that, in its genesis, there was no tectonic movements. This is because no signs of large-scale tectonic structures were identified in the region. However, as this thesis research demonstrates, there are faults growth that control the sedimentation and formation of the Holocene lagoon system, indicating the occurrence of those movements. The study is located in the regions of Mostardas, Tavares, São José do Norte and Rio Grande, in the state of Rio Grande do Sul. Foremost, satellite images and aerial photographs of the region were analyzed to investigate the geology and sedimentary characteristics, in addition of field trips, to observe gravitational deformational structures. Furthermore, surveys were carried out with low frequency GPR with a 50 MHz antenna (RTA), perpendicular to the coastline and structures of interest, percussion drillholes, carried out to identify the peat layer that outcrops on the beach in the district of Bujuru (RS), correlating them to GPR surveys. The thesis seeks to emphasize the process of mechanical subsidence present in the Pleistocene Barrier III, through a linear scarp more than 100 km long, constituted by a listric growth fault that controls the northwest margin of Lagoa do Peixe. Besides, it aims to highlight the evidence of deformational structures, controlling the stratigraphic and geomorphic features and the Holocene sedimentation of coastal ridges in the Quinta – Cassino (RS) region. It else aims to identify deformational traps that led to the occurrence of heavy mineral deposits in São José do Norte (RS).

Key-words: Ground Penetrating Radar; Heavy minerals deposits; Listric growth fault; Beach ridges; Mechanical subsidence.

LISTA DE FIGURAS

Capítulo 1

Figura 1.1. Mapa da Planície Costeira do Rio Grande do Sul, evidenciando os sistemas laguna-barreira (Modificado de TOMAZELLI & VILLWOCK, 1996)... 27

Figura 1.1.1. Área de estudo deste trabalho (Modificado de *Google Earth*)..... 28

Capítulo 2

Figura 2.1.1. Classificação dos movimentos e processos de transporte de massa subaéreos (Modificado de HIGHLAND & BOBROWSKY, 2008)..... 36

Figura 2.1.2. Diagrama esquemático mostrando os processos de declive por gravidade (Simplificado de SHANMUGAM, 2018). 38

Figura 2.1.3. Tipos de estruturas de movimento de massa em ambiente sub-aquoso. a) Movimentos rasos (SHANMUGAM, 2018) e b) movimentos profundos (p.ex. FERNANDES *et al.*, 2003). 39

Figura 2.1.4. Relações entre as tensões que desencadeiam os movimentos de massa. a) e b) Esforços que influenciam as forças de resistência do maciço terroso/rochoso. c) Discriminação dos parâmetros e forças que atuam nos movimentos de massa. d) Diagrama Mohr-Coloumb mostrando as relações de ruptura (z = profundidade na coluna de sedimentos; h = espessura total da coluna de sedimentos até a superfície de ruptura; α = ângulo de mergulho do declive topográfico; $\tau \cdot \cos(\alpha)$ = resistência ao cisalhamento dos sedimentos; W = componente vertical do esforço atuando sobre os sedimentos; $W \cdot \sin(\alpha)$ = esforço gravitacional atuando na direção do potencial plano de ruptura; c = coesão; A = ruptura dilatacional; B = ruptura contracional; C = ruptura por liquefação; D = carregamento cíclico até a ruptura) (ver HAMPTON *et al.*, 1996). 41

Figura 2.1.5. Diagrama Mohr-Coloumb mostrando os esforços que atuam na ruptura de maciços terrosos/rochosos. A seta azul indica o deslocamento no aumento das tensões iniciais ($\sigma_1, \sigma_2, \sigma_3$) até a ruptura; a seta vermelha indica a consequência do aumento da pressão de fluídos nos poros que resulta na diminuição da tensão efetiva ($\sigma_{ef} = \sigma_i - \sigma_f$). θ = ângulo de atrito interno da ruptura. 42

Figura 2.2.1. Falha de Pelotas (BR-41), descrita por Saadi *et al.* (2002; figura modificada). 45

Figura 2.2.2. Modelo de sombreamento de relevo mostrando elementos morfotectônicos associados à Província Costeira do Rio Grande do Sul e adjacências: Lineamento Jacuí – Porto Alegre (LJP), Sistema de Falhas Coxilha das Lombas (SFCL), Graben Guaíba (GG), Sinclinal de Torres (ST), Arco do Rio Grande (ARG) e o Alto de São Gabriel – Santa Maria (ASGM). Também estão indicados os locais de ocorrência de feições anelares ou hemi-anelares do baixo Taquari (T), do vale dos Sinos (S) e do alto Piratini (P). Mais a leste, estão marcadas as linearidades das margens internas das lagoas do Peixe (LP) e Mangueira (LM). Na área do Escudo, algumas falhas e zonas de cisalhamento se destacam no controle da topografia, sendo que os traços principais denotam paralelismo com linearidades observadas na Província Costeira. Em (B), está ressaltado o “arco do Rio Uruguai” (UY), acrescentando-se outros lineamentos regionais: Florianópolis (LFI) e Chui (LCh) (Modificado de FONSECA, 2006). 48

Figura 2.2.3. a) Mapa de localização do perfil PB-013 (Modificado do *Google Earth*). b) Radargrama mostrando a camada de turfa mergulhando em direção ao continente com uma antena de 50 MHz (FONTOURA, 2015). 49

Figura 2.2.4. Carta Síntese Morfoestrutural da Plataforma Continental do Rio Grande do Sul (Extraído de CORRÊA, 1994). 51

Figura 2.2.5. Modelo estrutural 3D do Cone do Rio Grande, sudeste brasileiro (Extraído de CASTILLO *et al.*, 2009). 52

Figura 2.2.6. Linha sísmica “228_312” no Cone do Rio Grande. As linhas pretas representam as principais falhas na região do Cone do Rio Grande. Notar as

falhas identificadas em direção à zona de praia, a falha principal (*master fault*) no talude, e falhas inversas na base do talude, todas emergindo à superfície do fundo oceânico (Santos, 2020). Observar os perfis em detalhe nas figuras seguintes..... 53

Figura 2.2.7. Flanco norte do Cone do Rio Grande, linha sísmica “277_336”. Ocorrência de falhas sintéticas e antitéticas normais e a formação de *graben* aflorante em fundo oceânico (Santos, 2020)..... 54

Figura 2.2.8. Flanco norte do Cone do Rio Grande, linha sísmica “231_465”. Ocorrência de falhas inversas que correspondem ao domínio compressivo da tectônica gravitacional na região (Santos, 2020)..... 54

Figura 2.2.9. Flanco sul do Cone do Rio Grande, linha sísmica “228_311”. Ocorrência de deslizamento translacional raso (*shallow landslide*), com falhas normais e inversas de duplo cavalgamento que seccionam o fundo oceânico (Santos, 2020)..... 55

Capítulo 3

Figure 1 – Rio Grande do Sul Coastal Plain location (A), its regional geological map (B), and the model for its depositional systems (C). Modified from Tomazelli & Villwock (1996) and Tomazelli *et al.* (2000). 59

Figure 2 – Location of the Lagoa do Peixe Growth Fault and the areas of detailed geological and geophysical surveying. A) Mostardas (northern), B) Tavares (central), C) Lagoa do Cará, and D) Bujuru (Southern) areas. 62

Figure 3 – Geological map of the Mostardas area, with the location of the GPR survey..... 66

Figure 4 – Geological map of the Tavares area, with the location of the GPR survey (A). Pleistocene Barrier III (B) crops out in the intersection of the fault trace and GPR lines (Talhamar Road). 67

- Figure 5 – Geological map of the Lagoa do Cará area, with the location of the GPR survey..... 67
- Figure 6 – Geological map of the Bujuru area (A), with the location of the GPR survey and the drill holes along GPR line 1 (B). 68
- Figure 7 – Radargram for Bujuru Line 01 (A) and boreholes description (B). Legend: 1) Light yellow sand; 2) Light yellow sand with coarse lamination (1-5 mm thick); 3) light yellow sand with gently inclined lamination (1-2 mm thick) and disseminated heavy minerals; 4) light yellow sand with thin horizontal lamination (1 mm) and disseminated heavy minerals; 5) Massive, dark gray sand with high quantity of heavy minerals; 6) Massive light yellow sand and disseminated heavy minerals; 7) Peat; 8) light yellow sand with gently arched lamination (1 mm); 9) isolated thin horizontal laminae of heavy minerals; 10) up to 2 cm recent root fragments; 11) small recent root fragments; 12) small disseminated shell fragments; 13) up to 1 cm shell fragments; 14) oxidized material; 15) oxidized (orange) dark gray sand; 16) heavy minerals concentration; 17) light yellow sand with fragmentary structure; 18) dispersed organic matter; 19) relicts of organic matter; 20) localized breccia structure; 21) dark yellow sand lamination..... 69
- Figure 8 – Fault truncation geometries for radar surface boundaries. A) Normal fault truncation. B) Growth fault truncation. C) reverse fault truncation. D) Thrust fault truncation. These types of truncations can be observed in radargrams of Reiss *et al.* (2003), Christie *et al.* (2009), Nobes *et al.* (2016) e Zhang *et al.* (2016). 71
- Figure 9 – Radargram for Tavares area (Talhamar Road), that cut across fault escarpment in the Lagoa do Peixe National Park. (A) Complete interpreted radargram, and (B) detail radargram showing the triangular and upper lagoonal radarfacies..... 75
- Figure 10 – Radargram for Lagoa do Cará area (A), also cutting the fault escarpment. (B) A detail showing that reflections for lateral facies of the dune (6a) laying on the structural high are interbedded with lagoonal deposits (4). 76
- Figure 11 – Radargram for Mostardas area, also cutting the fault escarpment. 77

Figure 12 – Evolutionary model for Lagoa do Peixe Growth Fault and linked sedimentation. A) Growth fault initiation and propagation. B) Propagation of fault tip zone (northeastward is shown) and deposition of the lower lagoonal radarfacies. C) Additional fault propagation and sedimentation of the triangular wedge lagoonal radarfacies. D) Last stages of fault propagation and sedimentation of the upper lagoonal radarfacies..... 81

Capítulo 4

Figure 1 – Rio Grande do Sul Coastal Plain location (**A**), its regional geological map (**B**), and the model for its depositional systems (**C**). Modified from Tomazelli and Villwock (1996) and Tomazelli *et al.* (2000). The first lagoon/barrier systems: (I): 325 ka; (II) 230 ka; (III) 123-125 ka; and (IV) 5.6 ka MIS. 90

Figure 2 – Geology of the Quinta – Cassino area, located to the south of Rio Grande channel..... 91

Figure 3 – Simplified geologic map of the Quinta area, showing the location of main GPR line surveys. Thick yellow lines separate the beach ridges sets. 98

Figure 4 – Simplified geologic map of the Quitéria area, showing the location of main GPR line surveys. 99

Figure 5 – Simplified geologic map of the Torotama area, showing the location of main GPR line surveys. 100

Figure 6 – Radargrams for GPR survey lines in the Quitéria subarea (Quinta escarpment, Rio Grande Brazil). A) Quitéria 1 GPR line in the north (Line 1). B) Quitéria 2 GPR line in the south (Line 2). Radarfacies ID as in Tabel 2. Green lines: normal listric faults. Thick yellow lines: Pleistocene – Holocene boundary surface. Thin yellow lines: Holocene radarfacies surfaces. 104

Figure 7 – Radargrams for GPR survey lines in the Quinta subarea (Quinta escarpment, Rio Grande Brazil). A) Quinta 40 GPR line in the north. B) Quinta 43 GPR line in the south. Legend as in Figure 6. 105

Figure 8 – Radargrams for GPR survey lines in the Torotama subarea (Quinta escarpment, Rio Grande Brazil). Legend as in Figure 6.....	105
Figure 9 – Radargrams for GPR survey lines in the Quinta subarea (limit between BR1 and BR2, Rio Grande Brazil). A) Quinta 21 GPR line in the north. B) Quinta 26 GPR line in the south. Legend as in Figure 6.	107
Figure 10 – Radargrams for GPR survey lines in the Quinta subarea (limit between BR1, BR2 and BR2, Rio Grande Brazil). A) Quinta 21 GPR line in the north. B) Quinta 26 GPR line in the south. Legend as in Figure 6.....	108
Figure 11 – Radargrams for GPR survey lines in the Quinta subarea (GPR Line 54: limit between BR1 and BR3, Rio Grande Brazil). Legend as in Figure 6..	108

Capítulo 5

Figure 1 – Rio Grande do Sul Coastal Plain location (A), its regional geological map and HM deposits placement (B), and the model for its depositional systems (C). Modified from Tomazelli & Villwock (1996) and Tomazelli <i>et al.</i> (2000). Lagoon/Barrier system ages according to Rosa <i>et al.</i> (2017).....	120
Figure 2 – Radargram in the Talhamar Road (Tavares, Brazil), cutting across Lagoa do Peixe Growth Fault (Tavares GPR line 2). See Table 1 for a description of the geophysical units and surfaces.	122
Figure 3 – Simplified geological map of the Retiro and Bujuru HM deposits area, showing the tip zone of the Lagoa do Peixe (1) and Retiro – Estreito (2) faults.	126
Figure 4 – Simplified geological map for Bujuru (A) and Retiro (B) HM deposits. Lagoa do Peixe (1) and Retiro – Estreito (2) normal fault traces define the Northwest escarpment against Pleistocene sediments. Legend GPR radargrams: a) Figure 9 radargram; b) Figure 10 radargram; c) Figure 11 radargram.....	127

Figure 5 – High resolution satellite images in the Lagoa do Peixe area from north (A) to south (E) showing the interplay of two clogging processes, from aeolian dunes construction (A), to gravity- and hydraulic-driven deposition (B), a combination of both (C), and the final fill of the lagoon by aeolian dunes (D,E).

..... 128

Figure 6 – High resolution satellite images in the Retiro (A) and Estreito (B) showing the predominance of aeolian dunes construction in these areas..... 129

Figure 7 – Stratigraphic relationships between peat layer and TD hosting HM in the structural high at Bujuru District. A) Peat layer cropping out at Bujuru beach under erosional fragmentation. B) Undulated contact between peat and dune sediments. C) Vertical peat fragment identified in an excavated trench. D) Horizontal peat fragment in an excavated trench. E) Natural vertical cut of HM layering close to interdune area. F) Orthogonal trench cut showing HM lamination; note higher HM concentration in the horizontal layering. 130

Figure 8 – Description of the percussion Drillholes Logs in the Bujuru area.
Borehole logs legend: 1) Light yellow sand; 2) Light yellow sand with coarse lamination (1-5 mm thick); 3) light yellow sand with gently inclined lamination (1-2 mm thick) and disseminated heavy minerals; 4) light yellow sand with thin horizontal lamination (1 mm) and disseminated heavy minerals; 5) Massive, dark gray sand with high quantity of heavy minerals; 6) Massive light yellow sand and disseminated heavy minerals; 7) Peat; 8) light yellow sand with gently arched lamination (1 mm); 9) isolated thin horizontal laminas of heavy minerals; 10) up to 2 cm recent root fragments; 11) small recent root fragments; 12) small disseminated shell fragments; 13) up to 1 cm shell fragments; 14) oxidized material; 15) oxidized (orange) dark gray sand; 16) heavy minerals concentration; 17) light yellow sand with fragmentary structure; 18) dispersed organic matter; 19) relicts of organic matter; 20) local breccia structure; 21) dark yellow sand lamination..... 132

Figure 9 – Radargram depicting deep structural relationships in the Bujuru area.
Radargram legend: i) white numbers: radarfacies as presented in Table 1; ii) green lines: normal faults; iii) thick yellow lines: ~1.0 m peat layer cropping out at

Bujuru beach; thin yellow lines: geophysical units/radarfacies; white lines: lateral stratification of dunes (6a in Table 1). Boreholes position is projected into the radargram..... 133

Figure 10 – PB-13 section structural features. **A)** Radargram close to **B)** PB-13 drillhole section. Drillhole section under permission of RGM S.A. Radargram legend as shown in Figure 9..... 133

Figure 11 – PB-13 section structural features. **A)** Radargram close to **B)** PB-01 drillhole section. Drillhole section under permission of RGM S.A. Radargram legend as shown in Figure 9..... 135

Figure 12 – Geologic-structural model for placer Bujuru and Retiro HM deposits (RGSCP, Brazil). A) The development of the structural trap (placer) for first stage of HM concentration. B) The third stage HM concentration and purification on Transgressive Dunes. 146

Figure 13 – Cartoon showing the development stages for structurally controlled lagoons, and the formation of Bujuru and Retiro HM deposits. Rate scale is only for illustration..... 148

LISTA DE TABELAS

Capítulo 3

Table 1 – Summary of the main stratigraphic units cropping out in the selected areas for GPR surveying. 63

Table 2 – Summary of radar surface boundaries (**s**) and radarfacies (**f**) distinguished for GPR survey lines in the Lagoa do Peixe and their interpretation (Mostardas – Tavares – Lagoa do Cará – Bujuru, RS, Brazil)..... 71

Capítulo 4

Table 1 – Summary of the main stratigraphic units cropping out in the selected areas for GPR surveying. 95

Table 2 – Summary of radar surface boundaries (**s**) and radarfacies (**f**) distinguished for GPR survey lines in the Quinta – Cassino area and their interpretation (RS, Brazil). 100

Capítulo 5

Table 1 – Summary of main radar radarfacies and surfaces distinguished for GPR survey lines in the Lagoa do Peixe and Bujuru HM deposit (RGSCP, Brazil). See Fontoura *et al.* (submitted) for a detailed description and analysis..... 122

Table 2 – HMs compositional differentiation and concentration as recorded in some investigations to compare with Bujuru and Retiro HM deposits. SKA = sillimanite+kyanite+andalusite..... 143

SUMÁRIO

AGRADECIMENTOS	v
RESUMO.....	viii
ABSTRACT	ix
LISTA DE TABELAS	xviii
ESTRUTURA DA TESE	23
CAPÍTULO 1	24
1. INTRODUÇÃO	25
1.1. ÁREA DE ESTUDO	28
1.2. OBJETIVOS:.....	29
1.2.1. OBJETIVOS GERAIS.....	29
1.3. OBJETIVOS ESPECÍFICOS:.....	29
1.4. PREMISSAS:.....	30
1.5. HIPÓTESES:	30
1.6. JUSTIFICATIVAS:	31
CAPÍTULO 2	33
2. ESTADO DA ARTE	34
CAPÍTULO 3	56
GRAVITY-DRIVEN LISTRIC GROWTH FAULT AND SEDIMENTATION CONTROL IN THE COASTAL PLAIN OF RIO GRANDE DO SUL, BRAZIL....	58
ABSTRACT	58

INTRODUCTION.....	59
GEOPHYSICAL AND GEOLOGICAL SURVEY METHODS.....	61
GEOLOGY OF THE SURVEYED AREAS.....	63
GEOPHYSICAL SURVEYS: FAULT GEOMETRY AND KINEMATIC.....	70
RADARFACIES AND SURFACES DESCRIPTION.....	71
BOUNDARY SURFACES AND RADARFACIES INTERPRETATION.....	77
EVOLUTION OF LAGOA DO PEIXE GROWTH FAULT AND SEDIMENTATION	79
CONCLUSION.....	82
REFERENCES (CAPÍTULO 3).....	84
CAPÍTULO 4.....	87
4. COMPROVANTE DE SUBMISSÃO DO ARTIGO 2.....	88
FAULT-CONTROLLED SUBSIDENCE AND BEACH RIDGES PROGRADATION IN QUINTA – CASSINO (RS) COASTAL PLAIN, BRAZIL.....	89
ABSTRACT.....	89
INTRODUCTION.....	89
GEOPHYSICAL AND GEOLOGICAL SURVEY METHODS.....	93
GEOLOGY OF THE SURVEYED AREAS.....	94
GEOPHYSICAL SURVEYS: FAULT GEOMETRY AND RADARFACIES.....	100
DISCUSSION ON EVOLUTION OF THE QUINTA – CASSINO STRANDPLAIN	109

CONCLUSION	110
REFERENCES (CAPÍTULO 4).....	112
CAPÍTULO 5	115
5. COMPROVANTE DE SUBMISSÃO DO ARTIGO 3.....	116
STRUCTURAL CONTROLS OF THE COASTAL BUJURU AND RETIRO HEAVY MINERALS DEPOSITS IN SOUTHERN BRAZIL.....	117
ABSTRACT	117
INTRODUCTION.....	118
GEOLOGICAL SETTING	119
GEOLOGICAL AND GEOPHYSICAL SURVEYING METHODS.....	123
STRUCTURAL AND GEOLOGIC CONTROLS OF HM DEPOSITS	124
GEOPHYSICAL STRUCTURES CONTROLLING HM DEPOSITS.....	130
DISCUSSION.....	135
CONCLUSIONS	149
ACKNOWLEDGEMENTS.....	150
REFERENCES (CAPÍTULO 5).....	150
CAPÍTULO 6	158
6. CONSIDERAÇÕES FINAIS	159
REFERÊNCIAS (CAPÍTULOS 1, 2 E 6).....	162

ESTRUTURA DA TESE

Esta tese de Doutorado está estruturada em forma de artigos publicados em periódicos conforme a norma 118 do Programa de Pós-Graduação em Geociências (PPGGEO/IG/UFRGS). Sendo subdividida da seguinte maneira:

Capítulo 1: Contempla a introdução ao tema abordado, a área de estudo, os objetivos do trabalho, a justificativa, as premissas e a hipótese da Tese.

Capítulo 2: Contém o estado da arte sobre o tema da pesquisa.

Capítulo 3: Artigo científico submetido (em avaliação) na Revista GEOPHYSICS: ***Gravity-driven listric growth fault and sedimentation control in the Coastal Plain of Rio Grande do Sul, Brazil.***

Capítulo 4: Artigo científico submetido (em avaliação) na Revista GEOPHYSICS: ***Fault-controlled subsidence and beach ridges progradation in Quinta – Cassino (RS) coastal plain, Brazil.***

Capítulo 5: Artigo científico submetido (em avaliação) na Revista ORE GEOLOGY REVIEW: ***Structural Controls of the Coastal Bujuru and Retiro Heavy Minerals deposits in Southern Brazil.***

Capítulo 6: Apresenta as considerações finais sobre o tema.

CAPÍTULO 1

1. INTRODUÇÃO:

Os ambientes costeiros ao redor do mundo possuem ampla ocupação populacional, devido a fatores climáticos, econômicos e de entretenimento. O controle sobre seus processos de formação e evolução são extremamente importantes para se compreender o ambiente costeiro como um todo. A Planície Costeira do Rio Grande do Sul (PCRS) será descrita, então, com relação a esses aspectos.

A Província Costeira do Rio Grande do Sul é constituída por dois importantes compartimentos geológicos (VILLWOCK & TOMAZELLI, 1995): i) o Embasamento e ii) a Bacia de Pelotas. A Planície Costeira do Rio Grande do Sul constitui a porção emersa (aflorante) da Bacia de Pelotas, que está situada entre o Complexo Cristalino Pré-Cambriano, que constitui o Escudo Sul-rio-grandense, e as sequências sedimentares e vulcânicas paleozoicas e mesozoicas da Bacia do Paraná (a oeste), e o Oceano Atlântico (a leste) (VILLWOCK, 1972).

O pacote sedimentar que se acumulou na Bacia de Pelotas assenta-se sobre rochas antigas que pertencem ao Escudo Sul-rio-grandense, na porção sul do Estado. Ao norte do paralelo que passa pela cidade de Porto Alegre, esse pacote sedimentar da Bacia de Pelotas repousa sobre as sequências sedimentares e vulcânicas, paleozoicas a mesozoicas, que integram a Bacia do Paraná (VILLWOCK & TOMAZELLI, 2007).

Estudos de Fontana (1990, 1996) mostraram que, desde o início de sua formação, a Bacia de Pelotas vêm sendo preenchida por um pacote de sedimentos com mais de 10 000 m de espessura, em que os folhelhos predominam sobre arenitos, calcilutitos e conglomerados. Essas litologias estão assentadas parte sobre a crosta continental, parte sobre rochas vulcânicas extrudidas no início da fase “*rift*” e parte, na zona mais distante da margem, sobre o assoalho oceânico.

Segundo Villwock & Tomazelli (2007), Rosa *et al.* (2011), Dillenburg & Barboza (2014), a origem da Bacia de Pelotas está indiscutivelmente relacionada com os acontecimentos geotectônicos que conduziram à abertura do Oceano

Atlântico Sul. Esse processo iniciou-se a partir do Jurássico, resultando na ruptura do bloco continental gondwânico e a posterior separação dos continentes africano e sul-americano.

Os trabalhos desenvolvidos por Villwock & Tomazelli (1995), Tomazelli & Villwock (2000), Tomazelli & Villwock (2005), Barboza *et al.* (2011), Rosa *et al.* (2011), Lima *et al.* (2013), Dillenburg & Barboza (2014), Dillenburg *et al.* (2017), Rosa *et al.* (2017) e Barboza *et al.* (2018), tem mostrado que os depósitos aflorantes na Planície Costeira do Rio Grande do Sul acumularam-se em sistemas deposicionais específicos desenvolvidos na região durante os períodos Neógeno e, principalmente, Quaternário. Esses depósitos são agrupados em: (1) um sistema de leques aluviais, que ocupa uma faixa contínua ao longo da parte mais interna da Planície Costeira, e (2) quatro distintos sistemas deposicionais transgressivos-regressivos do tipo laguna-barreira (Figura 1.1). Os sedimentos do sistema de leques foram retrabalhados pelos diversos eventos transgressivos-regressivos geradores dos sistemas de barreiras. Cada barreira, provavelmente, originou-se no limite atingido por uma transgressão e foi preservada devido à regressão da linha de costa forçada por uma queda glacio-eustática do nível do mar.

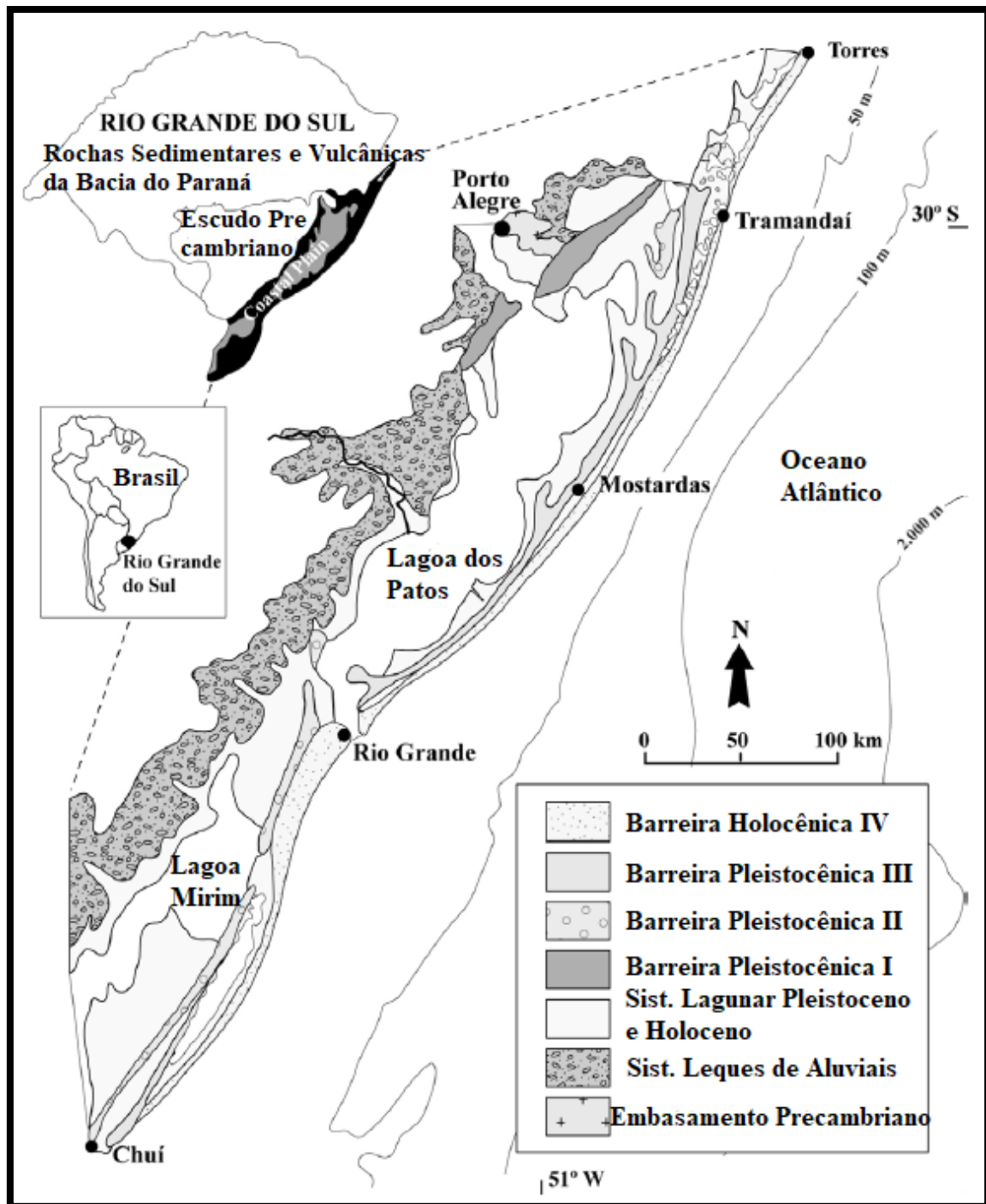


Figura 1.1. Mapa da Planície Costeira do Rio Grande do Sul, evidenciando os sistemas laguna-barreira (Modificado de TOMAZELLI & VILLWOCK, 1996).

1.1. ÁREA DE ESTUDO:

A área de estudo abrange os municípios de Rio Grande, São José do Norte, Tavares e Mostardas, no litoral sul e médio do Estado do Rio Grande do Sul (Figura 1.1.1). Foram divididas três áreas de detalhamento, são elas: área 1, área 2 e área 3 (ver capítulos 3, 4 e 5, respectivamente). A área de estudo tem acesso através da capital Porto Alegre pela BR 101 até Mostardas (cerca de 200 km) e pela BR 116 e, em seguida, pela BR 471 até o município de Rio Grande (cerca de 319 km). É necessário deslocar-se por balsa entre os municípios de Rio Grande e São José do Norte.

As localidades do Retiro e Estreito e, o distrito de Bujuru, situados no município de São José do Norte, apresentam setores com potencial rentável para a extração de minerais pesados. A empresa que possui a área requerida é a Rio Grande Mineração S/A.



Figura 1.1.1. Área de estudo deste trabalho (Modificado de *Google Earth*).

1.2. OBJETIVOS:

1.2.1. Objetivos Gerais:

A Planície Costeira do Rio Grande do Sul formou-se através de sistemas deposicionais específicos causados, entre outros fatores, pela transgressão e regressão do nível do mar nos últimos 325 ka (VILLWOCK & TOMAZELLI, 1995; TOMAZELLI & VILLWOCK, 2000; TOMAZELLI & VILLWOCK, 2005; BARBOZA *et al.*, 2011; ROSA *et al.*, 2011; LIMA *et al.*, 2013; DILLENBURG & BARBOZA, 2014; DILLENBURG *et al.*, 2017; ROSA *et al.*, 2017; BARBOZA *et al.*, 2018). Dentro desta perspectiva, a estabilidade tectônica da Bacia de Pelotas na sua porção emersa é apontada em diversos trabalhos publicados desde Villwock (1972).

O objetivo principal deste trabalho é dar sequência à identificação de estruturas deformacionais relacionadas à tectônica gravitacional atuante na Planície Costeira do Rio Grande do Sul a partir de 8 ka e no Cone do Rio Grande. Desde já, é importante deixar claro que os esforços dedicados ao conhecimento dos processos sedimentares que atuaram e atuam na PCRS, bem como os resultados alcançados, são amplamente reconhecidos.

A continuidade da identificação das estruturas deformacionais já apresentadas pretende avaliar o tipo de interação entre os processos essencialmente sedimentares que vêm sendo descritos e caracterizados pelos diversos pesquisadores nomeados acima e, os processos deformacionais que têm sido identificados.

1.3. Objetivos Específicos:

Os objetivos específicos, dentro destes quesitos, são:

- Identificar estruturas deformacionais neotectônicas de grande escala na PCRS através de levantamentos geofísicos, furos de sondagem, análise de fotografias aéreas, imagens do *Google Earth* e observações de campo .
- determinar os parâmetros e as condições para levantamentos geofísicos por *Ground Penetrating Radar* para elucidar as relações entre deformação e sedimentação;
- definir o controle geológico dos depósitos de minerais pesados (*placers*) na região de Retiro e Estreito (São José do Norte, RS).

1.4. PREMISSAS:

Estudos preliminares a regiões correlatas motivaram o avanço desse tema. Os lineamentos neotectônicos da Lagoa do Peixe e da Lagoa Mangueira encontrados por Fonseca (2006) e da escarpa erosiva da Quinta, segundo Godolphim (1985) são feições extremamente lineares indicativos de falha (Fonseca, 2006). Deste modo, propiciaram o aprofundamento do estudo nessa área.

1.5. HIPÓTESES:

Os trabalhos publicados por FONTOURA (2015), FONTOURA *et al.* (2015) e STRIEDER *et al.* (2015) detectaram a presença de falhas normais sintéticas e antitéticas através de levantamentos geofísicos com Georradar no Distrito de Bujuru (São José do Norte, RS).

A identificação de uma movimentação tectônica por meio de dobras, falhas normais e falhas inversas na região do Cone do Rio Grande (BUENO *et al.*, 2007; LÓPEZ, 2009; ROSA, 2009; CASTILLO *et al.*, 2009; CONTRERAS *et al.*, 2010; CARDOZO, 2011; SANTOS, 2020) indicam um modelo geológico-estrutural análogo ao encontrado na porção emersa da Bacia de Pelotas, pois estas estruturas desenvolvem-se pela ampliação de sua área de abrangência.

O trabalho de Santos (2020) demonstra que o Cone do Rio Grande constitui uma estrutura de deslizamento rotacional (*slump*) do tipo profundo (*deep-seated*), à qual se associam várias estruturas, predominantemente laterais, deslizamento translacional (*slides*) e rotacional (*slump*) raso. As estruturas mostram detalhes de falhas extensionais (normais), compressionais (cavalgamento) e dobras que emergem à superfície do fundo marinho, seccionando os refletores mais superficiais. Isto indica que os sedimentos recentes estão ainda sendo deformados pela tectônica gravitacional que define o Cone do Rio Grande (Santos, 2020).

A hipótese que está sendo proposta nesta tese introduz o componente tectônico-gravitacional nos estudos pré-existentes sobre os depósitos sedimentares aflorantes na Planície Costeira do Rio Grande do Sul.

A hipótese principal é complementada, então, pela hipótese de que deve haver uma relação de interação entre os processos essencialmente sedimentares que vêm sendo descritos e caracterizados pelos diversos pesquisadores e os processos deformacionais que têm sido identificados no Cone do Rio Grande e PCRS.

A aplicação dessas hipóteses está direcionada aos depósitos de minerais pesados (*placers*) na região de Retiro e Estreito (São José do Norte, RS).

1.6. JUSTIFICATIVAS:

A investigação das relações de interação entre os processos essencialmente sedimentares que vêm sendo descritos e caracterizados pelos diversos pesquisadores e os processos deformacionais que têm sido identificados abre novas perspectivas para o desenvolvimento científico e tecnológico regional em diferentes níveis.

O trabalho proposto, embora tenha uma motivação puramente acadêmica, atinge a área de geologia aplicada (prospecção mineral). Na região de estudo, um empreendimento mineiro está em fase de licenciamento (Rio

Grande Mineração S.A.). Conforme informações verbais do Geólogo Aureliano Nóbrega, “*durante o processo de modelagem e cubagem do depósito mineral, a correlação dos dados entre alguns dos furos de sondagem requereu a interpolação dos dados balizados por falhas*”. Com isso, faz-se a necessidade de intensificar os estudos com o objetivo de comprovar esta hipótese.

A confirmação da hipótese de trabalho também abre novas perspectivas de exploração mineral no Cone do Rio Grande. A aplicação desses resultados, em conjunto com os resultados que estão sendo apresentados por Santos (2020), na prospecção de óleo, gás e hidrato de gás na Bacia de Pelotas estão ainda para serem analisados.

CAPÍTULO 2

2. ESTADO DA ARTE:

A morfotectônica investiga as relações entre as formas de relevo e os movimentos neotectônicos. Os processos deformacionais e as estruturas presentes na crosta terrestre, a partir do Plioceno, estão reunidas no denominado Período Neotectônico. O termo Neotectônica é, atualmente, usado em substituição ao termo Diastrofismo, que se refere a qualquer dos movimentos da crosta terrestre produzidos por processos tectônicos, incluindo a formação de bacias oceânicas, continentes, platôs e cadeias de montanhas (NEUENDORF *et al.*, 2011).

Os abalos sísmicos aumentam de magnitude com a proximidade de regiões limítrofes a placas tectônicas. Em países como Japão, por exemplo, que é circundado pelas Placas Eurasiana, das Filipinas e do Pacífico, a ocorrência de eventos tectônicos é frequente, devido a movimentação desses blocos rochosos de dimensões quase continentais. O Brasil, por outro lado, encontra-se na região central da Placa Sul-Americana e, por isso, são raros os terremotos e maremotos de grande intensidade. Entretanto, ocorrem preferencialmente tremores de pequena intensidade registrados ao longo do nosso território (ASSUMPÇÃO *et al.*, 2016). Esses abalos sísmicos são resultados de processos deformacionais que ocorrem em profundidades < 10-15 km, predominantemente relacionados com falhas; daí a sua associação com as fraturas (falhas e juntas) neotectônicas.

O termo Tectônica Gravitacional reúne as estruturas deformacionais geradas por um campo tensional em que a principal componente ativa é vertical e relaciona-se com a força da gravidade (VARNES, 1958; DOTT Jr., 1963; VARNES, 1978). Esses processos estão normalmente posicionados próximo a taludes de média a alta inclinação e podem ocorrer tanto em ambiente aéreo – subaéreo, quanto em ambiente subaquoso (ALVES, 2015; SHANMUGAM, 2018).

O objetivo dessa revisão é focar na discriminação das estruturas e das condições de seu desenvolvimento em ambiente subaquoso. No entanto, dois trabalhos de revisão recentes (ALVES, 2015; SHANMUGAM, 2018) exploram à

exaustão a discriminação de estruturas produzidas pelo rompimento gravitacional de taludes, principalmente aqueles subaquosos, e as condições em que tais movimentos de massa ocorrem e são desencadeados. Shanmugam (2018) apresenta, ainda, uma lista com mais de 50 dos maiores movimentos gravitacionais de massa estudados nos últimos 100 anos, e mais 20 deles estudados em detalhe. Alves (2015), por seu turno, revisa a significância do deslizamento de blocos submarinos e as estruturas deformacionais associadas com sedimentos pouco coesos em bacias de águas profundas, base em dados de sísmica 3D e de afloramento.

Uma revisão dos temas apresentados à exaustão por Shanmugam (2018) e por Alves (2015) para fins deste trabalho parecem, portanto, desnecessária e redundante. Desta forma, optou-se por apresentar o artigo de Shanmugam (2018), de abordagem mais ampla, como anexo (Anexo 1).

O estudo aqui apresentado, abrange alguns conceitos básicos iniciais da mecânica e dos tipos de processos deformacionais desenvolvidos pela Tectônica Gravitacional, e deixa a revisão detalhada no formato publicado pelos recentes e originais artigos de Shanmugam (2018) e Alves (2015). Isso permite que esta tese se concentre na apresentação das evidências e das estruturas deformacionais documentadas para a Bacia de Pelotas e sua porção emersa (a PCRS).

2.1. CONCEITOS

Os conceitos apresentados neste subitem estão relacionados aos princípios básicos de movimentos de massa, que são fundamentais para a plena compreensão da Tese em andamento. As classificações para estes tipos de processos são variadas, tendo início com Varnes (1958) em seu artigo intitulado “*Landslide, types and processes*”, que agrupa todos os movimentos causadores de depósitos de transporte de massa (MTDs – *mass-transport deposits*), tanto em ambiente aéreo e subaéreo, quanto no ambiente submarino. Esses conceitos

foram atualizados por outros autores ao longo dos anos (DOTT, Jr, 1963, VARNES, 1978; LOCAT & LEE, 2002; SHANMUGAM, 2018).

Highland & Bobrowsky (2008) apresentaram uma atualização da classificação dos movimentos de transporte de massa subaéreos em (Figura 2.1.1):

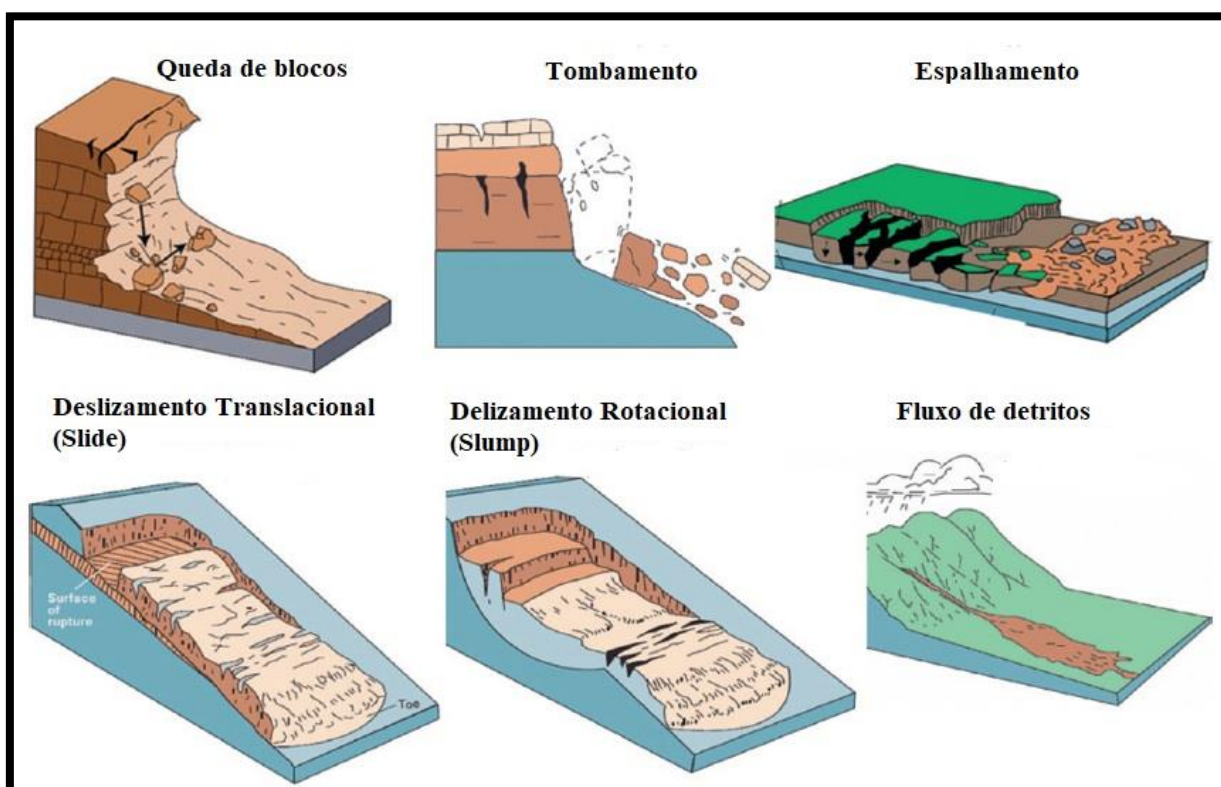


Figura 2.1.1. Classificação dos movimentos e processos de transporte de massa subaéreos (Modificado de HIGHLAND & BOBROWSKY, 2008).

- Queda: movimentos abruptos, descendentes, de rocha ou terra, ou ambos, que se desprendem de encostas íngremes ou falésias. A massa em queda pode quebrar com o impacto, começar a rolar em encostas mais íngremes e continuar até o terreno se aplainar;

- Tombamento: é reconhecido como a rotação para frente, em uma área muito inclinada, de uma massa de solo ou rocha em torno de um ponto ou eixo abaixo do centro de gravidade da massa deslocada. A queda é, às vezes, impulsionada pela gravidade exercida pelo peso do material em declive a partir da massa deslocada; outras vezes, a queda é causada por água ou gelo em rachaduras na massa;

- Espalhamento: extensão de um solo coeso ou massa rochosa combinada com a subsidência da massa fraturada do material coesivo em material subjacente mais macio. As propagações podem resultar da liquefação ou fluxo (e extrusão) do material subjacente mais macio. Os tipos de espalhamento incluem: de bloco, de liquefação e laterais;

- Deslizamento translacional (*Slide*): a massa em um deslizamento de terra translacional se move para fora, ou para baixo e para fora, ao longo de uma superfície relativamente plana com pouco movimento de rotação ou inclinação para trás. Os *slides* geralmente provocam estruturas deformacionais ao longo das discontinuidades geológicas, como falhas, juntas, superfícies de acamadamento ou, no contato entre rochas e solo;

- Deslizamento rotacional (*Slump*): deslizamento de terra no qual a superfície da ruptura possui concavidade voltada para cima e o movimento do deslizamento é mais ou menos rotacional em torno de um eixo paralelo ao contorno da inclinação. A massa deslocada pode, sob certas circunstâncias, mover-se como uma massa relativamente coerente ao longo da superfície de ruptura com pouca deformação interna;

- Fluxo de detritos: forma de rápido movimento de massa, no qual solo, rocha e/ou matéria orgânica soltos se combinam com a água para formar uma lama que flui encosta abaixo. Os fluxos de detritos podem ser mortais, pois se originam rapidamente e podem ocorrer sem qualquer aviso.

O comportamento mecânico baseado em processos subaquosos, nas regiões com instabilidade, extrema importância para a compreensão das deformações nesses ambientes. A figura 2.1.2 mostra, de modo simplificado, o

movimento e transporte de massa influenciado por gravidade para águas profundas. É possível notar que, a partir do aumento da profundidade/inclinação, a deformação altera-se de rúptil para dúctil; ou seja, a componente da gravidade é um agente modificador das estruturas deformacionais presente nos processos subaquosos.

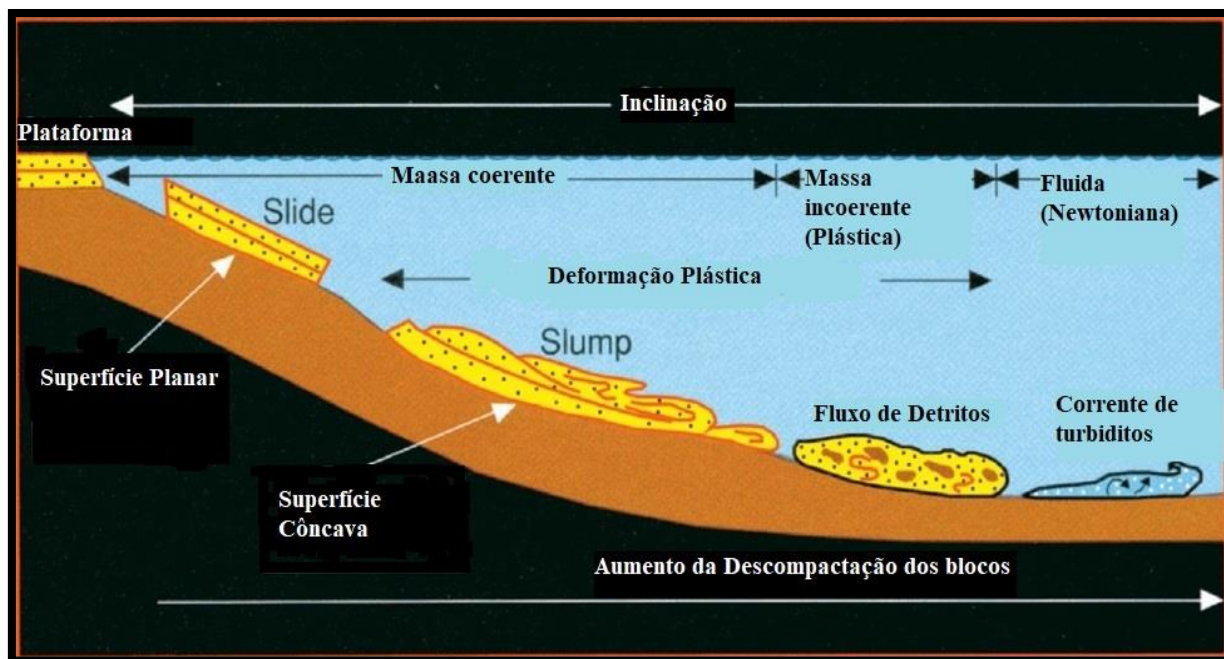


Figura 2.1.2. Diagrama esquemático mostrando os processos de declive por gravidade (Simplificado de SHANMUGAM, 2018).

Os tipos de movimentos discriminados acima são, ainda, classificados quanto a profundidade da superfície de ruptura (ver HAMPTON *et al.*, 1996). Nesse sentido, pode-se distinguir i) os movimentos rasos (*shallow slides/slumps*, Figura 2.1.3a) e ii) os movimentos profundos (*deep-seated slides/slumps*, Figura 2.1.3b).

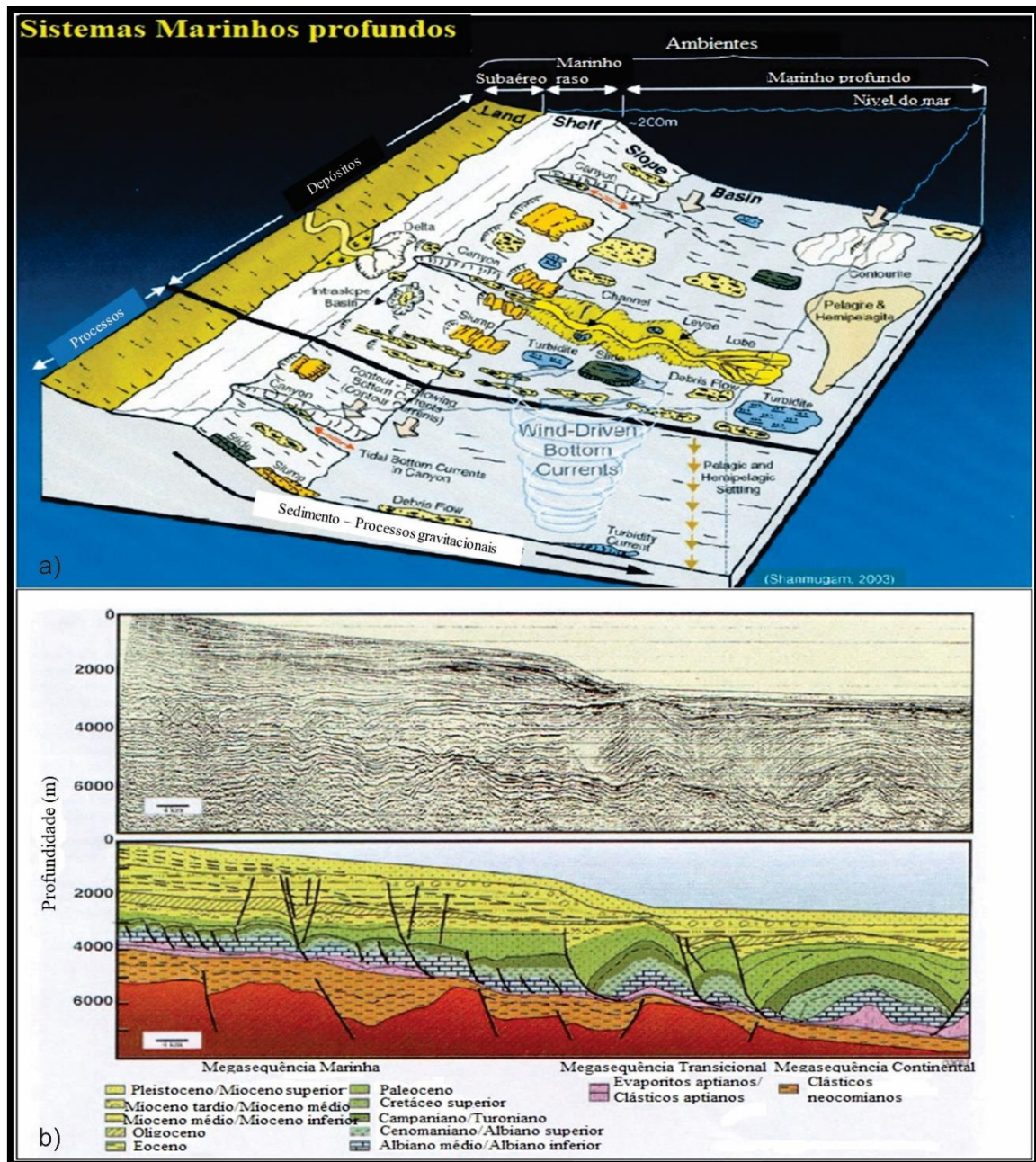
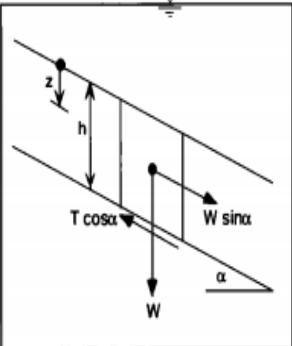
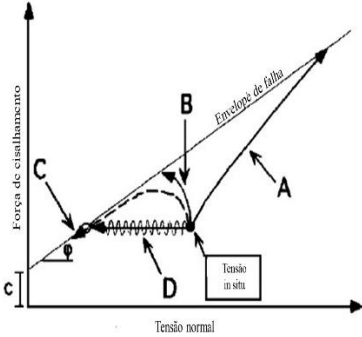


Figura 2.1.3. Tipos de estruturas de movimento de massa em ambiente sub-aquoso. a) Movimentos rasos (SHANMUGAM, 2018) e b) movimentos profundos (p.ex. FERNANDES *et al.*, 2003).

Os movimentos rasos de massa são normalmente investigados a partir de análises geomorfológicas e morfométricas (p. ex. CORRÊA, 1990), e, recentemente, por levantamentos sísmicos rasos. Os movimentos profundos,

por outro lado, desenvolvem feições geomorfológicas com escala mais semi-regional a regional, e são completamente descritos e quantificados a partir de levantamentos sísmicos profundos.

A causa dos movimentos submarinos de massa está ligada com a relação entre as tensões de resistência do maciço terroso/rochoso e as forças gravitacionais; o processo é iniciado quando a tensão de cisalhamento direcionada na declividade da superfície de ruptura (mecanismo desencadeador) excede a resistência do material (forças de resistência). O principal mecanismo desencadeador é a força gravitacional, mas estes esforços podem ser incrementados ou diminuídos por outros esforços (ver Figura 2.1.4).

a) Esforços que reduzem a resistência	b) Esforços que aumentam a resistência	c) Geometria do problema de escorregamento/deslizamento	d) Diagrama Mohr-Colomb para as relações de tensões
<ul style="list-style-type: none"> - Tremores de terra - Carga de ondas - Mudanças de n.m (maré) - Intemperismo 	<ul style="list-style-type: none"> - Tremores de terra - Carga de ondas - Mudanças de n.m (maré) - Diapirismo 		

- Sedimentação	- Sedimentação		
- Expulsão de gás	- Erosão		

Figura 2.1.4. Relações entre as tensões que desencadeiam os movimentos de massa. a) e b) Esforços que influenciam as forças de resistência do maciço terroso/rochoso. c) Discriminação dos parâmetros e forças que atuam nos movimentos de massa. d) Diagrama Mohr-Coloumb mostrando as relações de ruptura (z = profundidade na coluna de sedimentos; h = espessura total da coluna de sedimentos até a superfície de ruptura; α = ângulo de mergulho do declive topográfico; $\tau \cdot \cos(\alpha)$ = resistência ao cisalhamento dos sedimentos; W = componente vertical do esforço atuando sobre os sedimentos; $W \cdot \sin(\alpha)$ = esforço gravitacional atuando na direção do potencial plano de ruptura; c = coesão; A = ruptura dilatacional; B = ruptura contracional; C = ruptura por liquefação; D = carregamento cíclico até a ruptura) (ver HAMPTON *et al.*, 1996).

As rupturas também são influenciadas pela pressão de fluidos nos poros dos sedimentos. Nestas condições, o aumento da sobrecarga de sedimentos causa a sua compactação e o aumento da pressão nos poros. Este processo determina uma diminuição na pressão efetiva, o deslocamento das tensões para a esquerda do diagrama de Mohr-Coloumb (Figura 2.1.5), e a ruptura sob condições de baixa tensão de carregamento.

A condição de equilíbrio é controlada por (ver HAMPTON *et al.*, 1996):

$$F = \frac{\text{Esforço de cisalhamento } (W \cdot \sin \alpha)}{\text{Força de resistência gravitacional } (\tau \cdot \cos \alpha)} \quad F = \frac{\gamma' \cdot z \cdot \sin \alpha}{\sigma'_{\nu} \cdot \tan \theta'}$$

onde:

θ = ângulo de atrito interno ($^{\circ}$)

γ' = densidade dos sedimentos submersos (densidade dos sedimentos – densidade da água)

σ'_v = tensão vertical (gravidade) efetiva (kPa)

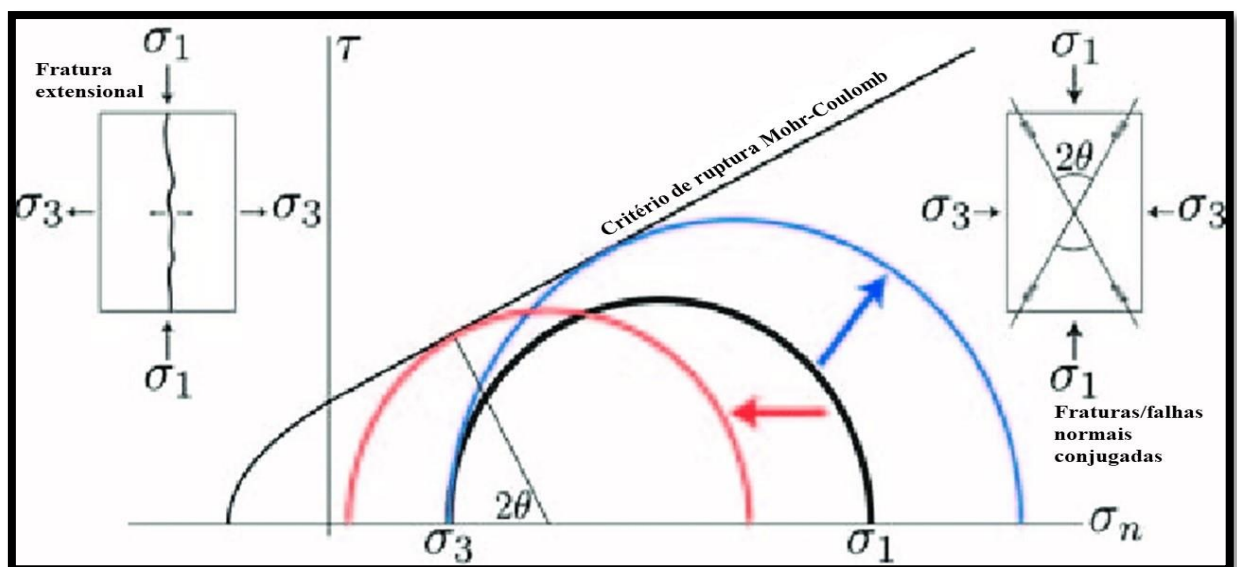


Figura 2.1.5. Diagrama Mohr-Coloumb mostrando os esforços que atuam na ruptura de maciços terrosos/rochosos. A seta azul indica o deslocamento no aumento das tensões iniciais ($\sigma_1, \sigma_2, \sigma_3$) até a ruptura; a seta vermelha indica a consequência do aumento da pressão de fluídos nos poros que resulta na diminuição da tensão efetiva ($\sigma_{ef} = \sigma_i - \sigma_f$). θ = ângulo de atrito interno da ruptura.

Quando $F = 1$, as tensões máximas de cisalhamento em planos adequadamente orientados são iguais à tensão de cisalhamento de resistência e, assim, o falhamento é iminente. Quando $F > 1$, a tensão de cisalhamento de resistência excede a tensão máxima de cisalhamento e o material no ponto considerado é estável.

2.2 EVIDÊNCIAS DE ATUAÇÃO NEOTECTÔNICA NA BACIA DE PELOTAS

Este subitem se propõe a apresentar a bibliografia disponível sobre as evidências da Neotectônica na Bacia de Pelotas. Com base no uso de metodologias como sensoriamento remoto, cartografia geológica e geofísica, os autores citados apresentam um padrão para as falhas presentes na região.

A PCRS é formada essencialmente por sistemas deposicionais do tipo laguna-barreira, conforme apresentado no item anterior desta monografia. Porém, indícios da presença de eventos neotectônicos nesta região têm sido publicados por alguns pesquisadores. O método básico para o reconhecimento destas estruturas deformacionais tem sido a Geomorfologia.

A Geomorfologia (ramo da geologia/geografia que se dedica a estudar as formas de relevo da superfície terrestre) é uma importante ferramenta de identificação de deformações neotectônicas. Estruturas como escarpas de falhas, represamento natural de drenagens e diferenças súbitas de altitudes de corpos geológicos idênticos são detectadas através do uso de levantamentos aerofotogramétricos, sensoriamento remoto e até mesmo em observações de campo.

O sensoriamento remoto é uma ferramenta que permite visualizar o arranjo espacial das estruturas e formas de relevo em superfície de maneira mais regionalizadas. O trabalho publicado por Cecarelli (1996) identifica e analisa feições causadas por processos neotectônicos por meio de técnicas de sensoriamento remoto aplicadas em imagens do sensor TM do satélite Landsat-5, em escala 1:100.000, no litoral médio da PCRS, lado oeste da Lagoa dos Patos, entre os municípios de Pelotas e Camaquã. O sensoriamento remoto é uma ferramenta que permite visualizar o arranjo espacial das estruturas e formas de relevo em superfície de maneira mais regionalizadas. Os resultados mostraram que estruturas tectônicas condicionam a instalação da drenagem e a orientação de formas de relevo nos depósitos de sedimentos aflorantes naquele segmento da Bacia de Pelotas. O estudo evidencia que as diversas feições

morfológicas e estruturais presentes na PCRS são indicadores de que existe, na região, uma tectônica atual com influência direta sobre a morfologia.

A Falha de Pelotas foi descrita por Saadi *et al.* (2002) próxima à costa do Estado do Rio Grande do Sul e indicada como o limite entre as rochas do embasamento Pré-cambriano (Cinturão Ribeira a oeste) e os sedimentos cenozoicos da Bacia de Pelotas (a leste). Conforme Saadi *et al.* (2002), existem zonas deprimidas ao longo da falha na Bacia de Pelotas, que são ocupadas por um sistema de lagos – principalmente “Lagoa dos Patos” e “Lagoa Mirim” (Figura 2.2.1).

Foi apresentado, ainda, por Fonseca (2006) uma revisão bibliográfica exaustiva das evidências de Neotectonismo na PCRS por diversos pesquisadores. Entre eles, Delaney (1965) reconhece feições estruturais condicionando parte da formação da PCRS (Sistema de Falhas Coxilha das Lombas). Delaney (1965) mostrou que, logo após a deposição da Formação Itapuã, ocorreu o Sistema de Falhas Coxilha das Lombas durante um período de mar mais alto que o atual. Müller Fo. (1970) identificou falhas de pequena amplitude, que resultaram na individualização da Lagoa dos Patos; elas formariam o alinhamento de falhas Mostardas – Itapuã – Coxilha das Lombas – Itapeva.

Por outro lado, Villwock (1972) desconsidera a intervenção da neotectônica no modelado da retilinidade da Coxilha das Lombas, embora não discuta a existência do falhamento. O estudo interpretou a Coxilha das Lombas como uma falésia na época da deposição da Formação Chuí. Esta feição foi marcada como a mais jovem do Pleistoceno da PCRS (DELANEY, 1965).

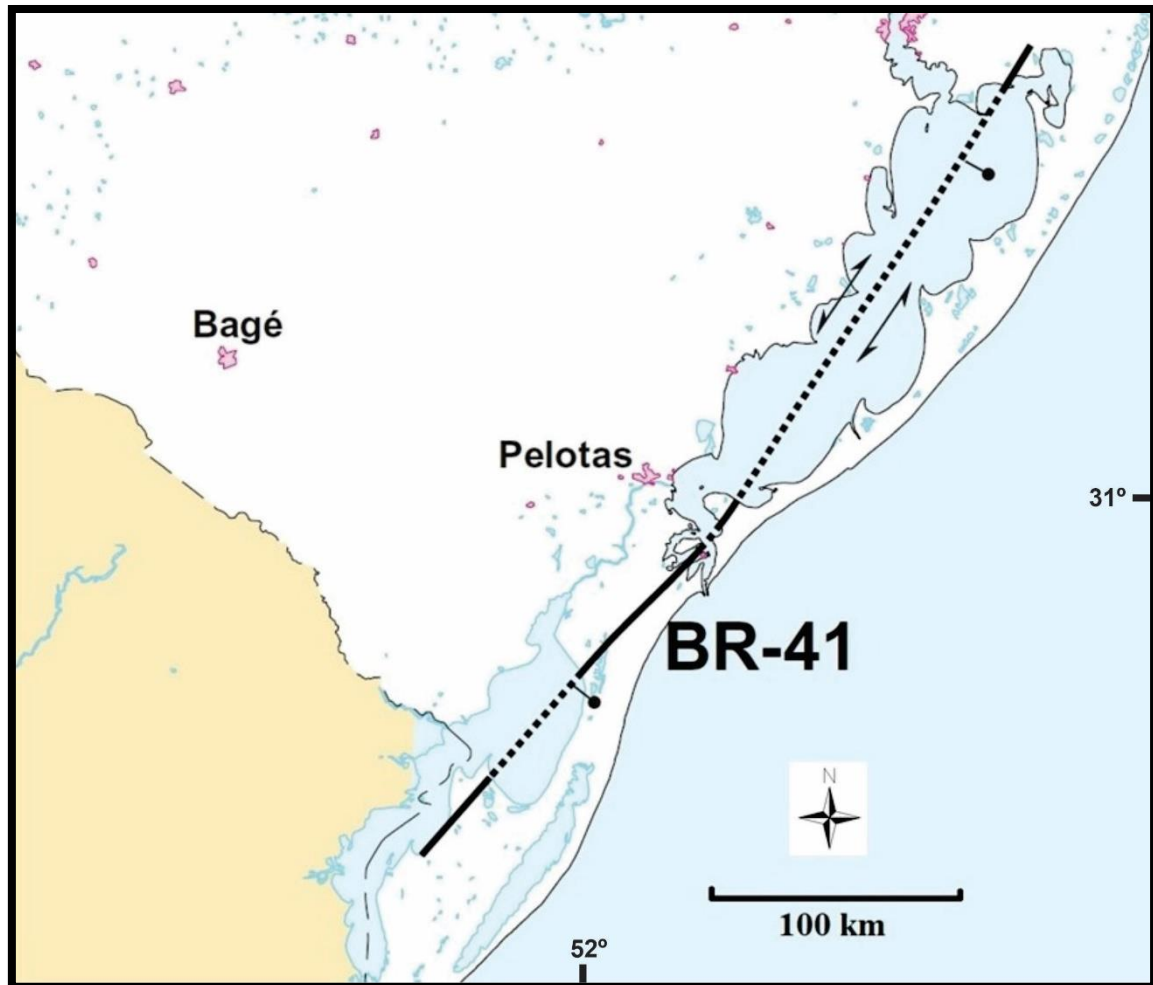


Figura 2.2.1. Falha de Pelotas (BR-41), descrita por Saadi *et al.* (2002; figura modificada).

Com base nesta revisão, Fonseca (2006) relata a necessidade de uma análise morfotectônica da Planície Costeira do Rio Grande do Sul para a detecção de atividades neotectônicas. O autor utilizou os elementos clássicos da geomorfologia para a identificação das feições morfotectônicas: escarpas de falhas, represamento natural de drenagens e gradientes de vales e encostas, dentre outros. Assim, Fonseca (2006) estudou a morfotectônica (relação entre drenagem e topografia) a partir da análise de bases cartográficas disponíveis, de imagens de sensores remotos e da bibliografia existente.

Este mesmo autor, Fonseca (2006) delimitou três macro-elementos morfotectônicos (Sistema de Falhas Coxilha das Lombas, Bacia de Porto Alegre, Lineamento Jacuí – Porto Alegre) no contexto da Planície Costeira do Rio Grande do Sul. O Lineamento Jacuí – Porto Alegre, por exemplo, é uma importante estrutura mostrada pelo autor, pois este lineamento secciona a Planície Costeira em duas partes. A primeira até Tramandaí (norte) apresenta lagoas/lagunas costeiras menores e/ou mais estreitas abrangendo somente as Barreiras III e IV e, a segunda, ao sul caracteriza-se por grandes lagunas (Patos e Mirim, Mangueira) que englobam os quatro sistemas deposicionais transgressivos-regressivos.

A análise e a compilação da bibliografia existente, o estudo topográfico e cartográfico preliminar (rede de drenagens), o sensoriamento remoto (LANDSAT e RADAR) e a investigação de campo com enfoque geomorfológico permitiram que Fonseca (2006) traçasse alguns lineamentos morfo-estruturais na PCRS e adjacências. Dentre os quais, os lineamentos da Lagoa do Peixe (LP) e Lagoa Mangueira (LM) cortam a área de estudo desta Tese (Figura 2.2.2 e suas explicações).

A influência das alterações altimétricas no relevo para a composição do terreno e o papel da drenagem dos rios na moldura desses depósitos sedimentares são relatadas por Fonseca (2006), com estruturas como: i) o Graben Guaíba, que corresponde a uma área rebaixada de 800 km² que influenciou a rede de drenagens regional e a sedimentação de depósitos quaternários; ii) a Sinclinal de Torres, que representa a maior projeção das unidades da Bacia do Paraná na direção do litoral; e iii) o Arco de São Gabriel, que proporcionou, por meio de sua denudação e da dinâmica tectono-isostática, as sequências sedimentares da Bacia de Pelotas.

No distrito de Bujuru, em São José do Norte (RS), foram realizados levantamentos geofísicos com georradar (GPR) por Fontoura (2015). A camada de turfa, que aflora no pós-praia e mergulha em direção ao continente, constitui um material geológico de condutividade mais alta do que sedimentos arenosos sobrepostos, ou mesmo do que os sedimentos silte-argilosos. Nesse sentido, os contatos da turfa com os sedimentos lagunares holocênicos (subjacentes) e

arenosos de natureza eólica (sobrejacentes) constituem refletores marcantes, pois apresentam alto contraste de impedância elétrica, que podem ser utilizados como camada guia no levantamento com georradar.

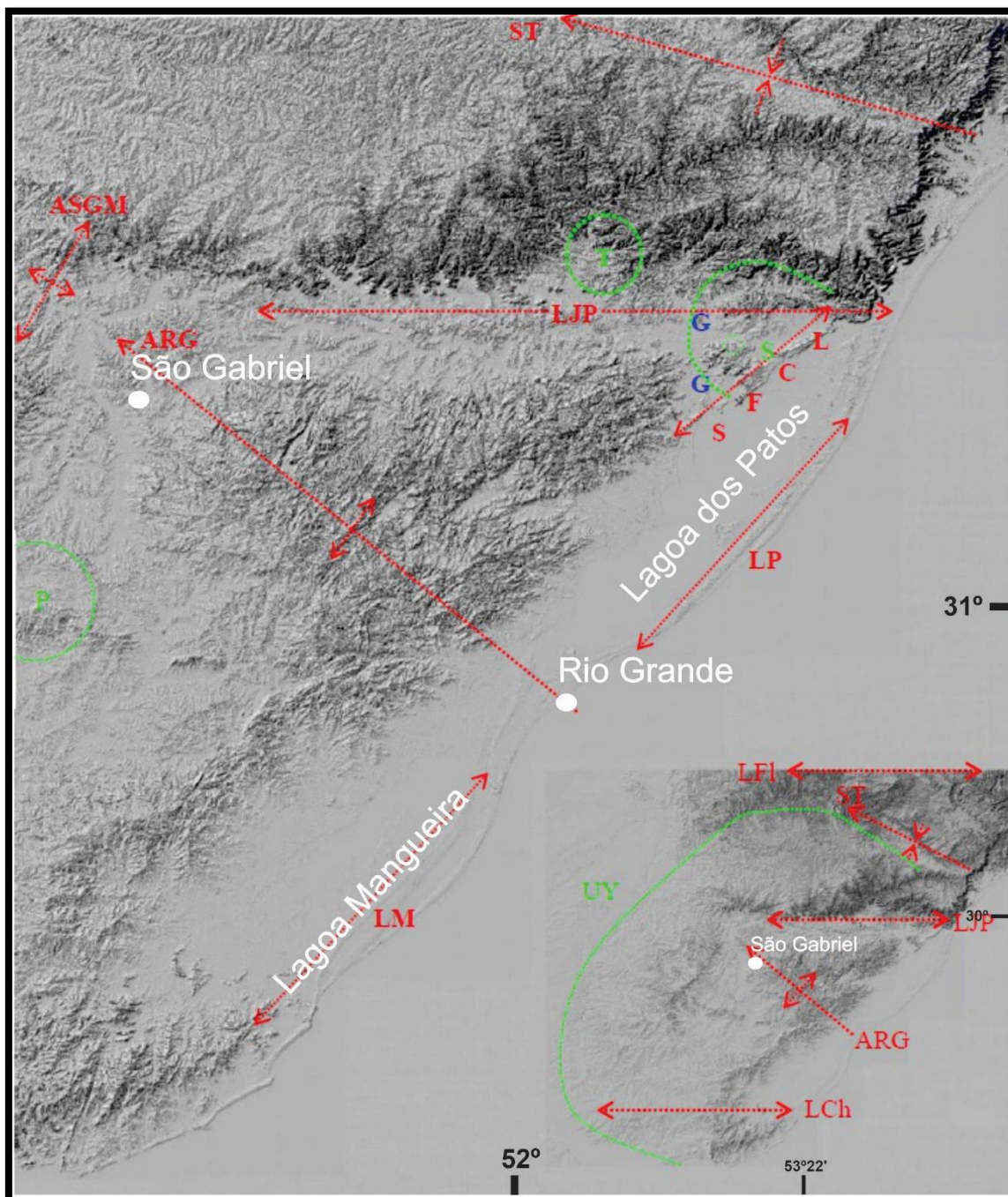


Figura 2.2.2. Modelo de sombreamento de relevo mostrando elementos morfotectônicos associados à Província Costeira do Rio Grande do Sul e adjacências: Lineamento Jacuí – Porto Alegre (LJP), Sistema de Falhas Coxilha das Lombas (SFCL), Graben Guaíba (GG), Sinclinal de Torres (ST), Arco do Rio Grande (ARG) e o Alto de São Gabriel – Santa Maria (ASGM). Também estão indicados os locais de ocorrência de feições anelares ou hemi-anelares do baixo Taquari (T), do vale dos Sinos (S) e do alto Piratini (P). Mais a leste, estão marcadas as linearidades das margens internas das lagoas do Peixe (LP) e Mangueira (LM). Na área do Escudo, algumas falhas e zonas de cisalhamento se destacam no controle da topografia, sendo que os traços principais denotam paralelismo com linearidades observadas na Província Costeira. Em (B), está ressaltado o “arco do Rio Uruguai” (UY), acrescentando-se outros lineamentos regionais: Florianópolis (LFI) e Chui (LCh) (Modificado de FONSECA, 2006).

A aquisição dos dados de GPR (Fontoura, 2015) no Distrito de Bujuru (São José do Norte, RS) foi produzida perpendicularmente à linha de costa, em direção ao interior do continente. A figura 2.2.3 mostra a camada guia de turfa sendo abruptamente interrompida por falha normal mergulhante em direção à praia. Além disso, é importante notar a presença de *drag-folds* associadas às falhas normais. As *drag-folds* são marcadas pela formação de antiforme no bloco superior (*capa*, *muro*, *footwall*) e sinforme no bloco abatido (*lapa*, *teto*, *hangingwall*), pois foram formadas pelo deslocamento numa superfície cisalhante que trunca sedimentos plásticos (camada de turfa) e sedimentos pouco coesos, genericamente designados *soft sediments*.

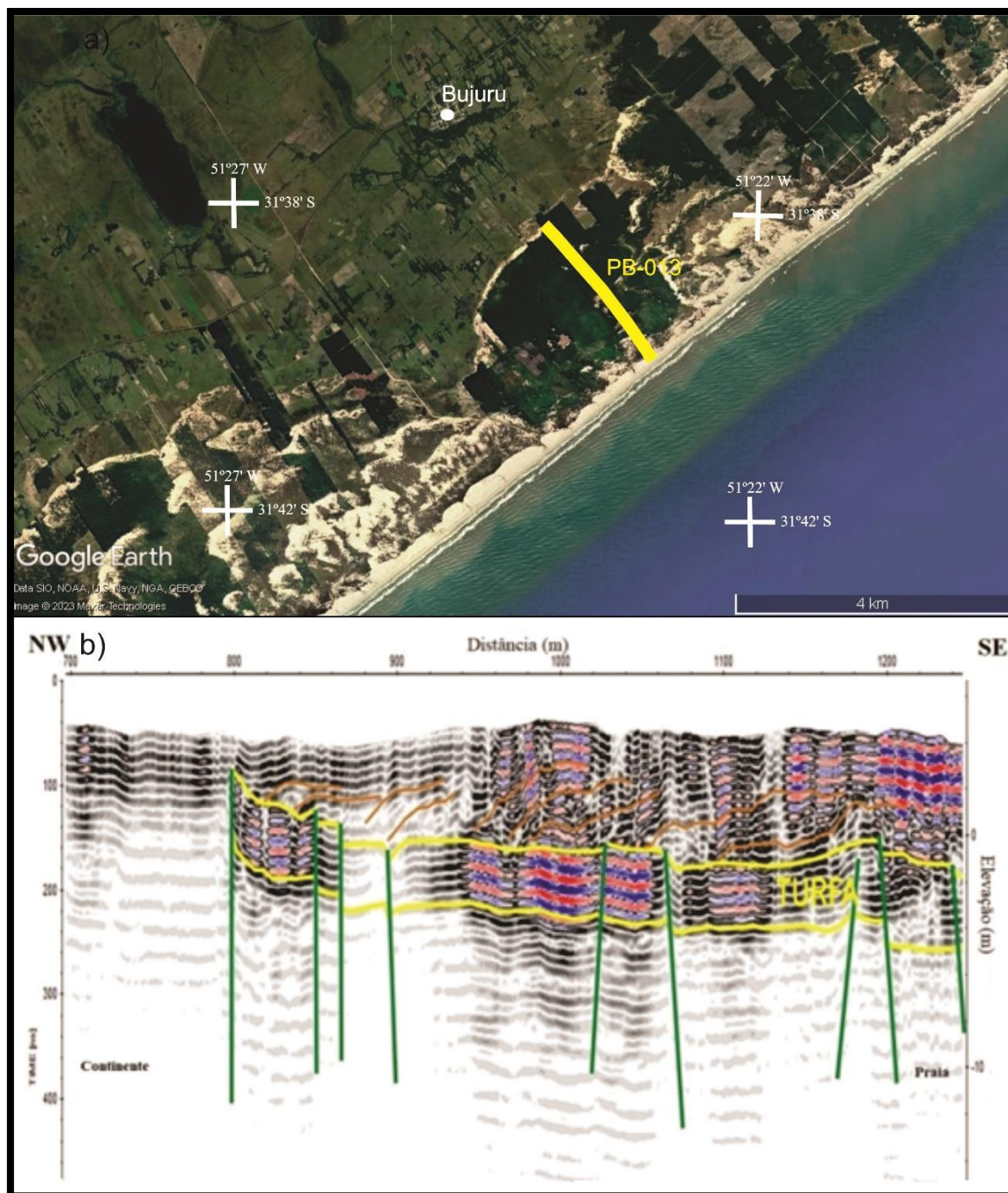


Figura 2.2.3. a) Mapa de localização do perfil PB-013 (Modificado do *Google Earth*). b) Radargrama mostra a camada de turfa mergulhando em direção ao continente com uma antena de 50 MHz (FONTOURA, 2015).

A identificação de falhas normais com mergulhos opostos (para oeste e para leste/sintéticas e antitéticas) sugere a existência de um par conjugado

cisalhante, cuja direção principal de esforço (σ_1) é vertical, ou seja, governado pela força gravitacional. O sistema de falhas do distrito de Bujuru registra o entroncamento de duas falhas lítricas principais, que são curvas em planta, que possuem a concavidade voltada para cima, e que se horizontaliza com a profundidade, na direção do talude continental. O conjunto de falhas normais sintéticas e antitéticas promovem o surgimento de *grabens* (com sinformes), que são os blocos rebaixados da camada guia de turfa, e de *horsts* (com antifformes), que são os blocos soerguidos da camada guia. Por fim, Fontoura (2015) conclui que os *placers* do distrito de Bujuru (São José do Norte, RS) são estruturalmente controlados pelas falhas gravitacionais lítricas da Lagoa do Peixe e de Rio Grande, as quais correspondem aos lineamentos morfo-estruturais dos Patos e da Mangueira indicados por Fonseca (2006). As falhas gravitacionais, conforme sintetizado por Jaboyedoff *et al.* (2013), têm natureza rotacional, não apenas em escala local como configurado pelas dobras de arrasto (*drag folds*).

Na plataforma continental adjacente ao Estado do Rio Grande do Sul, Corrêa (1990, 1994) identificou zonas de descontinuidades, estruturas sinformes e antifformes, *grabens*, *horsts* e falhas através de cartografia morfoestrutural, por meio da carta batimétrica de detalhe (Figura 2.2.4). Esta interpretação foi apresentada com base em fatores geológicos, estruturais, tectônicos e de variações do nível do mar (CORRÊA, 1994), a qual mostrou-se relação com as estruturas morfológicas encontradas nos depósitos sedimentares da Planície Costeira do Rio Grande do Sul.

O Cone do Rio Grande é caracterizado como uma espessa cunha sedimentar situada na Margem Continental do Rio Grande do Sul, na Bacia de Pelotas, em frente à cidade de Rio Grande (MARTINS *et al.*, 1972). Esta estrutura geológica situa-se entre as latitudes de 31° a 34°S e as longitudes de 45° a 51°W. O Cone do Rio Grande apresenta-se alongado na direção leste, estende-se por 550 km e tem sua largura máxima entre 350 a 400 km. Esta feição deposicional abrange o talude e a elevação continental, e alcança profundidades em torno de 4.000 m (Planície Abissal) (MARTINS, 1984).

O Cone do Rio Grande divide-se, geomorfologicamente, em i) porção superior, que compreende o talude superior, ii) cone médio, que abrange o talude

inferior, iii) a elevação continental, e iv) o cone inferior, que compreende a porção mais profunda dessa feição (MARTINS, 1984). Nos últimos anos, alguns pesquisadores têm encontrado mais indícios de que a tectônica gravitacional influenciou o processo de formação e evolução desta estrutura geológica.

A região do Cone do Rio Grande foi influenciada por eventos tectônicos desde o Período Cretáceo até o Recente. Em um trabalho realizado por meio de levantamentos sísmicos, Castillo *et al.* (2009) afirmam que a região do Cone do Rio Grande caracteriza-se por falhas normais, que foram originadas por *stress* distensivo gerado por blocos deslocados na zona proximal e falhas inversas na zona mais distal (Figura 2.2.5).

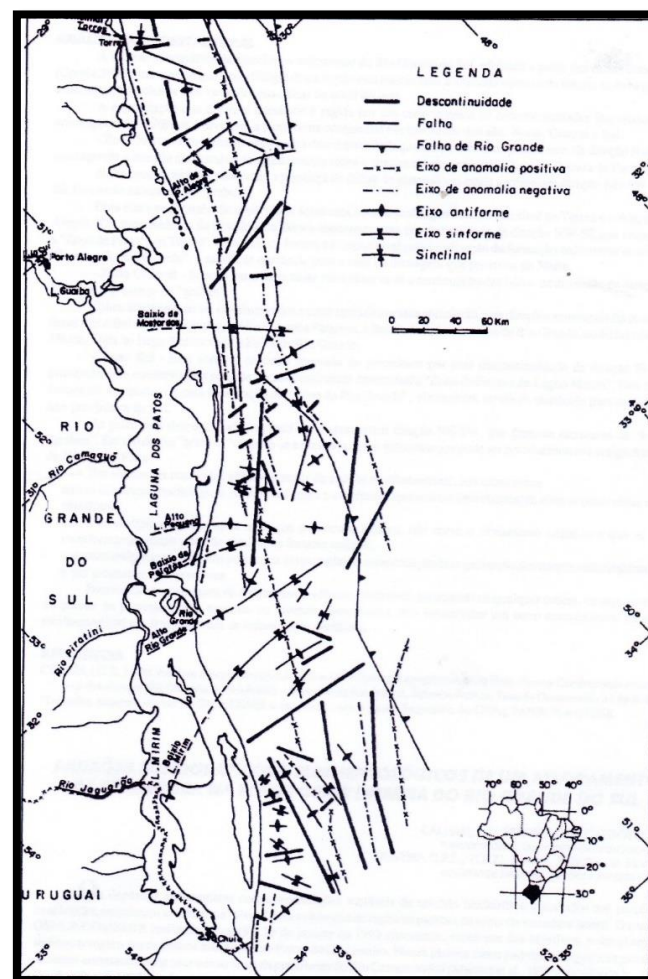


Figura 2.2.4. Carta Síntese Morfoestrutural da Plataforma Continental do Rio Grande do Sul (Extraído de CORRÊA, 1994).

A pesquisa de Santos (2020) demonstra que o Cone do Rio Grande constitui uma estrutura de deslizamento rotacional (*slump*) do tipo profundo (*deep-seated*), à qual se associam várias estruturas, predominantemente laterais, deslizamento translacional (*slides*) e rotacional (*slump*) raso (Figura 2.2.6). A figuras 2.2.7, 2.2.8 e 2.2.9 mostram detalhes de falhas extensionais (normais), compressionais (cavalgamento) e dobras que emergem à superfície do fundo marinho seccionando os refletores mais superficiais. Isto indica que os sedimentos recentes estão ainda sendo deformados pela tectônica gravitacional que define o Cone do Rio Grande (Santos, 2020).

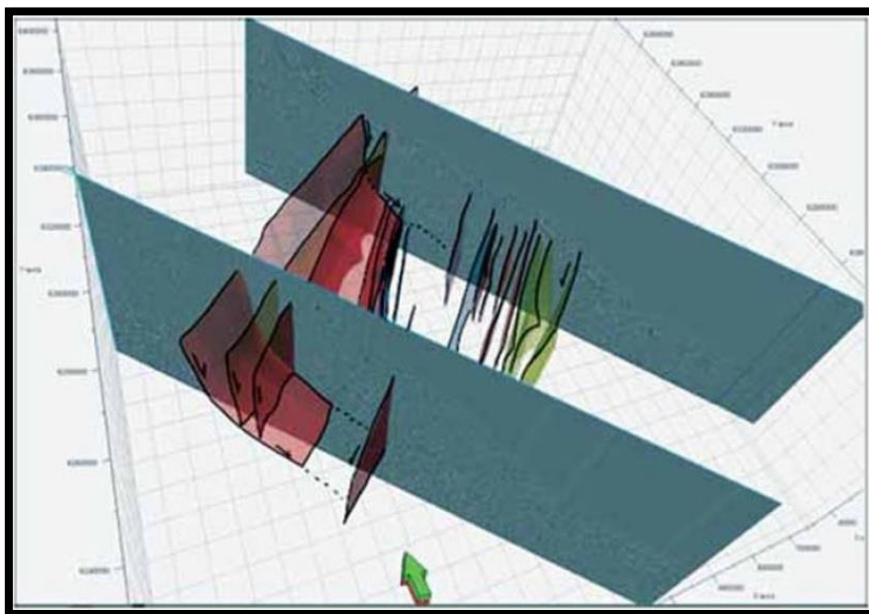


Figura 2.2.5. Modelo estrutural 3D do Cone do Rio Grande, sudeste brasileiro (Extraído de CASTILLO *et al.*, 2009).

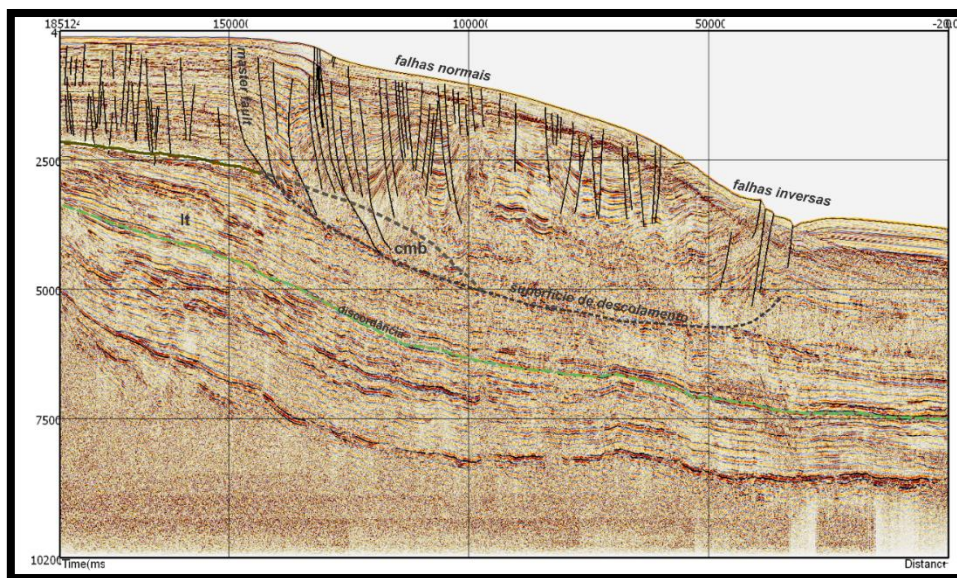


Figura 2.2.6. Linha sísmica “228_312” no Cone do Rio Grande. As linhas pretas representam as principais falhas na região do Cone do Rio Grande. Notar as falhas identificadas em direção à zona de praia, a falha principal (*master fault*) no talude, e falhas inversas na base do talude, todas emergindo à superfície do fundo oceânico (Santos, 2020). Observar os perfis em detalhe nas figuras seguintes.

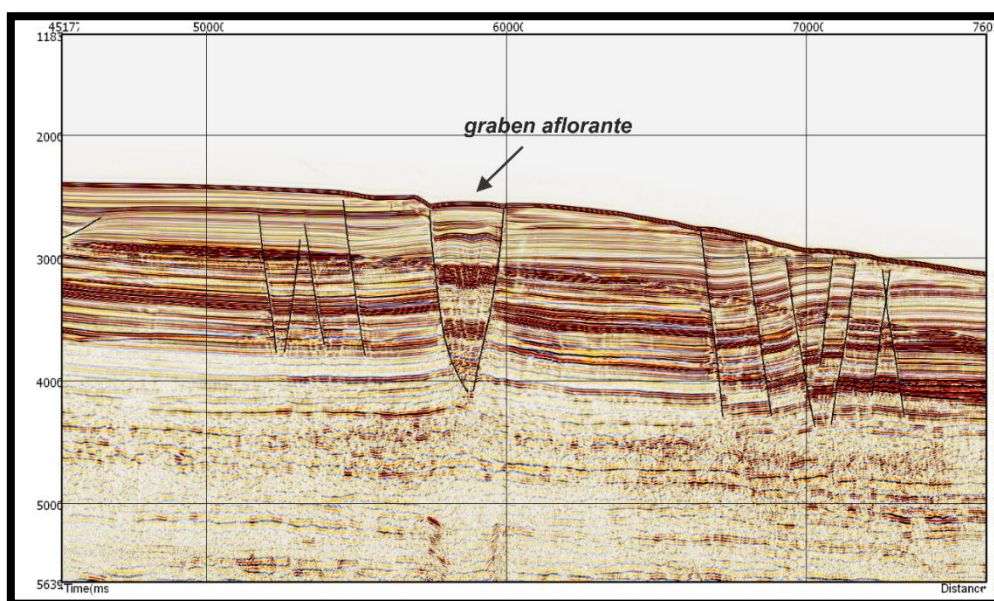


Figura 2.2.7. Flanco norte do Cone do Rio Grande, linha sísmica “277_336”. Ocorrência de falhas sintéticas e antitéticas normais e a formação de *graben* aflorante em fundo oceânico (Santos, 2020).

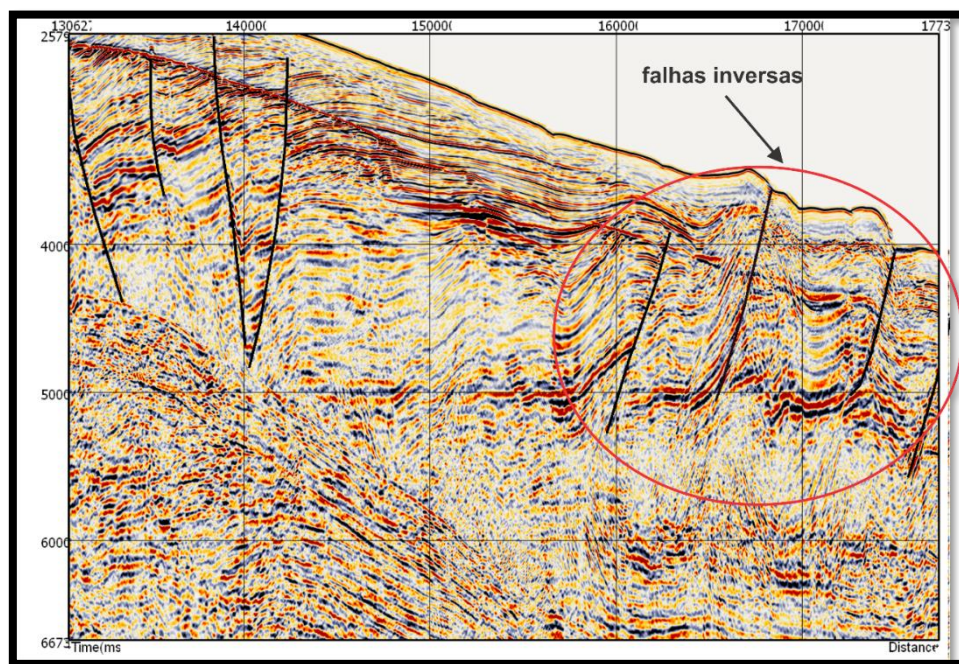


Figura 2.2.8. Flanco norte do Cone do Rio Grande, linha sísmica “231_465”. Ocorrência de falhas inversas que correspondem ao domínio compressivo da tectônica gravitacional na região (Santos, 2020).

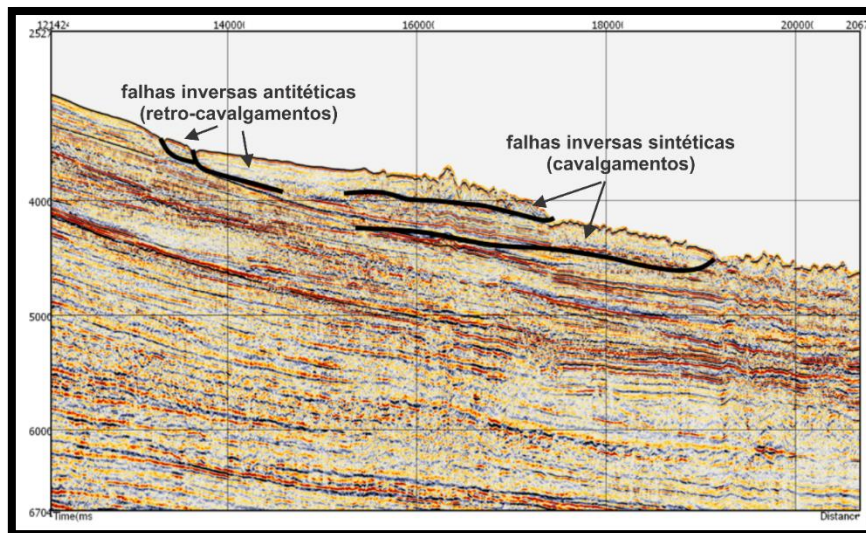


Figura 2.2.9. Flanco sul do Cone do Rio Grande, linha sísmica “228_311”. Ocorrência deslizamento translacional raso (*shallow landslide*), com falhas normais e inversas de duplo cavalgamento que seccionam o fundo oceânico (Santos, 2020).

CAPÍTULO 3

3. COMPROVANTE DE SUBMISSÃO DO ARTIGO 1:

☰ Geophysics

🏠 Home

✍ Author

🗉 Review

Submission Confirmation 🖨 Print

Thank you for your submission

Submitted to
Geophysics

Manuscript ID
GEO-2023-0474

Title
GRAVITY-DRIVEN LISTRIC GROWTH FAULT AND SEDIMENTATION CONTROL IN THE COASTAL PLAIN OF RIO GRANDE DO SUL, BRAZIL

Authors
Fontoura, Bruno
Strieder, Adelir
Corrêa, Iran
Mendes, Paulo
Calliari, Lauro

Date Submitted
14-Aug-2023

Author Dashboard

GRAVITY-DRIVEN LISTRIC GROWTH FAULT AND SEDIMENTATION CONTROL IN THE COASTAL PLAIN OF RIO GRANDE DO SUL, BRAZIL

ABSTRACT

High frequency, high resolution GPR surveys are successfully applied to investigate near-surface stratification architecture of sedimentary units in coastal plains and to define their depositional conditions. However, low frequency GPR surveys to investigate fault-related depositional systems at greater depths are scarce. This survey was designed to investigate a >100 km long linear escarpment that controls the northwest margin of the Lagoa do Peixe, an important lagoon in Rio Grande do Sul Coastal Plain (RGSCP, Brazil). The traditional approach points that RGSCP was developed by juxtaposition of four lagoons/barrier systems as consequence of sea level changes; no deformational structure is admitted to exist before. The low frequency GPR (50 MHz, RTA antenna) and geological surveys carried out in the RGSCP showed the existence of a large, gravity-driven listric growth fault controlling the Lagoa do Peixe escarpment and hangingwall sedimentation. The radargrams in four subareas along the Lagoa do Peixe Growth Fault could be interpreted following the seismic expression of rift-related depositional systems. The radargrams enabled to distinguish three main lagoonal deposition radarfacies. The lower lagoonal radarfacies is a convex upward unit, thicker close to growth fault; the radarfacies geometry indicates that fault displacement rate surpasses the sedimentation rate, and its upper stratum is aged ~ 3500 ^{14}C years BP. The second lagoonal radarfacies is a triangular wedge restricted to the lagoon depocenter, whose geometry indicates that fault displacement and the sedimentation rates kept pace. The upper lagoonal radarfacies is being deposited since 1060 ± 70 ^{14}C years BP, under sedimentation rate higher than fault displacement rate. The results indicate that low frequency GPR surveys can help in investigating fault-related depositional systems in coastal zones. They also point to a new approach in dealing with RGSCP stratigraphy.

INTRODUCTION

The Rio Grande do Sul Coastal Plain (RGSCP) is the emerged part of the gently sloping Pelotas Basin continental shelf, the southernmost of Brazil's Atlantic basins. This coastal plain is up to 100 km wide and extends for more than 600 km. The RGSCP was formed by juxtaposition of sedimentary deposits derived from deltaic alluvial plains and four lagoons/barrier systems developed as consequence of sea level changes from Middle Pleistocene to Holocene (Villwock *et al.*, 1986). The first lagoon/barrier system (I) has an estimated age of 325 ka. The following systems have absolute ages of 230 ka (II), 123-125 ka (III), and 5.6 ka (IV) MIS (Figure 1).

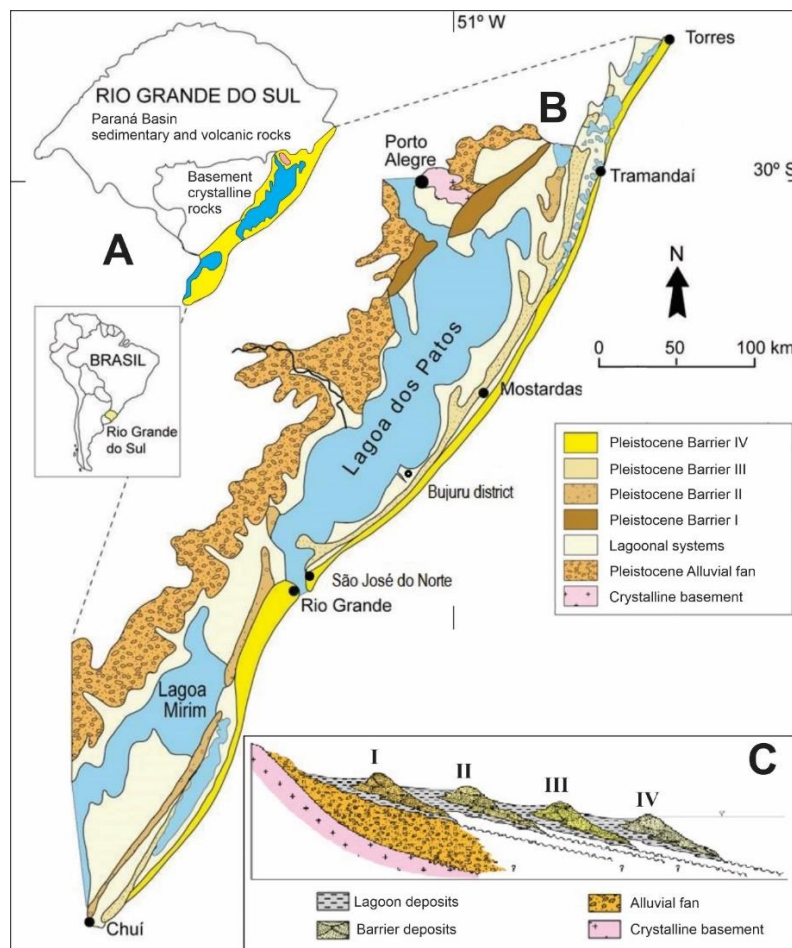


Figure 1 – Rio Grande do Sul Coastal Plain location (A), its regional geological map (B), and the model for its depositional systems (C). Modified from Tomazelli & Villwock (1996) and Tomazelli *et al.* (2000).

The RGSCP lagoons/barrier system was defined based on sedimentary facies, depositional systems, and chronostratigraphic techniques (Tomazelli & Villwock 1996, Tomazelli *et al.* 2000). No neotectonic deformational episode is considered for RGSCP lagoons/barrier sedimentary strata juxtaposition: *“the Pelotas Basin has remained oblivious to major tectonic movements, which translates into the symptomatic absence of faulting. If there were any, they resulted from aseismic processes in the sedimentary package that today constitutes the slope of the continental margin”* (Villwock 1972).

Recently, some records of neotectonic activity in the RGSCP has been identified. Fonseca (2006) produced a wide investigation for neotectonic records in the RGSPC based on geomorphic features, small-scale field structures, and remote sensing images (LANDSAT, SRTM). Fonseca (2006) was able to identify significant neotectonic records and *“suggested systematic campaigns of field to structural and geophysical data-collecting in the identified areas”*. Fontoura *et al.* (2015) and Strieder *et al.* (2015) showed preliminary evidence of major faults in the RGSCP. Cooper *et al.* (2016, 2018) have also showed evidence for major deformation in the Santa Catarina Coastal Plain.

The aim of this paper is to show a large-scale fault in the RGSCP, which cut across Pleistocene coastal barrier (III) and controls Holocene barrier (IV) and lagoon system development. 50 MHz RTA Ramac GPR surveys, drillholes and field surveys were carried out in order to determine the regional structural framework developed by the Lagoa do Peixe Growth Fault.

GEOPHYSICAL AND GEOLOGICAL SURVEY METHODS

The Lagoa do Peixe Growth Fault is named after the Lagoa do Peixe National Park, a conservation unit established due to Decreto nº 93.546/1986 (Figure 2). The Lagoa do Peixe, in fact a lagoon, is home to large amounts of migratory birds coming from the Northern (summer) and Southern (winter) hemispheres.

The northwestern border of the Lagoa do Peixe is a steep escarpment, whose actual altitude differences amount up to 10 m. This escarpment is close to deeper water sheet, which is poorly maintained during the dry season of the *La Niña* periods. The southeastern border is gently dipping toward northwest, and its connection with Atlantic Ocean is cancelled during the dry seasons.

The Lagoa do Peixe escarpment was previously regarded as a geomorphic lineament possibly due to a neotectonic structure (Fonseca, 2006). This geomorphic lineament is clearly defined in satellite images as a N40E trending, >100 km long escarpment. Based on these geomorphic features, four areas for geophysical and geological survey were selected: i) Mostardas (northern), ii) Tavares (central), iii) Lagoa do Cará, and iv) Bujuru (see Figure 2 for details). The surveyed areas were focused to geophysically investigate what kind of geological structure controls the escarpment in its entire extend.

The geophysical surveys were carried out through 50 MHz RTA Ramac equipment. This frequency was selected to investigate that structure as deep as possible (>20m depth was attained with good resolution). The mean EM wave velocity was estimated to be 0.08 m/ns, so that vertical resolution is ~0.8 m. Then, the EM wavelength is not adequate small-scale structures of sedimentary units, but to their geometry and continuity.

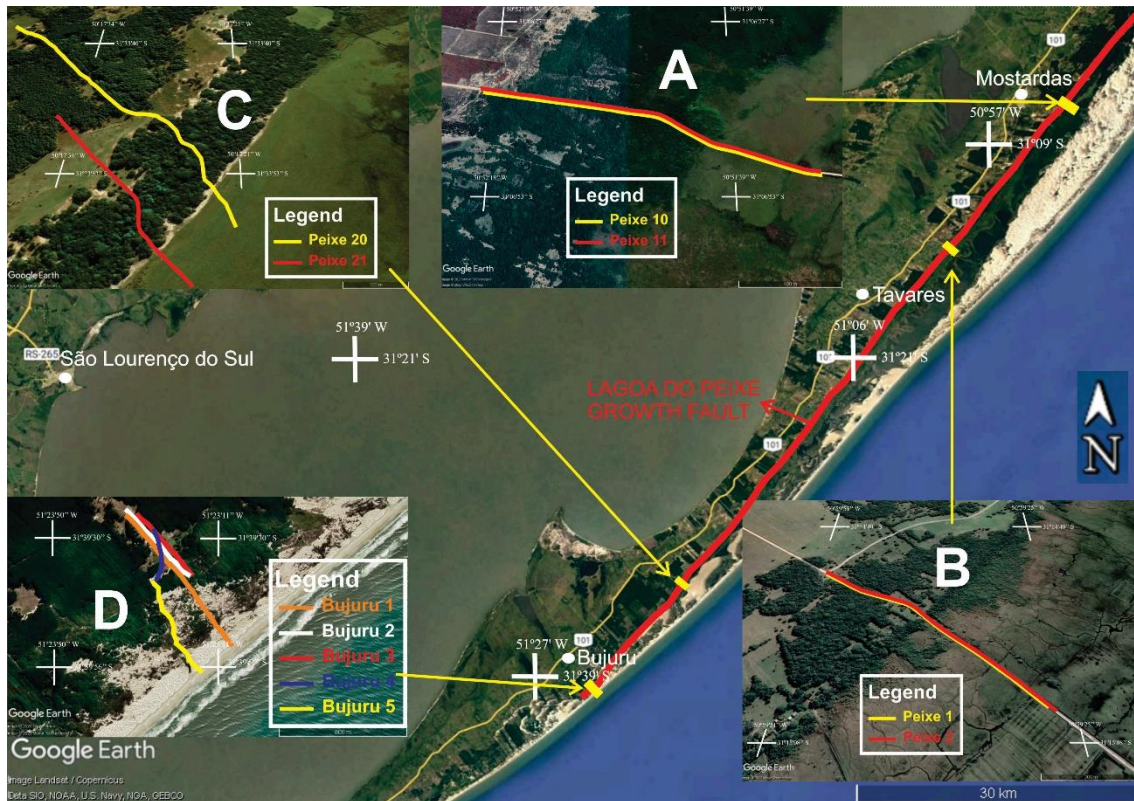


Figure 2 – Location of the Lagoa do Peixe Growth Fault and the areas of detailed geological and geophysical surveying. A) Mostardas (northern), B) Tavares (central), C) Lagoa do Cará, and D) Bujuru (Southern) areas.

Two parallel GPR lines were surveyed in Mostardas, Tavares and Lagoa do Cará areas. The Mostardas and Tavares GPR lines were surveyed in gravel roads cutting across Lagoa do Peixe. Lagoa do Cará (a lake isolated from the main Lagoa do Peixe due to sedimentation) was profiled in a secondary road as long as possible into the clogged lagoon. In the Bujuru area, five parallel and oblique lines were surveyed, since no water filled depression is present and a better scanning for the fault geometry can be produced.

The GPR survey lines were all accompanied by DGPS (Emlid, Reach RS+ model, base and rover receptors) control, with kinematic and post-processed corrections (Leica Geo Office and PPP-IBGE). The GPR line positioning procedure do permit a high horizontal (7mm + 1ppm), and vertical precisions (14mm +1 ppm).

The Bujuru area was drilled to determine the sand thickness covering the peat layer, and the stratigraphic features of the Pleistocene barrier (III). Three percussion drill cores were sampled and correlated with GPR survey line (Bujuru01 line). It was selected to drill because the peat layer does not crop out in the actual beach, and the GPR survey line ends at beach; thus, it was possible to control the geophysical signature of the peat layer.

GEOLOGY OF THE SURVEYED AREAS

The geologic survey of the detailed areas was carried out through aerial-photographs, high resolution Google images, and field work. The aim of the geologic survey was to investigate the main surficial sedimentary units over which GPR survey lines were conducted, to define their main geological features that can contribute to discriminate them in radargrams. The aim was not to fully characterize each sedimentary unit in terms of their sedimentological properties.

Figures 3 to 6 present simplified geological maps that are result of aerial photographs, Google high resolution images and field work. Table 1 summarizes the main lithological features of each stratigraphic unit distinguished during the geological survey.

Table 1 – Summary of the main stratigraphic units cropping out in the selected areas for GPR surveying.

Stratigraphic unit		Geological and lithological features
Aeolian covers		Thin sheets of fine-grained sands (≤ 1 m thick) covering mainly the structural highs. Locally, it can develop a small dune up to 2-3 m high.
Holocene Barrier IV	Holocene dunes II	Active dunes close to the Atlantic Ocean, making part of the actual dune system building the Holocene Barrier IV.

	Holocene dunes I	Inactive dunes underlying the active ones. They seem to be coarser grained than actual ones and are anchored by native grass and bushes.
	Holocene Lagoonal deposits	Fine-grained sands and silts interlayered with variable proportions of organic matter and clays in depressed areas.
	Pleistocene Barrier III	Fine to medium-grained sands, mostly horizontal, parallel stratification, slightly compacted, and Fe ³⁺ hydroxides and clay impregnated.

The Pleistocene Barrier III is a key stratigraphic unit for GPR surveys since it rests as a structural high west of the Lagoa do Peixe Growth Fault scarp. This structural high may be recognized in two erosional tiers (10-15 m, and 5-8 m) above mean sea level (see Figure 3B, Tavares geological map). It is best exposed in the Talhamar Road (Tavares area), at the erosional retreating fault scarp (Figure 4B). On the other side, the west limit of the Pleistocene Barrier III is not fault bounded, but erosional, as can be seen by several embayment controlled by actual drainage.

The Holocene Lagoonal deposits rests at < 3 m above mean sea level. Parallel stratification of silts and fine-grained sands and peat rich layers or lenses ($\geq 0,5$ m thick) are present. An upper peat layer crops out in some segments along the beach in the investigated area when it is being eroded. A gentle folding and faulting of this upper peat layer controls its outcropping.

The Holocene Lagoonal deposits are also present in the west limit of the Pleistocene Barrier III structural high, where they are under the influence of the Lagoa dos Patos. These lagoonal deposits are not in the scope of this investigation, since their actual limits are not fault-bounded.

The Holocene Barrier IV system is under construction close to the Atlantic Ocean. It is made up by aeolian dunes migrating from NE toward SW. This dune system discordantly overlays the Holocene Lagoonal deposits in the Lagoa do

Peixe National Park. This feature is best recognized in segments where the upper peat layer crops out and is under erosion. In some places, where actual active dunes are not present, it is possible to recognize a previous, vegetated dune blanket that seems to have been developed by winds blowing more easterly. The Holocene Barrier IV system advances over and clogs the eastern margin of the Lagoa do Peixe, as can be seen in figures 3 to 6.

The west fault-bounded margin of the Lagoa do Peixe, on the other hand, presents a number of wedge aprons that can be recognized to clog the lagoon. It is to be noted that these wedge aprons are in high angle to fault trace (see Figure 4) and do reflect erosion of the Pleistocene Barrier III footwall making up the scarp.

In the Bujuru area (Figure 6), the Holocene Barrier IV system almost completely covers the Holocene Lagoonal deposits and the Lagoa do Peixe Growth Fault; just a small window could be recognized, where GPR lines were surveyed. Two GPR lines were extended to the shoreface, since the upper peat layer does not crop out there, but 2-3 km to the southwest and to the northeast. In this way, a drilling campaign was conducted to investigate the peat layer presence in that position (Figure 7).



Figure 3 – Geological map of the Mostardas area, with the location of the GPR survey.

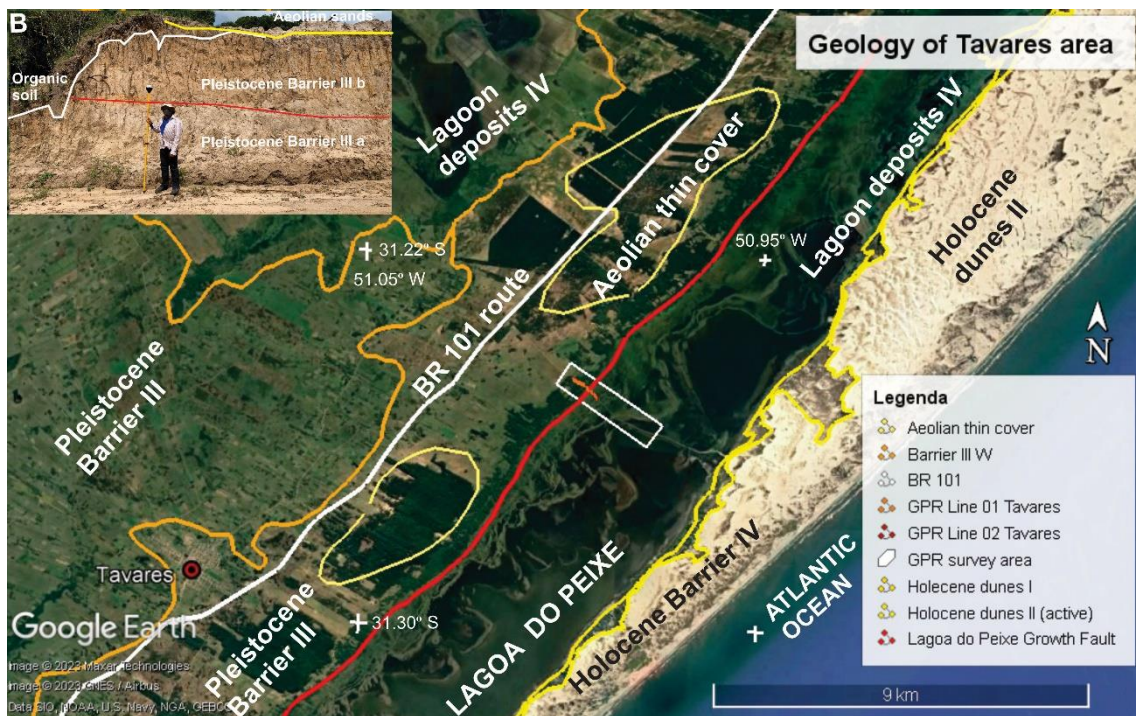


Figure 4 – Geological map of the Tavares area, with the location of the GPR survey (A). Pleistocene Barrier III (B) crops out in the intersection of the fault trace and GPR lines (Talhamar Road).

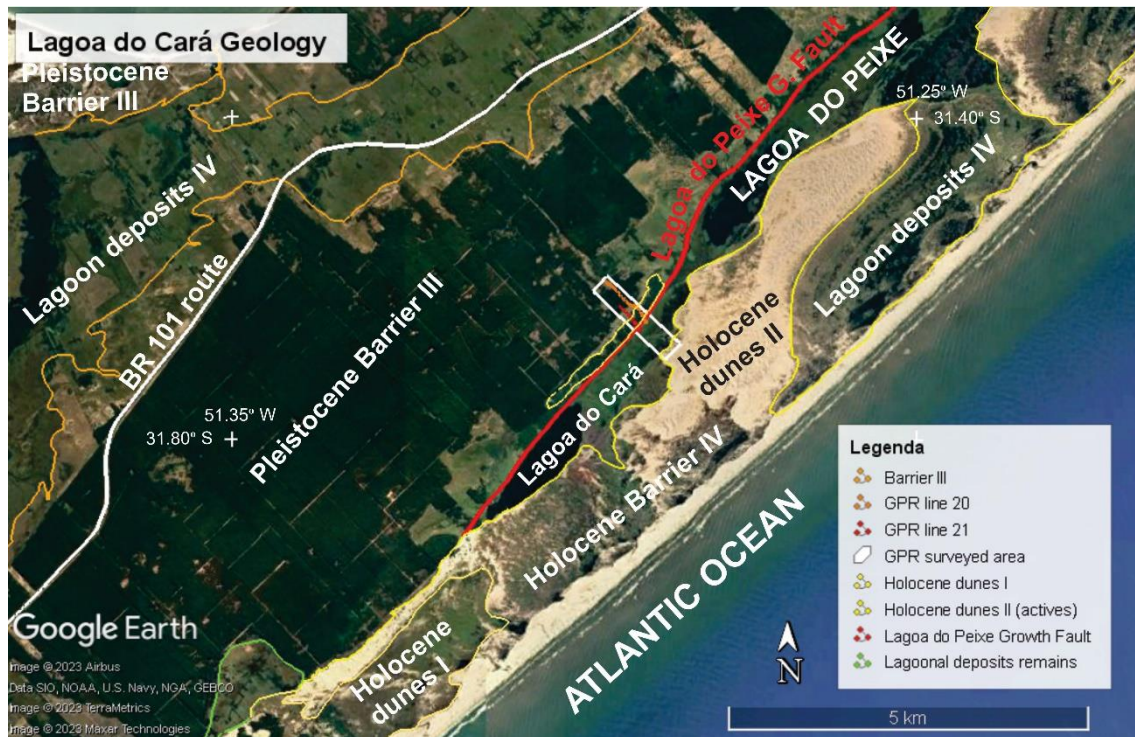


Figure 5 – Geological map of the Lagoa do Cará area, with the location of the GPR survey.

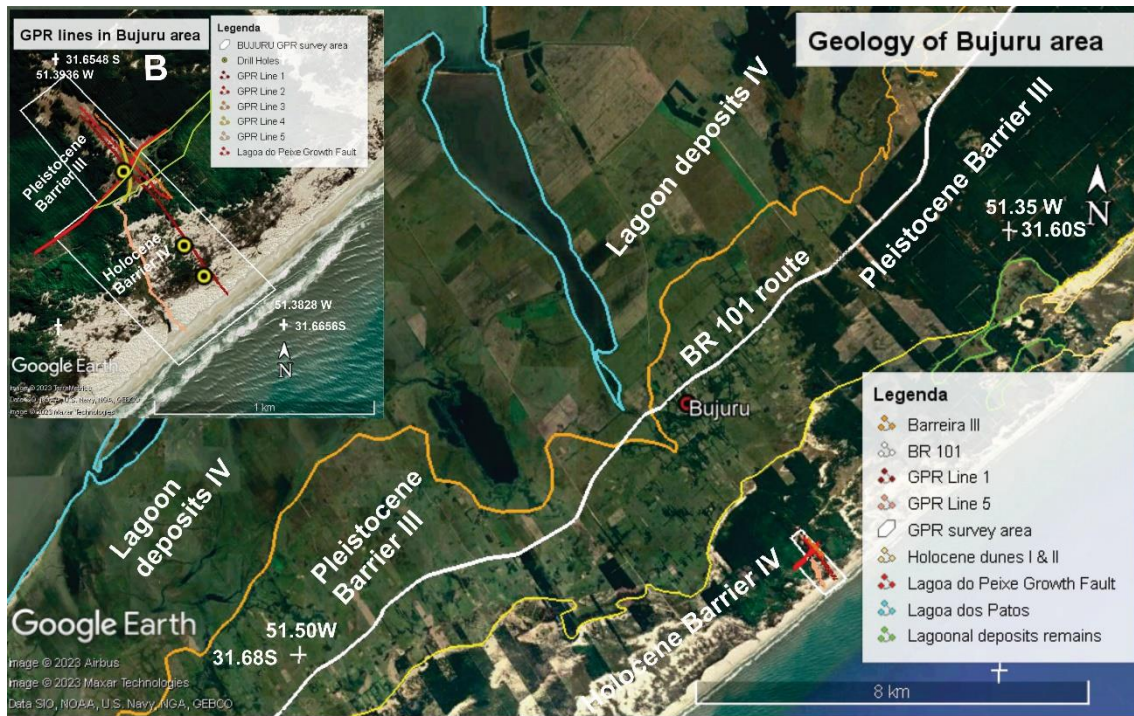


Figure 6 – Geological map of the Bujuru area (A), with the location of the GPR survey and the drill holes along GPR line 1 (B).

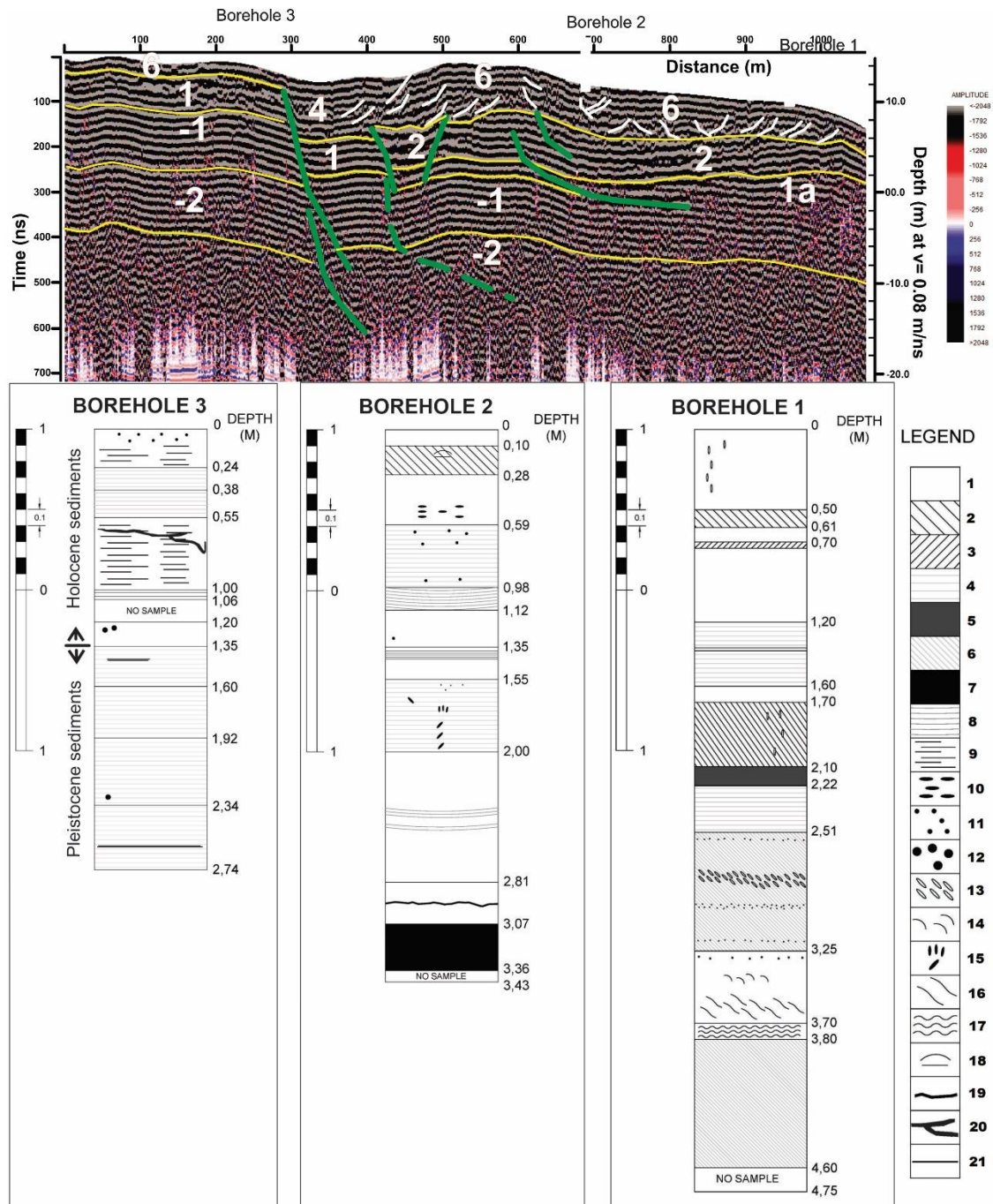


Figure 7 – Radargram for Bujuru Line 01 (A) and boreholes description (B). Legend: 1) Light yellow sand; 2) Light yellow sand with coarse lamination (1-5 mm thick); 3) light yellow sand with gently inclined lamination (1-2 mm thick) and disseminated heavy minerals; 4) light yellow sand with thin horizontal lamination (1 mm) and disseminated heavy minerals; 5) Massive, dark gray sand with high quantity of heavy minerals; 6) Massive light yellow sand and disseminated heavy minerals; 7) Peat; 8) light yellow sand with gently arched lamination (1 mm); 9) isolated thin horizontal laminas of heavy minerals; 10) up

to 2 cm recent root fragments; 11) small recent root fragments; 12) small disseminated shell fragments; 13) up to 1 cm shell fragments; 14) oxidized material; 15) oxidized (orange) dark gray sand; 16) heavy minerals concentration; 17) light yellow sand with fragmentary structure; 18) dispersed organic matter; 19) relicts of organic matter; 20) localized breccia structure; 21) dark yellow sand lamination.

Figure 7 shows the peat layer presence at depth in the Bujuru investigated area (Figure 6B), as predicted from its gentle folding structure. Figure 7A also shows that upper peat layer covers a well-defined radarfacies, which displays parallel, continuous reflections with wavelength larger than adjacent ones. This radarfacies is made up by more conductive material (clays, silt and organic matter - peat, for example) and is lay discordantly over previous radarfacies (see *toplap* feature in position below Borehole 1 in figure 7A). Then, it is envisaged that peat layer cropping out at beach is a stratum covering the lower lagoonal radarfacies developed due to Lagoa do Peixe Fault.

A thin aeolian sand blanket (≤ 1 m thick) is widespread in the structural high made up by Pleistocene Barrier III. But, it is locally thicker (up to 2-3 m) close to the fault scarp, where isolated or a sequence of few dunes can be recognized. Some of these thicker covers were emphasized in maps shown in figures 3 to 6.

GEOPHYSICAL SURVEYS: FAULT GEOMETRY AND KINEMATIC

The radarfacies discrimination followed Neal (2004) proposal. However, it was necessary to include fault truncation geometries for radarfacies boundary reflectors (Figure 8). Then, radarfacies discrimination was based on the following criteria: i) geometry of reflectors at boundaries, ii) shape of reflections, iii) dip of reflections, iv) relationship between reflections, v) reflections continuity, and vi) truncation of reflections.

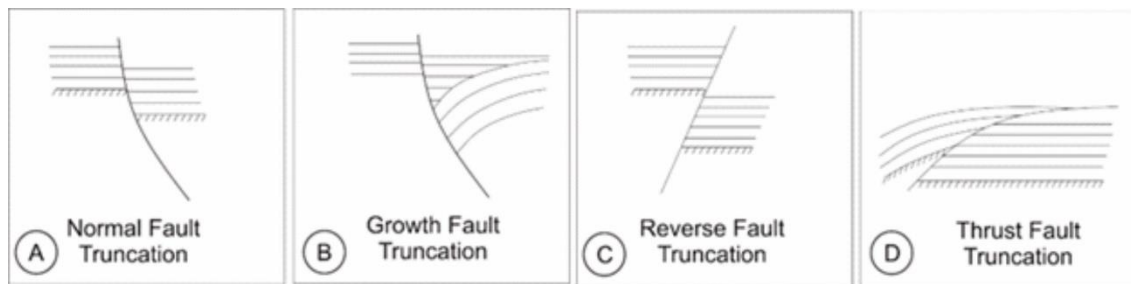


Figure 8 – Fault truncation geometries for radar surface boundaries. A) Normal fault truncation. B) Growth fault truncation. C) reverse fault truncation. D) Thrust fault truncation. These types of truncations can be observed in radargrams of Reiss *et al.* (2003), Christie *et al.* (2009), Nobes *et al.* (2016) e Zhang *et al.* (2016).

Radarfacies and surfaces description

The description of the identified radar surface boundaries (**s**) and radarfacies (**f**) follows the chronologic sequence proposed by Neal and Roberts (2001) and Neal (2004). Table 2 summarizes the radar surface boundaries and radarfacies distinguished in the Lagoa do Peixe – Bujuru area.

Table 2 – Summary of radar surface boundaries (**s**) and radarfacies (**f**) distinguished for GPR survey lines in the Lagoa do Peixe and their interpretation (Mostardas – Tavares – Lagoa do Cará – Bujuru, RS, Brazil).

Stage	Facies ID	DESCRIPTION	INTEPRETATION
1	LP-f _{n+1} -ps	Pleistocene sediments (poorly compacted) cropping out west of Lagoa do Peixe escarpment (Barrier III)	Pleistocene sediments cropping out at the footwall top west of fault escarpment (Barrier III)
1a	LP-f _{n+1} -pf	Radarfacies underlying the lower lagoonal unit, displays regular reflections which are truncated	Pre-fault radarfacies undergone hangingwall collapse and erosion

		(<i>toplap-offlap</i>) by its upper boundary	
	LP-s_{n+1}-gf	Upward concave listric geometry surface that truncate Pleistocene sediments (west) and lower lagoonal unit (east)	Listric gravitational growth fault. See also associated branching normal faults.
	LP-s_{n+2}-et	<i>Offlap-toplap</i> for reflectors underlying lower lagoonal unit; maybe an erosional truncation	An erosional surface developed on the down-throwing hangingwall before fault controlled lagoonal accumulation
2	LP-f_{n+2}-pe	Convex upward arcuated lower lagoonal unit, displaying <i>onlap</i> for lowermost reflections in the thickest zones, close to listric surface, and parallel reflections for uppermost strata	Lagoonal accumulation during the first stage of fault displacement resulted in its convex geometry and greater thickness close to fault surface
	LP-s_{n+3}-ol	Surface at the top of the lower lagoonal unit, in the outcropping peat layer, showing <i>onlap</i> reflections for overlying radarfacies.	An increase in water depth giving rise to <i>onlap</i> of horizontal sedimentary layer on both sides in the lagoon depocenter.
3	LP-f_{n+3}-lag	Horizontal reflections in a hangingwall triangular area close to listric surface, showing <i>onlap</i> upon lower lagoonal unit and listric surface.	Localized sediment accumulation while fault displacement advanced, during a second stage of fault displacement, clogging Lagoa do Peixe depocenter (triangular wedge).
	LP-s_{n+4}-dl	Discrete <i>onlap-downlap</i> features upon previous radarfacies on both margins of the Lagoa do Peixe.	Surface defining the vanishing stage of fault displacement, and the third stage of sediment accumulation in the Lagoa do Peixe.

4	LP-f_{n+4}-lag	Upward arcuated reflections at both Lagoa do Peixe margins, showing alternating <i>onlap-downlap</i> and <i>toplap-offlap</i> features.	Third stage of lagoonal sediment accumulation, characterized by the interbedding of lagoon sediments and sands from emerged areas on both sides of the Lagoa do Peixe.
5	LP-f_{n+5}-es	Dipping sinuous reflections in the Lagoa do Peixe escarpment, showing discrete downlap with lagoon sediment reflections.	Erosional degradation of the fault escarpment and deposition as interbedded layer of sands and lagoon sediments
	LP-s_{n+n}-df	Minor truncation of inner reflections of radarfacies	Minor listric normal faults merging into master one, or diachronic synthetic and antithetic normal faults
	LP-s_{n+5}-dl	Irregular surface underlying recent dune sediments	Surface upon which recent dune sediments prograde
6	LP-f_{n+6}-dm	Horizontal and steeply dipping sigmoidal reflections, as also as thin horizontal reflection near the topographic surface	Recent dunes and thin wind cover overlying previous sedimentary radarfacies: 6a – steeply dipping reflections: lateral limbs of recent dunes; 6b – horizontal reflections: frontal dune strata, and thin wind covers
Types of radarfacies (f)			Types of boundary surfaces (s)
<p>ps = Pleistocene sediments</p> <p>pf = pre-fault unit underlying lower lagoonal</p> <p>pe = lower lagoonal, underlying peat layer</p> <p>lag = sediments clogging the lagoon</p> <p>es = erosional sediments close to escarpment</p> <p>dm = recent dunes and thin wind covers (Upper Holocene)</p>			<p>gf = growth fault</p> <p>et = erosional truncation</p> <p>ol = onlap</p> <p>dl = downlap</p> <p>df = diachronic normal faults</p>

The most important GPR lines (Figure 9) were surveyed in the Talhamar Road, perpendicular to the Lagoa do Peixe escarpment. They display the most complete surface boundaries and radarfacies chronologic sequence. Figure 8 reveals a concave boundary surface (**LP-s_{n+1}-gf**) that is steeply dipping in the westside, and gently dipping toward east. It truncates two main radarfacies: Pleistocene sediments (**LP-f_{n+1}-ps**), and the lower lagoonal unit (**LP-f_{n+2}-pe**).

The geophysical signature of the lower lagoonal radarfacies (**LP-f_{n+2}-pe**) shows it is westward dipping and convexly arcuated. It is also noticed that it is thicker close to the concave truncation surface (**LP-s_{n+1}-gf**). The lowermost reflectors of the lower lagoonal unit also show onlap features in the thicker segment close to the concave truncation.

The radarfacies underlying the lower lagoonal unit displays erosional truncation in its upper boundary (*toplap*), which is evidenced close to the concave boundary surface (**LP-s_{n+1}-gf**).

A close view of this boundary truncation surface (Figure 9B) shows a triangular feature delimited by the upper boundary surface of the lower lagoonal radarfacies and the fault truncation surface. The inner reflectors in this triangle show onlap over both west and east boundary surfaces. The sedimentary unit overlying the lower lagoonal radarfacies in the fault hangingwall can be distinguished into two radarfacies: i) the triangular area radarfacies (**LP-f_{n+3}-lag**) restricted to the fault truncation hangingwall, which is onlapping both the concave truncation surface and the convex upper boundary for lower lagoonal radarfacies; and an ii) upper extended radarfacies (**LP-f_{n+4}-lag**), which display alternating *toplap-offlap* and *downlap-onlap* reflections features in both west and east sides of the lagoon.

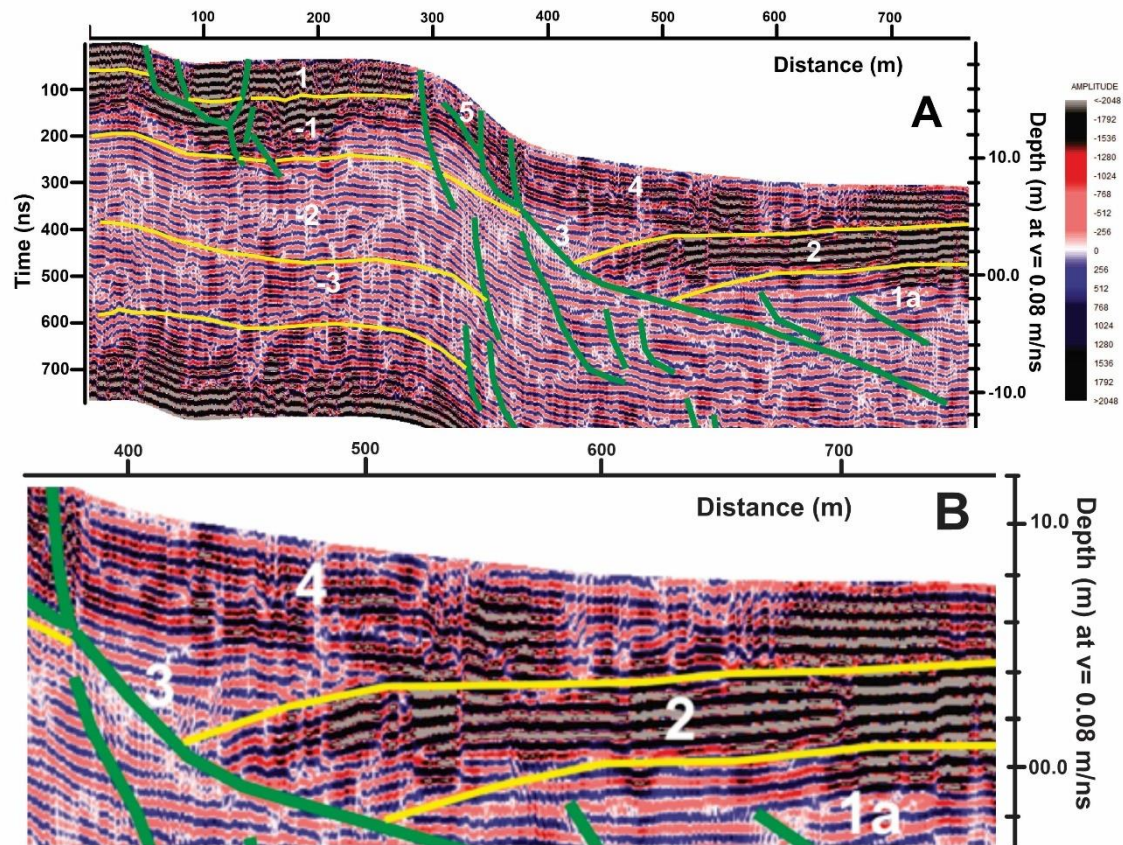


Figure 9 – Radargram for Tavares area (Talhamar Road), that cut across fault escarpment in the Lagoa do Peixe National Park. (A) Complete interpreted radargram, and (B) detail radargram showing the triangular and upper lagoonal radarfacies.

The alternation of reflection features seems to indicate interbedding of lagoon sediments and that derived from erosion in emersed margins. This feature is better seen in figure 10, where a thick Holocene dune lies on the top of footwall escarpment (structural high), and its east lateral strata (**LP-f_{n+6}-dm** - 6a) flows into the lagoon. Escarpment degradation by erosion (**LP-f_{n+5}-es**) is also responsible for interbedding with lagoon sediments (**LP-f_{n+4}-lag**) (see Figure 11).

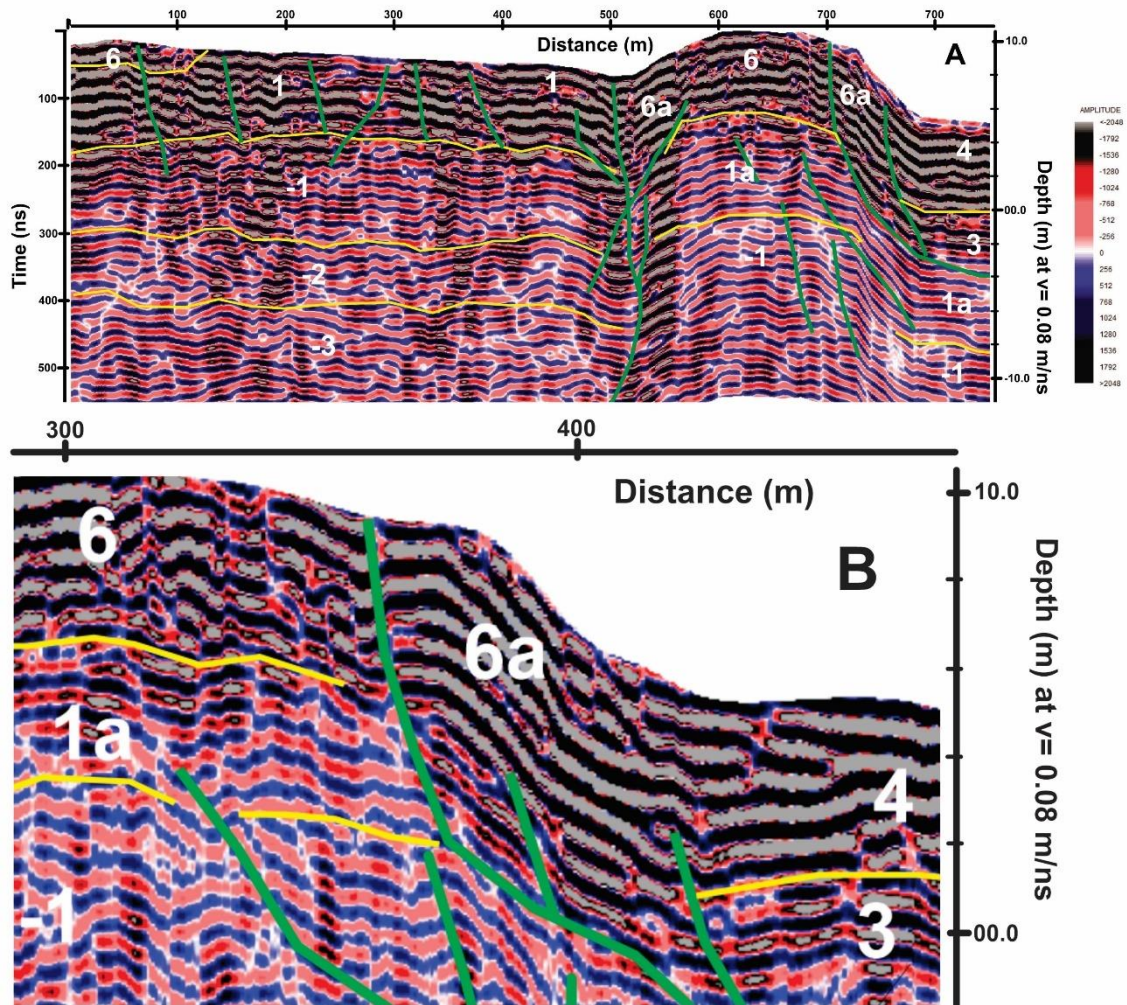


Figure 10 – Radargram for Lagoa do Cará area (A), also cutting the fault escarpment. (B) A detail showing that reflections for lateral facies of the dune (6a) laying on the structural high are interbedded with lagoonal deposits (4).

A number of diachronic synthetic and antithetic normal faults (**LP-s_{n+n}-df**) can be seen in the radargrams (e.g. Figures 10A and 11). They cut across different radarfacies. The deeper ones often merge into the master growth fault or seem to merge to a master concave fault that could not be traced continuously at this resolution scale. A group of conjugated faults are close to the actual surface and are related to topographic depression.

It is to be noted that downthrow displacement of the growth fault in the Bujuru and Mostardas areas is lesser than in Tavares area. Bujuru and Mostardas areas near the tip zone of the main Lagoa do Peixe Growth Fault, which is covered by actual dune system (Holocene Barrier IV). It is also to be observed that the lower lagoonal unit (**LP-f_{n+2}-pe**) was not recorded close to the Lagoa do Peixe fault escarpment in the Lagoa do Cará (Figure 10A) and Mostardas (Figure 11). This indicates that lower lagoonal unit (**LP-f_{n+2}-pe**) was not deposited in that areas due to the fact that lateral growth fault propagation reaches those areas after lower lagoonal unit ceased to be deposited, or there exists some fault branch midway to the beach controlling lower lagoonal deposition.

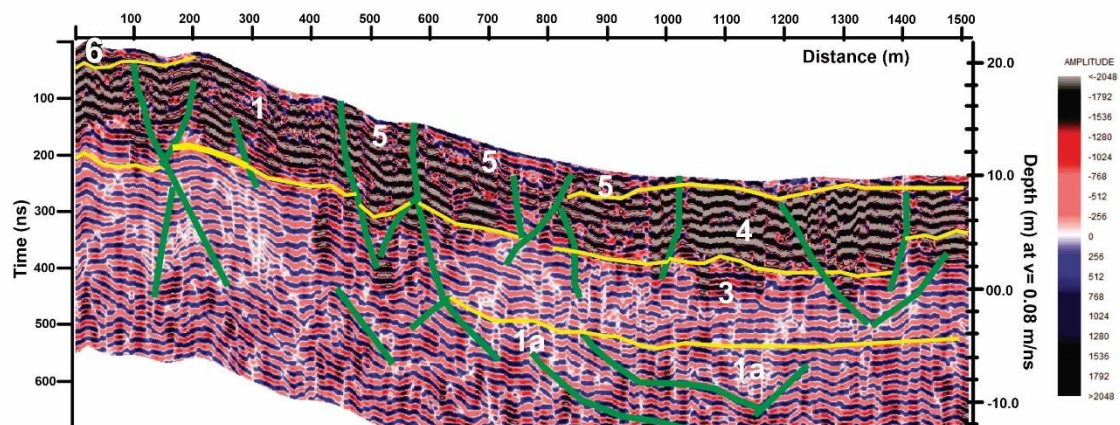


Figure 11 – Radargram for Mostardas area, also cutting the fault escarpment.

Boundary surfaces and radarfacies interpretation

The concave boundary surface (**LP-s_{n+1}-gf**) shows a number of features that can be interpreted as an emersed listric growth fault due to Quaternary gravitational neotectonic event in the RGSCP (Pelotas Basin): i) upward concave geometry, that flattens seaward; ii) exposes Pleistocene sediments at top of the footwall escarpment; iii) controls lower lagoonal sediments accumulation at

hangingwall as it deepens (convex geometry and thickness toward the fault); iv) controls depocenter for lagoonal sedimentation of overlying radarfacies (triangular geometry area). These features are in accordance to that summarized by Chapman (1983).

The kinematics of the listric growth fault may be linked to the deposition of the sedimentary radarfacies (Table 2). The subaerial evolution of this listric gravitational growth fault can be related to the rift-related depositional systems described by Prosser (1993), but 1-2 orders of magnitude smaller.

The evolution of sediment deposition while the listric gravitational fault displacement grows can also be distinguished into stages as proposed by Prosser (1993). The radarfacies underlying the lower lagoonal one is interpreted as a pre-fault sedimentary unit (**LP-f_{n+1}-pf**) since its upper boundary displays *offlap-toplap* reflectors truncation.

The pre-fault sedimentary radarfacies (**LP-f_{n+1}-pf**) also shows a gentle convex arcuated geometry close to listric growth fault (Figure 9). Projection of this arc suggests that it dip less than the lower lagoonal radarfacies, and it seems that the pre-fault sedimentary strata underwent minor hangingwall collapse according to the fault displacement amount. In such a subaerial condition, the onset of the fault displacement can favour erosion by stream along strike in the faulted and rotating hangingwall.

The main stage of fault displacement is characterized by sedimentation in a broad area and the predominant accumulation of sediments higher in conductive properties, such as clays and peat, to give rise the lower lagoonal radarfacies (**LP-f_{n+2}-pe**). The onlapping of the lowermost strata reflections close to the listric growth fault shows that fault displacement outpaces peat accumulation. Toward the top of lower lagoonal radarfacies, the sediment accumulation and fault displacement rates seem to keep pace.

The second stage of fault controlled lagoonal accumulation was taken in a restricted triangular area just in the Lagoa do Peixe depocenter (**LP-f_{n+3}-lag**), after a period of low sediment supply. The reflection geometry and *onlap*

relationship suggest the fault displacement and sedimentation kept pace during this period. However, the gently eastward dipping upper reflections of this radarfacies suggest that sediment supply could have slightly surpassed fault displacement.

The vanishing stage of fault displacement is characterized by sedimentary supply from emerged areas on both margins of the Lagoa do Peixe (**LP-f_{n+4}-lag**). The alternate reflections (*onlap-downlap*, and *toplap-offlap*) at its margins suggests interbedding of lagoon sediments and sands. This is particularly distinguished in upper reflections close to the growth fault, due to escarpment erosion (**LP-f_{n+5}-es**), and sand flow of Holocene dune lateral limbs (**LP-f_{n+6}-dm**).

EVOLUTION OF LAGOA DO PEIXE GROWTH FAULT AND SEDIMENTATION

The Lagoa do Peixe Growth Fault makes part of the gravitational tectonic affecting Pelotas Basin since Upper Miocene (Castillo *et al.*, 2009; Santos, 2020). Santos (2020) showed that Pelotas Basin gravitational tectonics started in the continental slope, and upper normal fault branches propagate westward into the platform.

The description and interpretation of radarfacies and surfaces (Tables 2 and 3) show that it is possible to discuss an evolutionary model for this area of the RGSCP. But, for a complete preliminary scenario, it is interesting to introduce some absolute ages for key sedimentary units.

There exist few radiogenic ages for detailed peat layer investigation in the Lagoa do Peixe area. On the other hand, Bauermann (2003) presented a detailed palynomorphologic investigation, including ¹⁴C ages for peat deposits cropping out north of Lagoa do Peixe. Bauermann (2003) investigated thick peat deposits and found 27.775±155 - 12.948±66 ¹⁴C years BP to lowermost interval (Barrocadas area; 5,75 m and 3,10 m depth), 10.974±49 ¹⁴C years BP to middle interval (Águas Claras area; 2,70 m depth), and 3.879±30 - 3.163±29 ¹⁴C years BP to the upper interval (Águas Claras - 1,70 m depth – and Barrocadas – 1,50 m depth - areas).

In the Bujuru area, Weschenfelder *et al.* (2008) determined ages for two organic-rich mud intervals recovered in a drillcore: 9400±140 Cal BP (23.2 m depth; ~10.000 ¹⁴C years), and 7370±150 Cal BP (5.0 m depth; ~8.300 ¹⁴C years). In another core drilled in the same area, Medeanic *et al.* (2001) found 7.370±150 ¹⁴C years BP (~6.330±47 Cal BP) for organic-rich mud at 3,33 m depth.

Close to the SW end of the Lagoa do Cará, Dillenburg *et al.* (2004) carried out a sequence of nine drillholes to recover material (2 shell samples, and 3 peat samples) for radiocarbon dating. Shell samples were collected close to the Atlantic Ocean, in fine (muddy) sand underlying peat, and recorded ages of 3390±130 and 3490±70 ¹⁴C years BP; it represents the upper stratum of the lower lagoonal radarfacies here described. Peat samples showed decreasing ages (1060±70, 350±60, and 380±80 ¹⁴C years BP) from east to west, where the Lagoa do Peixe escarpment anchors the peat and the underlying lagoonal sediments.

These results make possible to discuss an evolutionary model for the Lagoa do Peixe area. Figure 12 shows the structural evolution of the Lagoa do Peixe Growth Fault and the sedimentation control in its tectonically sinking area.

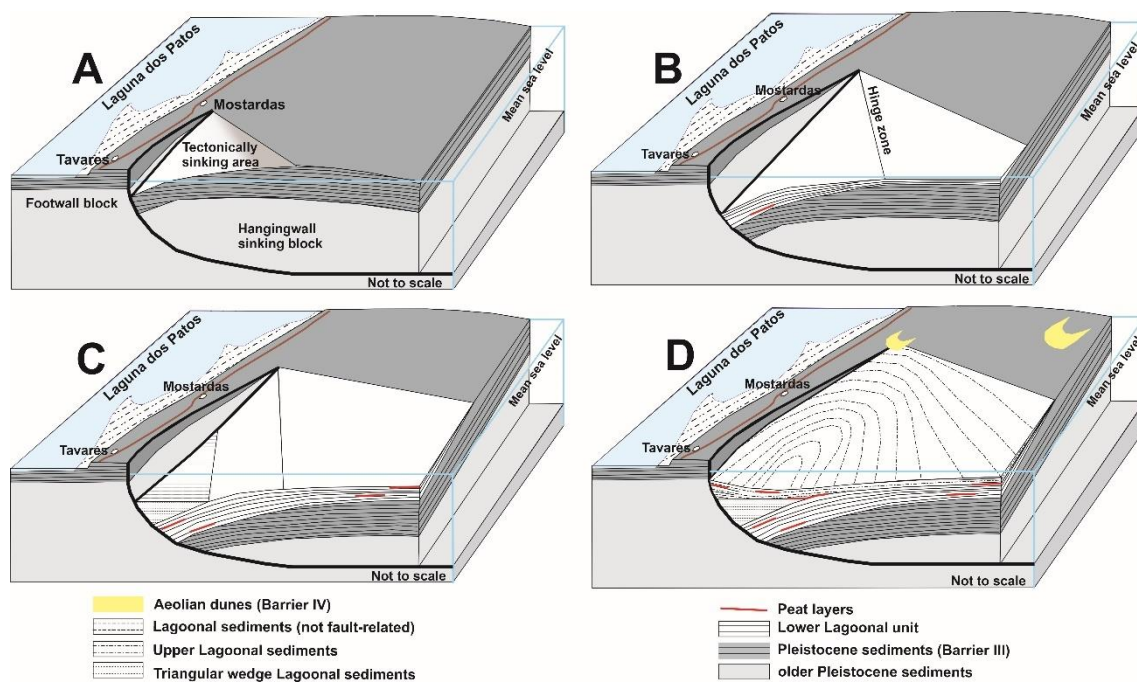


Figure 12 – Evolutionary model for Lagoa do Peixe Growth Fault and linked sedimentation. A) Growth fault initiation and propagation. B) Propagation of fault tip zone (northeastward is shown) and deposition of the lower lagoonal radarfacies. C) Additional fault propagation and sedimentation of the triangular wedge lagoonal radarfacies. D) Last stages of fault propagation and sedimentation of the upper lagoonal radarfacies.

The propagation of gravitational growth faults controls the local basin geometry and depocenter. The fault propagation rate controls mainly the sedimentary units' (radarfacies) geometry. The fault propagation, along its trend and dip, increases the area under tectonic subsidence, and then the local basin area for sedimentation. High fault propagation rates (outpacing sedimentation) develop an asymmetric basin and locate its depocenter close to fault. Low fault propagation displaces basin depocenter far away from fault and turns the basin geometry more symmetric. All these principles (derived from Prosser, 1993) apply to the Lagoa do Peixe Growth Fault and its local lagoonal basin (Figure 12A-D).

The first stage of fault displacement and sedimentation (Lower lagoonal radarfacies, **LP-f_{n+2}-pe**) seems to be initiated in the Lower Holocene (before 9400±140 Cal BP, Weschenfelder *et al.* 2008) in this area. Several organic-rich mud layers are to be expected during the first stage of this rapidly subsiding, low sedimentation rate tectonic basin (Figure 12B).

In the second stage (**LP-f_{n+3}-lag**), the fault displacement and sedimentation keep pace, and sedimentation is restricted to the local basin depocenter. This radarfacies does not crop out and was not drilled yet for direct investigation (Figure 12C). The triangle edges of this radarfacies decreases in sizes toward the northeast and southwest fault tip lines, giving rise to a wedge-like sedimentary unit clogging the hangingwall of a fault-bounded local basin.

The third lagoonal stage (Upper lagoonal radarfacies, **LP-f_{n+4}-lag**) is characterized by an eastward basin depocenter dislocation, due to sedimentation rates largely outpacing fault displacement (Figure 12D). During this stage, the

sedimentary influx comes from west (structural high = fault footwall) and east (local basin hinge zone). This upper lagoonal radarfacies also contains a number of peat layers, as recorded by Dillenburg *et al.* (2004): 1060 ± 70 , 350 ± 60 , and 380 ± 80 ^{14}C years BP. This observation is in accordance with this local basin geometry, as depicted in figure 12D.

The peat layer cropping out in the beach (Figure 7) ages 1060 ± 70 ^{14}C years BP. It overlays the lower lagoonal radarfacies (**LP-f_{n+2}-pe**), which aged ~ 3500 ^{14}C years BP (Dillenburg *et al.*, 2004). Then, there exists a ~ 2500 years timespan between both radarfacies. This timespan can accomplish sedimentation of the second, wedge-like radarfacies.

Recent aeolian dunes migration (toward the southwest) is the main process of Lagoa do Peixe clogging. Erosion of the footwall structural high is also contributing to a minor scale. However, these processes were not detailed here since they are best evaluated with high frequency GPR investigations.

CONCLUSION

These geological and GPR surveys show that Lagoa do Peixe is a fault-controlled lagoon. The Lagoa do Peixe Growth Fault is a gravitational listric fault established in the Rio Grande do Sul Coastal Plain (RGSCP). The fault displacement controlled different stages of sedimentation in the tectonically subsiding Lagoa do Peixe, and it actually is under a clogging process due to erosion of fault escarpment, and Holocene aeolian dunes migration (Barrier IV).

The Lagoa do Peixe Growth Fault shows that, at least in this area, the non-tectonic lagoon-barrier systems approach should be reviewed. Growth fault, gravitationally driven control on geometry and sedimentation in the RGSCP introduces new complexities to the lagoon-barrier approach. Structural highs, fault overlapping zones, transfer faults are all significant underlying features, as well as fault displacement and sedimentation rates.

This new investigation approach is being carried on other areas, in order to evaluate the extent the gravitational tectonic took in the RGS coastal plain. However, it is soon to extrapolate these results to others lagoon systems in the RGSCP. Despite the length and significance of the Lagoa do Peixe, it is close to Atlantic Ocean, while the other ones are located landward, and must be investigated using the same approach here discussed.

REFERENCES (CAPÍTULO 3)

Bauermann, S.G. 2003, Análises palinológicas e evolução paleovegetacional e paleoambiental das turfeiras de Barrocas e Águas Claras, Planície Costeira do Rio Grande do Sul, Brasil. Doutoral thesis, Universidade Federal do Rio Grande do Sul, Porto Alegre (Brazil).

Castillo, L.L.A., T.S. Kazmierczak, and F. Chemale. Jr., 2009, Rio Grande Cone tectono-stratigraphic model - Brazil: seismic sequences: Earth Sciences Research Journal, **13(1)**: 42–53.

Chapman, R.E., 1983, Early Deformation of Sedimentary Basins Growth Structures; in R.E. Chapman, ed, Petroleum Geology, Developments in Petroleum Science Series, Elsevier Ed., **16**, pp. 23–40.

Christie, M., G.P. Tsoflias, D.F. Stockli, and R. Black, 2009, Assessing fault displacement and off-fault deformation in an extensional tectonic setting using 3-D ground-penetrating radar imaging: Journal of Applied Geophysics, **68**, 9–16.

Cooper, J.A.G., A.N. Green, R.P. Meireles, A.H.F. Klein, J. Souza, and E.E. Toldo, 2016, Sandy barrier overstepping and preservation linked to rapid sea level rise and geological setting: Marine Geology, **382**, 80–91.

Cooper, J.A.G., R. P. Meireles, A. N. Green, A.H.F. Klein, and E.E. Toldo, 2018, Late Quaternary stratigraphic evolution of the inner continental shelf in response to sea-level change, Santa Catarina, Brazil: Marine Geology, **397**, 1–14.

Dillenburg, S.R., L.J. Tomazelli, and E.G. Barboza, 2004, Barrier evolution and placer formation at Bujuru southern Brazil: Marine Geology, **203**, 43–56.

Fonseca, V.P., 2006, Estudos morfotectônicos aplicados à planície costeira do Rio Grande do Sul e adjacências: Doutoral thesis, Universidade Federal do Rio Grande do Sul.

Fontoura, B.S., A.J. Strieder, J.S. Behling, R.S. Wetzel, R.S.S. Duarte, T.C. Silva, P.R. Mendes, A.A.V. Nobrega, and L.J. Calliari, 2015, Structural control of HM placer deposits at RGS (Brazil) Coastal Plain using ground penetrating radar: 8th International Workshop on Advanced Ground Penetrating Radar (IWAGPR), IEEE, P0153.

Neal, A., 2004, Ground-penetrating radar and its use in sedimentology: principles, problems and progress: *Earth-Science Reviews*, **66**, 261–330.

Neal, A., and C.L. Roberts, 2001, Internal structure of a trough blowout, determined from migrated ground-penetrating radar profiles: *Sedimentology*, **48**, 791–810.

Nobes, D.C., H.M. Jol and B. Duffy, 2016, Geophysical imaging of disrupted coastal dune stratigraphy and possible mechanisms, Haast, South Westland, New Zealand: *New Zealand Journal of Geology and Geophysics*, **59(3)**, 426–435.

Prosser, S., 1993, Rift-related linked depositional systems and their seismic expression: Geological Society, London, Special Publications, **71**, 35–66.

Reiss, S., K.R. Reicherter, and C.D. Reuther, 2003, Visualization and characterization of active normal faults and associated sediments by high resolution GPR, *in* C.S. Bristow, and H.M. Joe, eds, *Ground Penetrating Radar in Sediments*: Geological Society, London, Special Publications, **211**, 247–255.

Santos, A.C.O., 2020, Tectônica Gravitacional no Cone do Rio Grande, Bacia de Pelotas (RS): Doctoral thesis, Universidade Federal do Rio Grande.

Strieder, A.J., B.S. Fontoura, J.S. Behling, R.S. Wetzel, R.S.S. Duarte, T.C. Silva, P.R. Mendes, A.A.V. Nobrega, L.F.H. Niencheski, and L.J. Calliari, 2015, Gravitational tectonics evidences at RGS (Brazil) Coastal Plain using Ground Penetrating radar: 8th International Workshop on Advanced Ground Penetrating Radar (IWAGPR), IEEE, P0151.

Tomazelli, L.J., S.R. Dillenburg, and J.A. Villwock, 2000, Late Quaternary geological history of Rio Grande do Sul coastal plain, southern Brazil: *Revista Brasileira de Geociências*, **30(3)**, 470–472.

Tomazelli, L.J., and J.A. Villwock, 1996, Quaternary geological evolution of Rio Grande do Sul coastal plain, southern Brazil: *Anais da Academia Brasileira Ciências*, **68(3)**, 373–382.

Villwock, J.A., 1972, *Contribuição à Geologia do Holoceno da Província Costeira do Rio Grande do Sul*: M.S. thesis, Universidade Federal do Rio Grande do Sul.

Villwock, J.A., L.J. Tomazelli, E.L. Loss, E.A. Dehnhardt, N.O. Horn Filho, F.A. Bachi, and B.A. Dehnhardt, 1986, Geology of the Rio Grande do Sul Coastal Province, *in* J. Rabassa, ed., *Quaternary of South America and Antarctic Peninsula*: A.A. Balkema, Rotterdam, **4**, 79–97.

Weschenfelder, J., S. Medeanic, I.C.S. Corrêa, and S. Aliotta, 2008, Holocene Paleoinlet of the Bojuru Region, Lagoa dos Patos, Southern Brazil: *Journal of Coastal Research*, **24**, 99–109.

Zhang, C., H. Wang, Y. Liao, Z. Lu, and J. Tang, 2016, Differential control of syndepositional faults on sequence stratigraphy and depositional systems during main rift I stage in the southeastern fault zone of Qingxi Sag, Jiuquan Basin, Northwestern China: *Journal of Petroleum Exploration and Production Technology*, **6**, 145–157.

CAPÍTULO 4

4. COMPROVANTE DE SUBMISSÃO DO ARTIGO 2:

02/10/2023, 09:31

Gmail - Thank you for submitting your manuscript, GEO-2023-0580, to GEOPHYSICS



Bruno Silva da Fontoura <fontoura.bs@gmail.com>

Thank you for submitting your manuscript, GEO-2023-0580, to GEOPHYSICS

Geophysics <onbehalfof@manuscriptcentral.com>

2 de outubro de 2023 às 09:11

Responder a: geopapers@seg.orgPara: adelirstrieder@outlook.com, adelirstrieder@gmail.comCc: CLee-Petricek@seg.org, fontoura.bs@gmail.com, adelirstrieder@outlook.com, adelirstrieder@gmail.com, iran.correa@ufrgs.br, paulomdes@gmail.com, afbruch@gmail.com, acirolini@gmail.com

02-Oct-2023

Re: GEO-2023-0580, "FAULT-CONTROLLED SUBSIDENCE AND BEACH RIDGES PROGRADATION IN QUINTA – CASSINO (RS) COASTAL PLAIN, BRAZIL", Fontoura, Bruno; Strieder, Adelir; Corrêa, Iran; Mendes, Paulo; Bruch, Alexandre; Cirolini, Angélica

Dear Dr. Adelir Strieder:

Thank you for submitting your manuscript listed above to GEOPHYSICS. Please refer to the manuscript number in all correspondence. Your paper is undergoing review.

Please note that the SEG Board approved author-fee changes for papers submitted on or after 1 February 2020. Learn more at <https://library.seg.org/GEO-page-charges>.

Please see <https://library.seg.org/GEO-process> for manuscript processing schedules. For manuscript status, please check your Author Center at <https://mc.manuscriptcentral.com/geophysics>.

If you have uploaded your paper to a preprint server, please check SEG's preprint policy to ensure your paper's compliance with this policy: <https://library.seg.org/preprints>.

If you experienced problems uploading your files, click the "Get help now" button in the upper right corner at <https://mc.manuscriptcentral.com/geophysics>. This link brings up a new window that contains instructions, answers to frequently asked questions, and a method to send a question to the ScholarOne Manuscripts support team. If necessary, contact Callie Lee-Petricek (geopapers@seg.org) at the SEG Business Office, but first you should contact the ScholarOne Manuscripts support team for assistance.

Kind regards,
Prof. Alison Malcolm
Editor-in-Chief, GEOPHYSICS

***ScholarOne Manuscripts is transitioning to a new platform. Please encourage your team to whitelist both amazon.com and manuscriptcentral.com to ensure receipt of future e-mails related to your paper's submission and review.

FAULT-CONTROLLED SUBSIDENCE AND BEACH RIDGES PROGRADATION IN QUINTA – CASSINO (RS) COASTAL PLAIN, BRAZIL

ABSTRACT

GPR investigations have been applied to investigate very near-surface stratification of sedimentary units in coastal plains and to define their depositional conditions. This paper presents, however, low-frequency GPR survey to investigate fault-related depositional systems at greater depths. The Quinta – Cassino area in the Rio Grande do Sul Coastal Plain (RGSCP, Brazil) shows a wide strandplain that is made up of very long, continuous, and linear geomorphic features (beach ridges). This strandplain extends for ~70 km southward. The beach ridges show low-angle truncations against the Quinta escarpment, and also truncations in the strandplain. The traditional approach points that RGSCP was developed by juxtaposition of four lagoons/barrier systems as consequence of sea level changes; no deformational structure is admitted to exist before. The low frequency GPR (50 MHz, RTA antenna) and geological surveys carried out in this area showed the existence of listric fault controlling the beach ridges in the escarpments and hanging-wall blocks. The radargrams could distinguish Pleistocene basement unit anticlockwise rotation, thickening of beach ridges radarfacies close to listric normal faults, and horst structures. These deformational features indicate that the extensional zone of a large-scale gravity-driven structure controlled the mechanical subsidence for the RGSCP Holocene sedimentation and its stratigraphic and geomorphic features. The results point to a new approach in dealing with RGSCP Holocene evolution.

INTRODUCTION

The Rio Grande do Sul Coastal Plain (RGSCP) is the emerged segment of the Pelotas Basin, the southernmost of Brazil's Atlantic basins. It is up to 100 km wide and extends for more than 600 km in NE direction. The RGSCP has been characterized by juxtaposition of deltaic alluvial plains and four

lagoons/barrier systems (Figure 1) developed as consequence of sea level changes from Middle Pleistocene to Holocene (Villwock *et al.*, 1986).

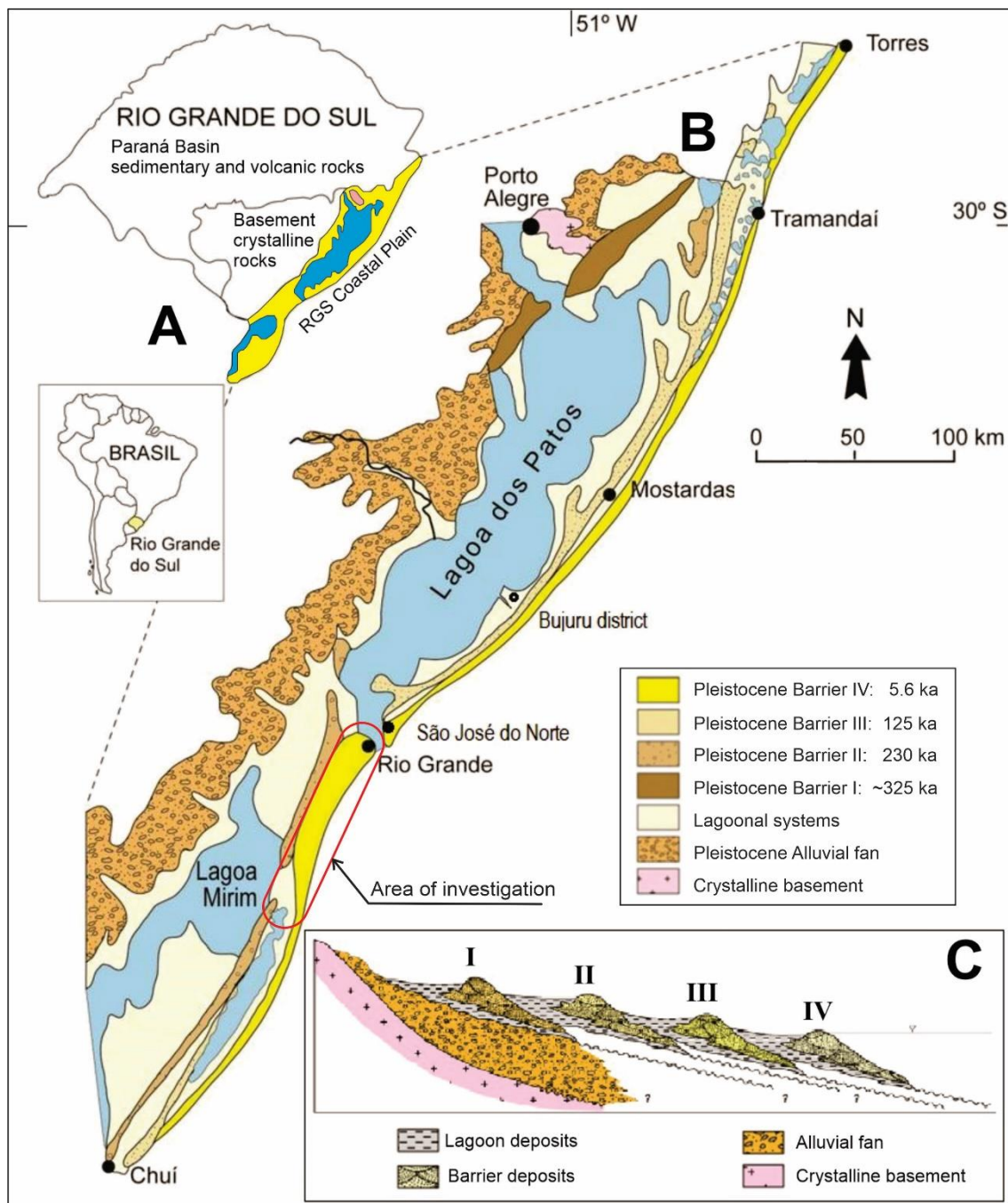


Figure 1 – Rio Grande do Sul Coastal Plain location (A), its regional geological map (B), and the model for its depositional systems (C). Modified from Tomazelli and Villwock (1996) and Tomazelli *et al.* (2000). The first lagoon/barrier systems: (I): 325 ka; (II) 230 ka; (III) 123-125 ka; and (IV) 5.6 ka MIS.

The RGSCP Holocene deposits (Barrier/Lagoon system IV) exhibit a much wider extent in the segment to the south of Rio Grande channel. It is dominated by an expressive half-fan series of linear features (beach ridges, Figure 2).



Figure 2 – Geology of the Quinta – Cassino area, located to the south of Rio Grande channel.

The wide strandplain developed to the south of the Rio Grande channel was first described by Godolphin (1985) and is limited to the west by an erosional cliff due to the Quinta Transgression (Pleistocene – Holocene transition). Godolphin (1985) proposed minor sea level oscillations during the Holocene regressive stage, to give rise a series of seven sets of coastal ridges (FR1: 6000 y.BP; to FR7: from 350 y.BP).

Long and Paim (1987) also distinguished seven sets of linear to curvilinear ridges (F1 to F7) based on truncation relationships and described the contact between Pleistocene and Holocene sediments as an erosional cliff. On the other hand, Long and Paim (1987) argued that F1 ridges series were developed by lower deposition energy conditions due to the widen of the Lagoa dos Patos estuary. The following ridges sets, arcuated to the ocean, were developed as a consequence of meandering and channeling changes under the influence of the Rio Grande channel outlet flow (Long and Paim, 1987).

Milana *et al.* (2016) produced a detailed map of individual ridges of the Holocene strandplain in the Quinta – Cassino area of the RGSCP, and distinguished at least 18 sets of coastal ridges, grouped into 5 stages. Milana *et al.* (2016), based on ridges lineaments truncation, ridges topographic altitude and ridges erosion evidence, suggested different conditions of longshore sediment transport, wind intensity and sediment supply in building the successive prograding coastal ridges sets.

Dillenburg *et al.* (2017), on the other hand, identified 6 sets of relict foredune ridges, whose limits between are distinguished by ridge truncations and the formation of transgressive dune sheets (TDS). According to Dillenburg *et al.* (2017), the Quinta – Cassino barrier progradation during Holocene was not uniform. The variable rates of progradation would be due to changes in sediment budget produced by environmental changes (changes in the wave climate, wind and precipitation). Dillenburg *et al.* (2017) argued that, at time of first foredune ridges set formation (6 ka), the sea level was still rising; and, that the following foredune ridges set were developed regressive sea level.

The previous investigations are based on sedimentary facies, depositional systems, chronostratigraphic techniques, and environmental conditions. No neotectonic deformational episode and no mechanical subsidence is considered for RGSCP sedimentary strata juxtaposition: “*the Pelotas Basin has remained oblivious to major tectonic movements, which translates into the symptomatic absence of faulting. If there were any, they resulted from aseismic processes in the sedimentary package that today constitutes the slope of the continental margin*” (Villwock 1972).

Fontoura *et al.* (2015) and Strieder *et al.* (2015), however, showed preliminary evidence of major faults in the RGSCP. Cooper *et al.* (2016, 2018) have also showed evidence for major deformation in the Santa Catarina Coastal Plain. And Fontoura *et al.* (submitted) presented a detailed GPR investigation to reveal a major growth fault at Lagoa do Peixe National Park.

The aim of this paper is to show that a large-scale fault controls mechanical subsidence and sedimentation of the prograding beach ridges in the Quinta – Cassino strandplain (RGSCP). 50 MHz RTA Ramac GPR surveys and field surveys were carried out in order to determine the regional structural framework developed by the Quinta Fault and its branches.

GEOPHYSICAL AND GEOLOGICAL SURVEY METHODS

The Pleistocene – Holocene contact in the Quinta area (RGSCP) has been characterized as an erosional cliff (Godolphin, 1985; Long and Paim, 1987). It is a low relief, gently arcuated (in plain view) escarpment that extend from Quinta (north) to Lagoa Mirim (south, Uruguay border). The Pleistocene sediments to the west of the escarpment are classified as Barrier II and III (Villwock *et al.*, 1986; Tomazelli and Villwock, 1996), and stand up into a low plateau, 10-15 m above the actual sea level.

Fonseca (2006) regarded this curvilinear geomorphic feature to a neotectonic structure (Mangueira Lineament). Based on this geomorphic feature, three areas were selected for geophysical and geological survey: i) Quinta

(southern), ii) Quitéria (central), and iii) Torotama (see Figure 2 for location). These selected areas were surveyed to geophysically investigate what kind of geological structure controls the escarpment.

The geophysical surveys were carried out through 50 MHz RTA Ramac equipment. This frequency was selected to investigate that structure as deep as possible (>20 m depth was attained with good resolution). The mean EM wave velocity was estimated to be 0.08 m/ns, so that vertical resolution is ~0.8 m. Then, the EM wavelength is not adequate small-scale structures of sedimentary units, but to their geometry and continuity.

Two parallel GPR lines were surveyed in Torotama and Quitéria areas, along gravel roads cutting across Pleistocene – Holocene escarpment. In the Quinta area, five parallel and oblique lines were surveyed, since no water filled depression is present and a better scanning for the fault geometry can be produced. Another three survey areas were defined to investigate the contact between the sets 1 and 2, and 1 and 3 (Figure 2), as defined by Godolphin (1985) and Long and Paim (1987). The GPR lines were surveyed perpendicular to high angle regarded to the Quinta escarpment, beach ridges and TD direction.

The GPR survey lines were all accompanied by DGPS (Emlid, Reach RS + model, base and rover receptors) control, with kinematic and post-processed corrections (Leica Geo Office and PPP-IBGE). The GPR line positioning procedure do permit a high horizontal (7 mm + 1 ppm), and vertical precisions (14 mm +1 ppm).

GEOLOGY OF THE SURVEYED AREAS

A geologic survey was carried out through aerial-photographs, high resolution Google images, and field work in the area under geophysical investigation, to investigate the main surficial sedimentary units over which GPR data were acquired. Such investigation helps to define the main geological features and contribute to discriminate them in radargrams. The aim was not to fully characterize each sedimentary unit in terms of their sedimentological

properties and inner structures, but to identify the sedimentary unit's organization (architecture) and the deformational structures.

The simplified geological maps images analysis and field work are presented in figures 3 to 5, and table 1 summarizes the main lithological features of each stratigraphic unit distinguished during the geological survey.

Table 1 – Summary of the main stratigraphic units cropping out in the selected areas for GPR surveying.

	Stratigraphic unit	Geological and lithological features
B A R R I E R I V	Lagoonal deposits	Fine-grained sands and silts interlayered with variable proportions of organic matter and clay being deposited close to Lagoa dos Patos.
	Dunefield Barrier	Transgressive Dune Sheets (TDS) and Transgressive Dunes (TD) developed by NE onshore winds.
	Alluvial fan	Fans of sand due to erosion by drainage cutting across the fault escarpment.
	Beach ridges	Narrow and very elongated sand ridges, intercalated with narrow depressions of mud and marsh, both parallel to shoreline
	Pleistocene Barrier III	Fine to medium-grained sands, mostly horizontal, parallel stratification, slightly compacted, and impregnated by Fe ³⁺ hydroxides and clay.

The Pleistocene Barrier III is the key stratigraphic unit for GPR surveys, and it crops out to the west of the Quinta escarpment (an erosional cliff, or a fault scarp?). Westward, the Pleistocene Barrier III is not fault bounded, but there exists an erosional terrace, that separates it from Barrier II. This both Pleistocene systems may be recognized by two erosional tiers (13-18 m, and 4-11 m) above mean sea level (Figure 2 and 5).

The Holocene Barrier (IV) is composed by different sedimentary deposits, as recognized in fieldwork (Table 1). These sedimentary deposits are named due to their geometric, descriptive features, and crosscutting relationships, in order to distinguish them in the geophysical sections.

The Beach ridges makes up a strandplain that is wider in the Rio Grande channel (north), and narrows toward the south. These beach ridges are linear to curvilinear features and can be continuously followed by more than 20 km. The ridges and the depressions are 70 to 300 m wide. The ridge-depression couples show truncations that make possible to distinguish at least 8 major sets (Figures 2 and 3); the truncation trace is also a curvilinear feature that can be followed by more than 100 km. Sets 1 to 7 are those initially proposed by Godolphin (1985) and Long and Paim (1987), while set 8 is interpreted in the northeastern segment, close to marine Rio Grande port dike.

The aim of this paper is not to investigate inner sedimentary structures or sedimentological features, but the fault geometry and the sedimentary unit's architecture in this large strandplain south to Rio Grande channel. In this way, the main nomenclature and definitions take the descriptive character based on Otvos (2012), who defined beach ridges as: "*Shore-parallel, narrow, elongated sand or gravel ridge formed by wave action near high tide-level on high-tidal beach berm surfaces, often directly underlain by intertidal sediments. Usually capped by a foredune ridge. Shore-parallel backshore dune ridges accumulated by wind over eolian sand sheet that may, in turn overlie prograded intertidal beach deposits also belong to this category*"; and strandplain as: "*Prograded beach ridge plain composed of locally truncated sets of broadly shore-parallel intertidal sand or gravel ridges, usually capped by dunes. Forms the surface in regressive barrier islands, barrier spits, and mainland barriers*".

Alluvial fans are distinguished at the base of the Quinta escarpment, related to incised drainage cutting across that scarp (Figure 3). They are composed by sandy material eroded from the structural high and deposited upon the beach ridges, since they interrupt the ridges in plan view. These features were reported by Godolphin (1985) and Milana *et al.* (2016).

The dunefield barrier is well developed in the shore zone, where a belt of climbing transgressive dunes (TD) overlay the beach ridges. Landward, the transgressive dune sheets (TDS) predominate, and TD are sometimes isolated and lower than those present in shore zone. It is interesting to note that thicker TDS are developed just west of the trace-line separating beach ridges sets (Figure 3). It is also interesting to observe that TDS bypass Quinta escarpment and give rise a narrow belt of TDS and some groups of TD. In both cases, TDS is seeing to migrate upslope.

The actual Lagoonal sediments in the northern segment of the area are deposited by Lagoa dos Patos. Figure 4 shows the Lagoonal sediments truncating the beach ridges. Southward, in the Taim National Park, TD and TDS sediments cover their lagoonal deposits.

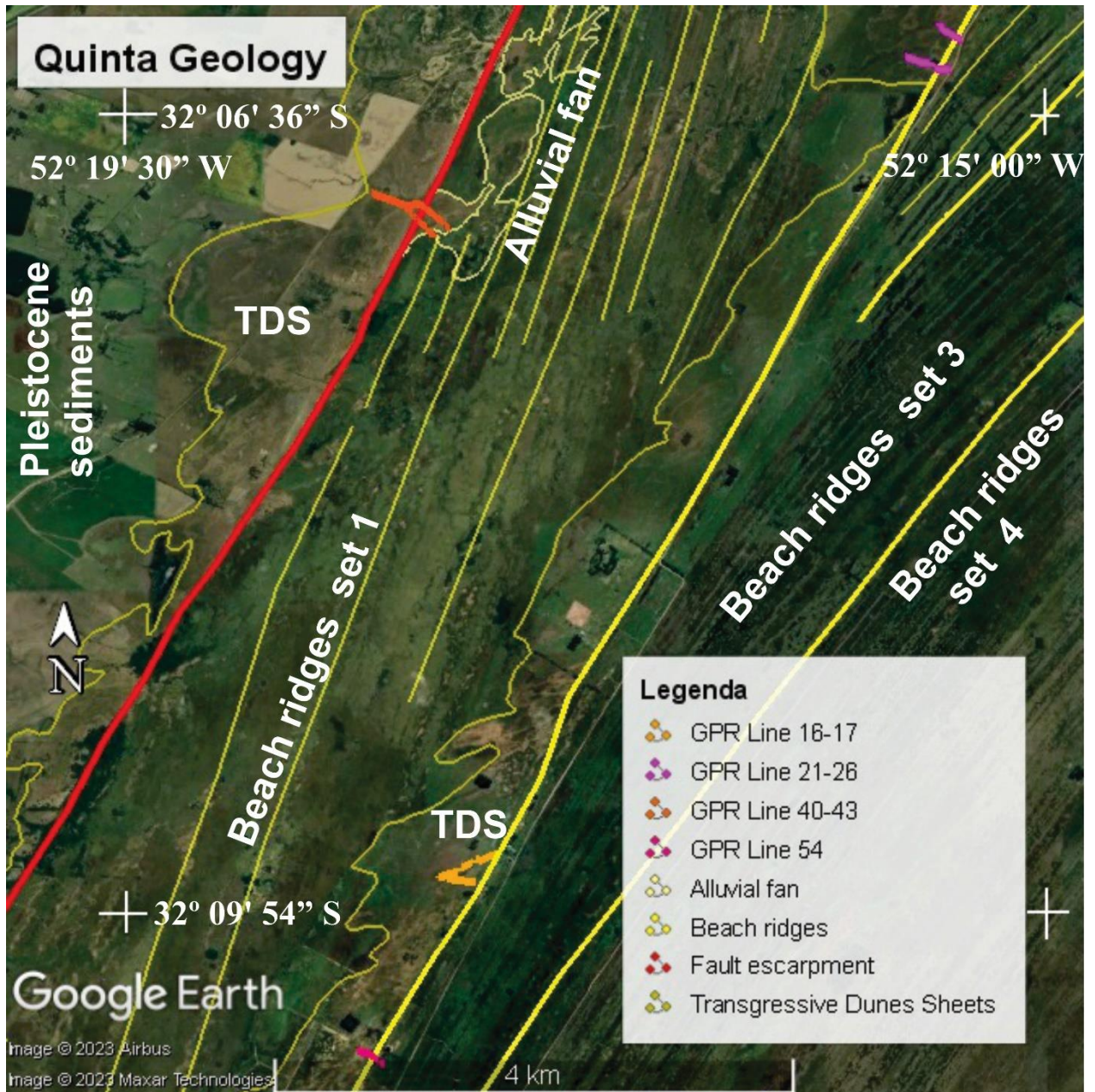


Figure 3 – Simplified geologic map of the Quinta area, showing the location of main GPR line surveys. Thick yellow lines separate the beach ridges sets.

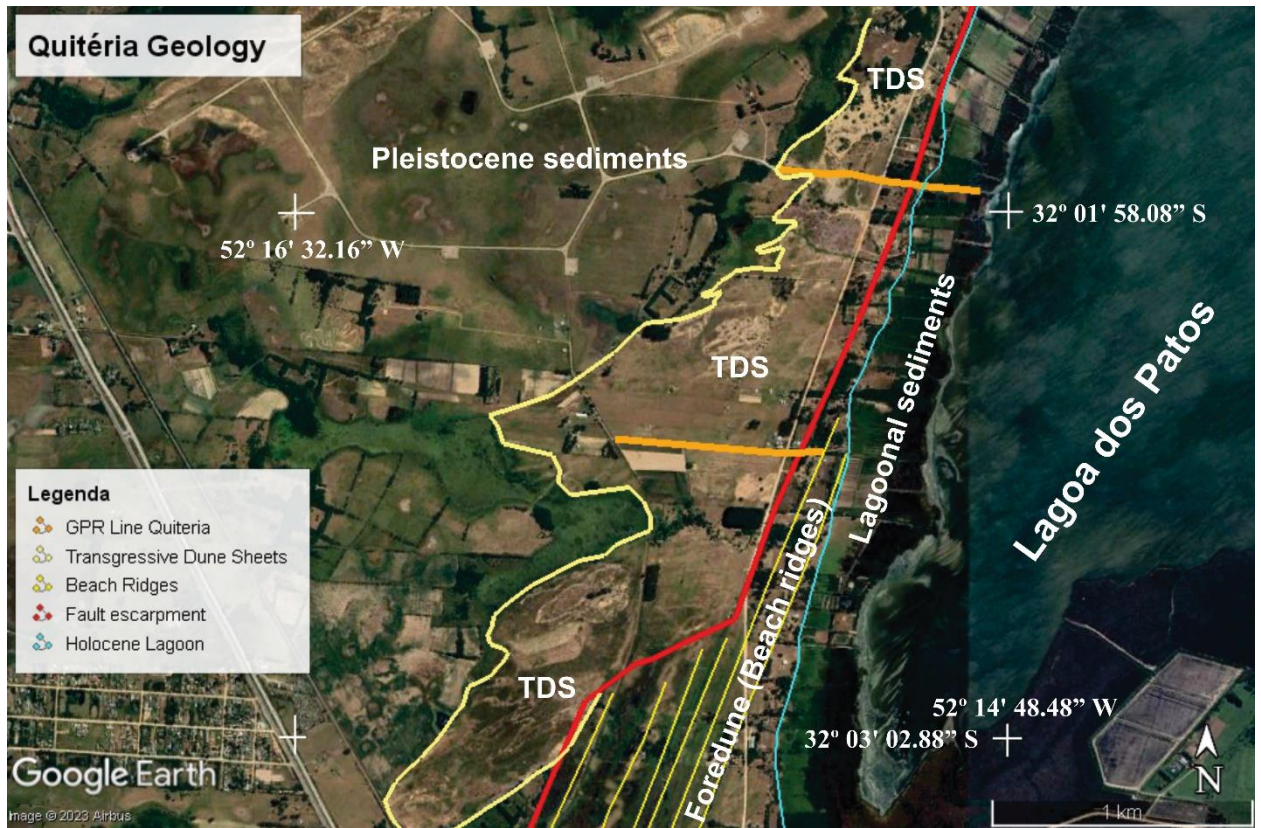


Figure 4 – Simplified geologic map of the Quitéria area, showing the location of main GPR line surveys.

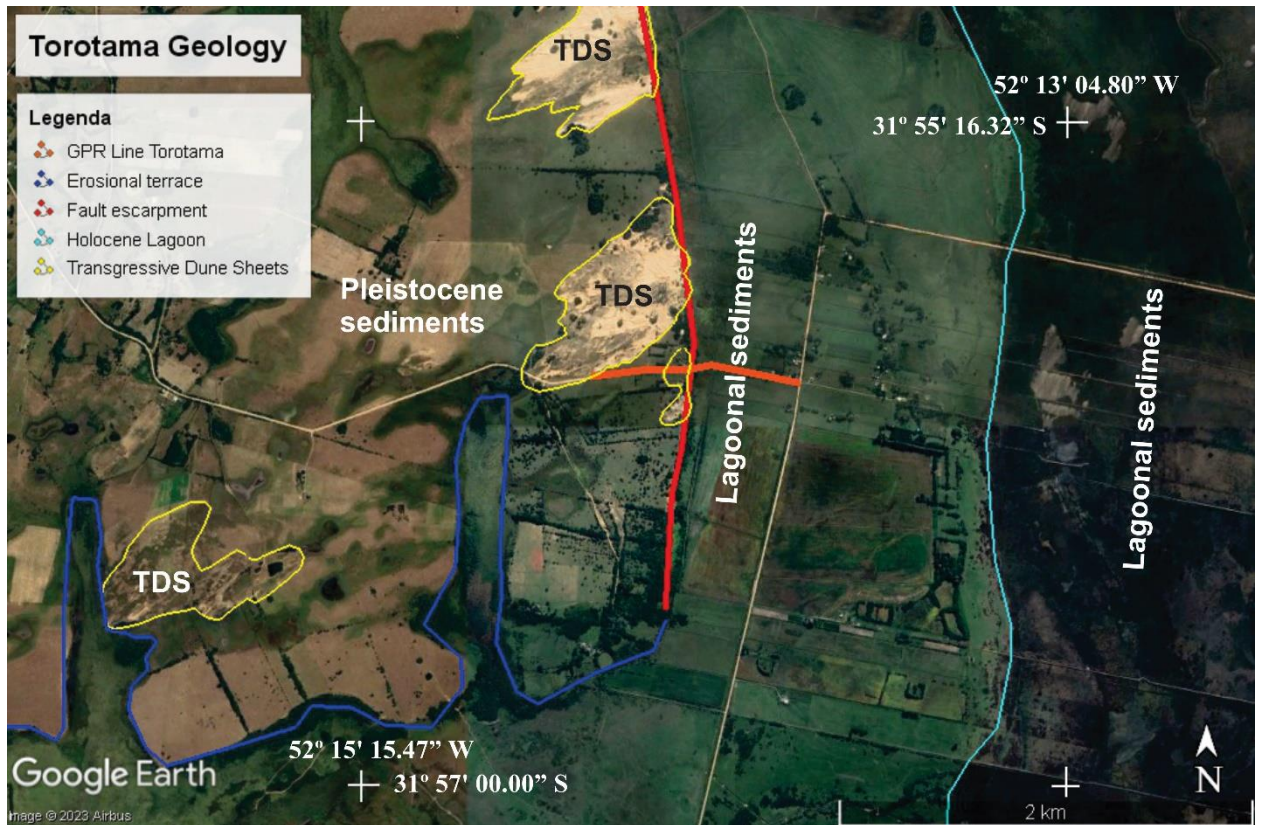


Figure 5 – Simplified geologic map of the Torotama area, showing the location of main GPR line surveys.

GEOPHYSICAL SURVEYS: FAULT GEOMETRY AND RADARFACIES

The radarfacies discrimination followed Neal (2004) proposal and Fontoura *et al.* (submitted) proposal for radarfacies boundary reflectors truncation geometries due to faults. The description of the identified radar surface boundaries (**s**) and radarfacies (**f**) follows the chronologic sequence proposed by Neal and Roberts (2001) and Neal (2004). Table 2 summarizes the radar surface boundaries and radarfacies distinguished in the Quinta – Cassino area.

Table 2 – Summary of radar surface boundaries (**s**) and radarfacies (**f**) distinguished for GPR survey lines in the Quinta – Cassino area and their interpretation (RS, Brazil).

Stage	Facies ID	DESCRIPTION	INTEPRETATION
-1	QC-f _{n-1} - pf	Radarfacies underlying the upper Pleistocene sediments, displays regular reflections which are truncated (<i>toplap-offlap</i>) in its upper boundary	Pre-fault radarfacies undergone hanging-wall collapse and erosion
1	QC-f _{n+1} - ps	Pleistocene sediments (poorly compacted) cropping out west of Quinta escarpment (Barrier III).	Pleistocene sediments cropping out at the footwall top west of fault escarpment (Barrier III). It also undergone hanging-wall collapse and erosion
	QC-s _{n+2} - et	<i>Offlap-toplap</i> for reflectors of the underlying lower Pleistocene sediments	An erosional surface developed on the top of footwall block and on down-throwing hangingwall
	QC-s _{n+1} - lf	Upward concave listric geometry surface that truncate Pleistocene sediments (west) and beach ridges radarfacies (east)	Listric normal fault. See also associated branching normal faults.
2	QC-f _{n+2} - br	Eastward gently dipping reflectors, some upper western arched crests, displaying <i>onlap</i> against normal faults and its subunits, and downlap on Pleistocene basement	Beach ridges stacks with different crest preservation degree
	QC-s _{n+3} - tl	Surface at the top of the beach ridges radarfacies, showing <i>toplap</i> for underlying reflectors	Irregular surface that is the unconformity overlying beach ridges radarfacies
3	QC-f _{n+3} - af	Horizontal and irregular reflectors in the hanging-wall close to listric surface	Alluvial fans: local sedimentary accumulation of sand due to drainage erosion from the structural high (fault footwall)
	QC-s _{n+4} - dl	Discrete <i>onlap-downlap</i> features upon previous radarfacies on Quinta	Surface defining the unconformity between overlying TD and TDS and

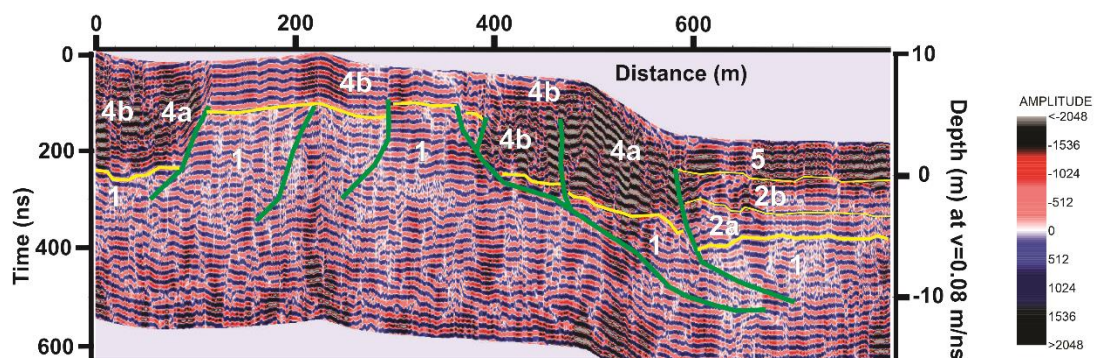
		escarpment, or horizontal irregular reflectors far from escarpment	the underlying beach ridges radarfacies
4	QC-f_{n+4}-tds	Horizontal and steeply dipping sigmoidal reflections, as also as thin horizontal reflection near the topographic surface	Transgressive dunes (TD) and thin dune sheets (TDS) overlying previous sedimentary radarfacies: 6a – steeply dipping reflections: lateral limbs of recent dunes; 6b – horizontal reflections: frontal dune strata, and thin wind covers
	QC-s_{n+5}-tl	Surface at the top of the beach ridges radarfacies, showing toplap for underlying reflectors	Unconformable irregular surface that limits the underlying beach ridges radarfacies
5	QC-f_{n+5}-lag	Horizontal well defined reflectors far from fault escarpment, showing discrete toplap for underlying radarfacies	Lagoonal sediments close to Lagoa dos Patos, showing some interfingering with aeolian TDS sediments
	QC-s_{n+n}-df	Minor truncation of inner reflections of radarfacies	Minor listric normal faults merging into master one, or diachronic synthetic and antithetic normal faults
Types of radarfacies (f)			Types of boundary surfaces (s)
ps = Pleistocene sediments pf = pre-fault units underlying the Pleistocene br = beach ridges af = alluvial fans lag = lagoonal sediments tds = transgressive dunes and dune sheets			lf = listric normal fault et = erosional truncation ol = onlap dl = downlap tl = toplap df = diachronic normal faults

Figures 6, 7 and 8 present radargrams for GPR lines which location is shown in figures 4, 3 and 5, respectively. Figure 6a shows that lateral (**QC-f_{n+4}-td**: 4a) and frontal (**QC-f_{n+4}-td**: 4b) radar signature for TD overlay a structural high (a horst) made off Pleistocene sediments (**QC-f_{n+1}-ps**) radarfacies. Figure 6

reveals upward concave boundary surfaces (**LP-s_{n+1}-lf**) that flatten in dip direction, which characterize a listric normal fault. They truncate lateral upper radarfacies, as also the lateral Pleistocene radarfacies. In the eastern end of the radargrams (Figures 6a,b), Pleistocene radarfacies are unconformably overlain by beach ridges radarfacies (**QC-f_{n+2}-br**).

The beach ridges radarfacies (**QC-f_{n+2}-br**) shows parallel eastward gently dipping reflectors overlapping the listric fault (**LP-s_{n+1}-lf**). It can be distinguished as a stack of different beach ridges subunits, which display downlap and toplap relationships with lower and upper geophysical units, respectively (Figure 6b). The western limit of beach ridges subunits may show arched reflectors (like an anticlinal), which are regarded to relict berm feature.

The beach ridges radarfacies are unconformably overlain by alluvial fan radarfacies (**QC-f_{n+3}-af**: Figure 7) and by lagoonal deposits radarfacies (**QC-f_{n+5}-lag**: Figures 6, 8) close to Lagoa dos Patos. The reflectors of these both upper radarfacies seem to be conformably overlaying beach ridges mainly far from the fault scarp, but this appears to result from resolution of the low frequency antenna. In fact, figures 3 and 4 clearly show that these upper radarfacies are unconformably overlaying beach ridges.



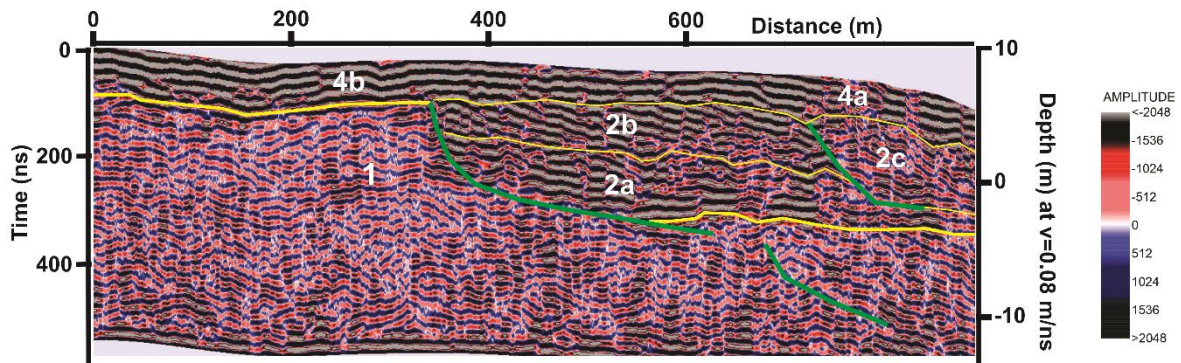
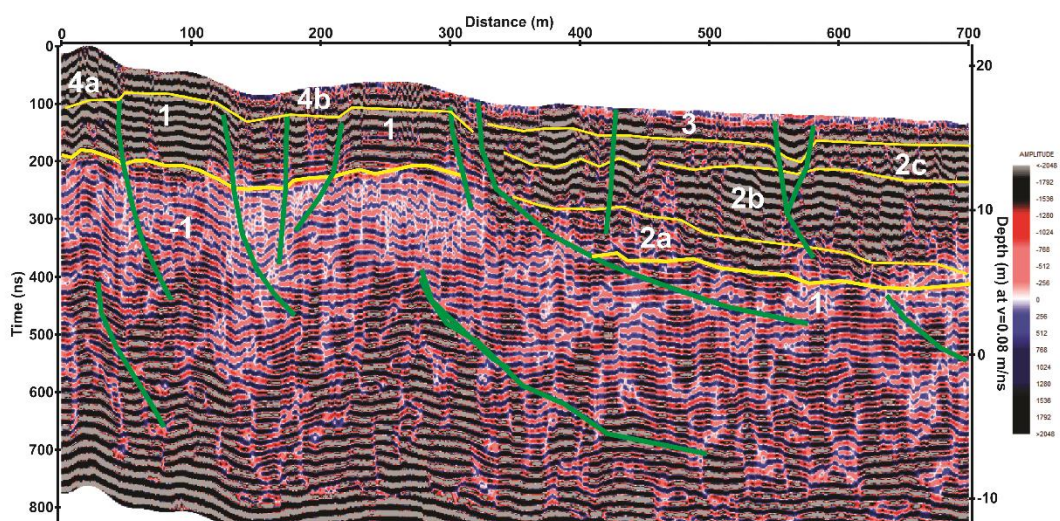


Figure 6 – Radargrams for GPR survey lines in the Quitéria subarea (Quinta escarpment, Rio Grande Brazil). A) Quitéria 1 GPR line in the north (Line 1). B) Quitéria 2 GPR line in the south (Line 2). Radarfacies ID as in Tabel 2. Green lines: normal listric faults. Thick yellow lines: Pleistocene – Holocene boundary surface. Thin yellow lines: Holocene radarfacies surfaces.

The alluvial fan radarfacies (**QC-f_{n+3}-af**) is a thin sand sheet (1-2 m) due to Pleistocene footwall block erosion (Figure 7). But, actually, erosion is also on TDS climbing fault scarp and on footwall block summit. Consequently, it is hard to distinguish between alluvial fan reflectors (**QC-f_{n+3}-af**), TDS (**QC-f_{n+4}-td**), and lagoonal deposits (**QC-f_{n+5}-lag**), at their contact zone using 50 MHz GPR antenna (Figures 6, 7, 8). Interfingering is observed in thick deposits at fault scarp base.



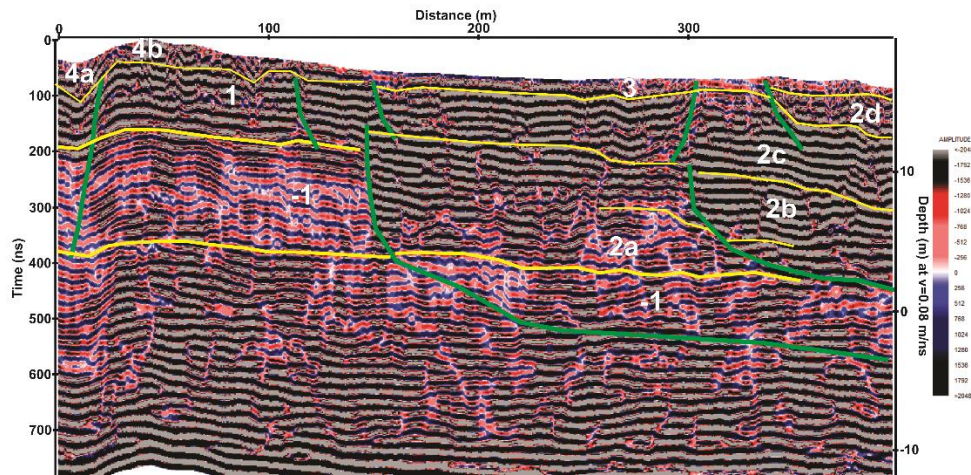


Figure 7 – Radargrams for GPR survey lines in the Quinta subarea (Quinta escarpment, Rio Grande Brazil). A) Quinta 40 GPR line in the north. B) Quinta 43 GPR line in the south. Legend as in Figure 6.

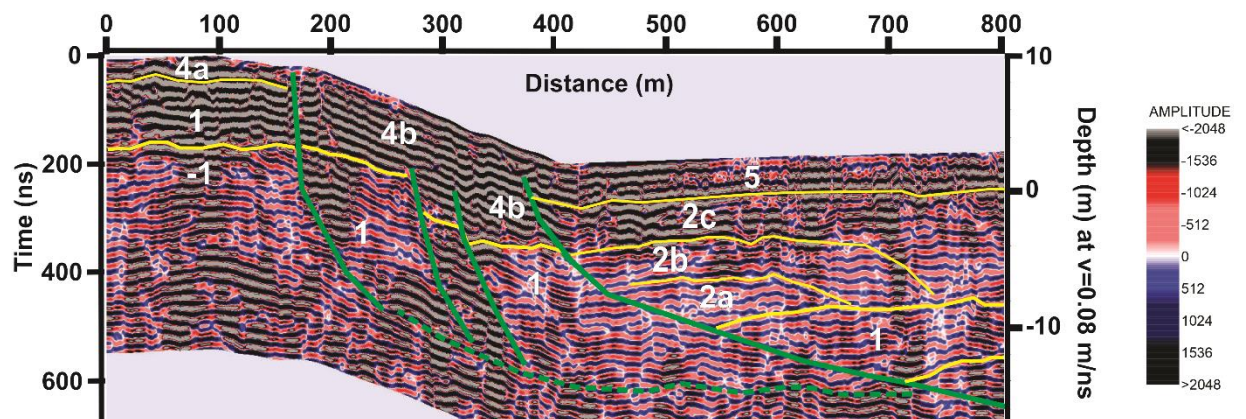
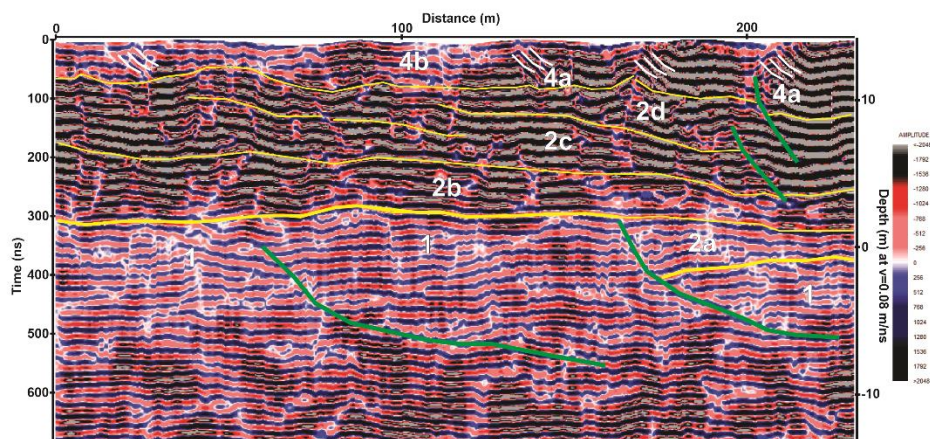


Figure 8 – Radargrams for GPR survey lines in the Torotama subarea (Quinta escarpment, Rio Grande Brazil). Legend as in Figure 6.

Figure 6, 7 and 8 show an upward inclination for Pleistocene reflectors (like a drag fold) or its gentle anticlockwise rotation in the hanging-wall blocks. These features suggest varying fault displacement rates and amount of displacement, block to block.

A second group of GPR lines was located to investigate the trace separating beach ridges 1, 2 and 3, since they merge toward the south (see Figure 3). Figures 9 and 10 show the stacking subunits of gently dipping foreshore reflectors of the beach ridges radarfacies (**QC-f_{n+2}-br**). The beach ridges radarfacies subunits can be distinguished by onlap features at their base. In some cases, the upper arched berm reflectors can be observed to climb the lower subunit, which displays a toplap feature suggesting erosion (Figure 11). This upper arched berm reflectors is similar to well preserved beach ridges GPR signature presented by Vespremeanu-Stroe *et al.* (2016).

The main normal fault influence is observed in the displacement of Pleistocene sedimentary unit, the basement for beach ridges sediments deposition. The hanging-wall of the lowermost beach ridges radarfacies (**QC-f_{n+2}-br**) subunit is thicker and correlates with a greater number of beach ridges subunits.



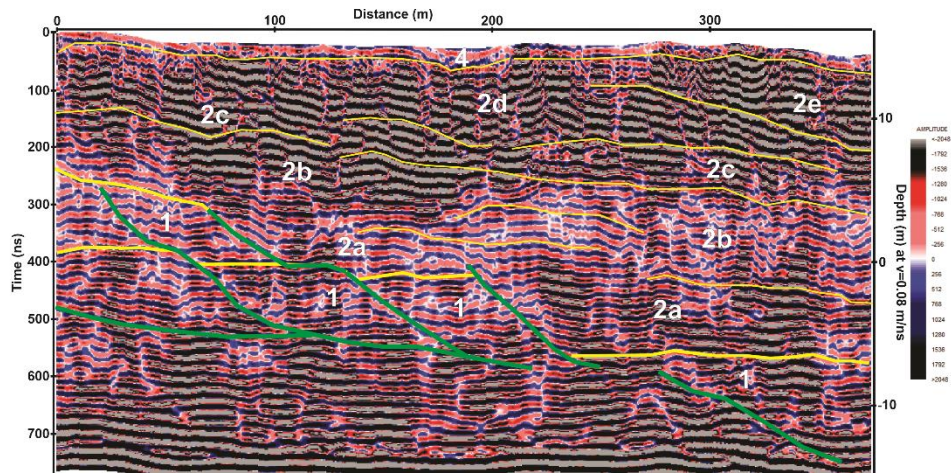
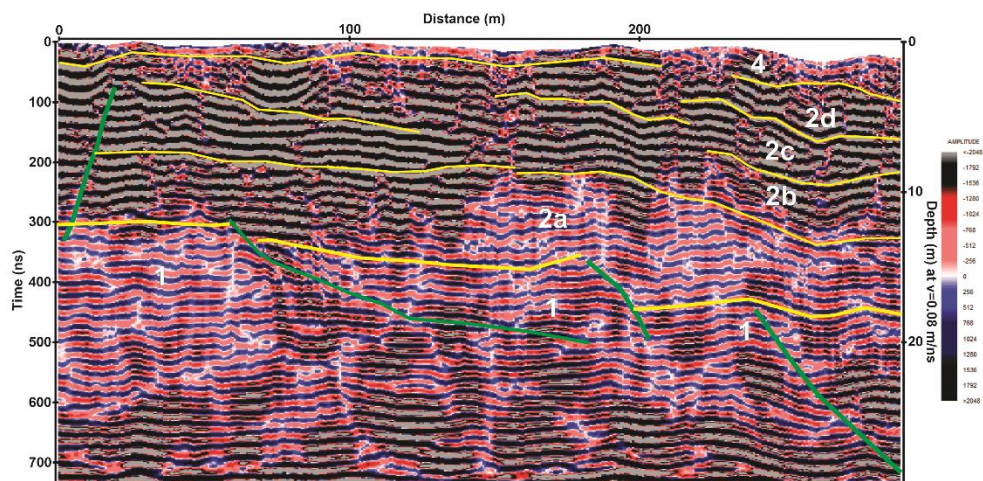


Figure 9 – Radargrams for GPR survey lines in the Quinta subarea (limit between BR1 and BR2, Rio Grande Brazil). A) Quinta 21 GPR line in the north. B) Quinta 26 GPR line in the south. Legend as in Figure 6.



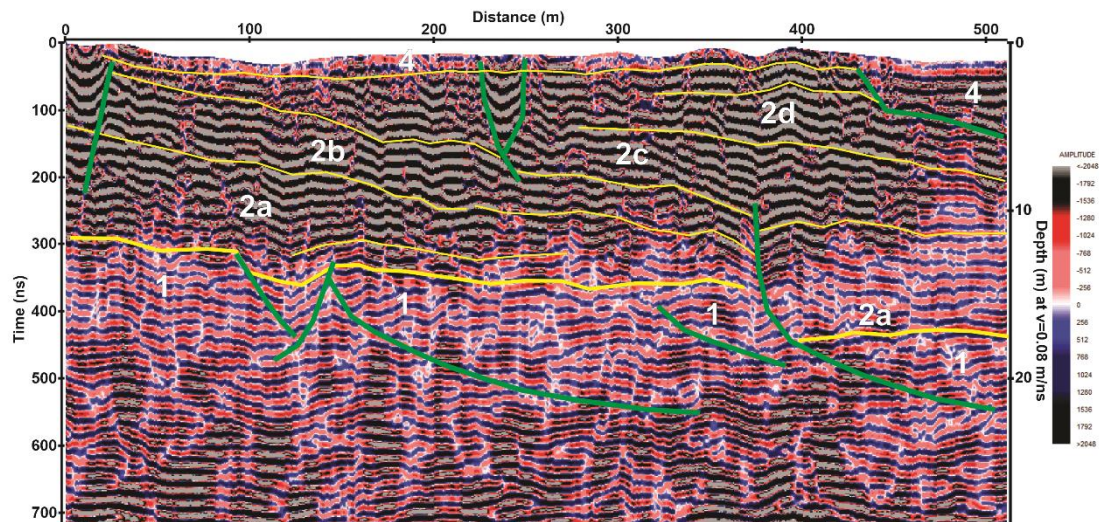


Figure 10 – Radargrams for GPR survey lines in the Quinta subarea (limit between BR1, BR2 and BR2, Rio Grande Brazil). A) Quinta 21 GPR line in the north. B) Quinta 26 GPR line in the south. Legend as in Figure 6.

Figure 11 (GPR Line 54) is located well to the south of the merging traces for BR1, BR2 and BR3 sets. It shows a horst structure similar to that shown in figure 6A (Quiteria 1 GPR line). The downlap feature at the base of the beach ridges radarfacies (**QC-f_{n+2}-br**) indicates its limit with Pleistocene basement.

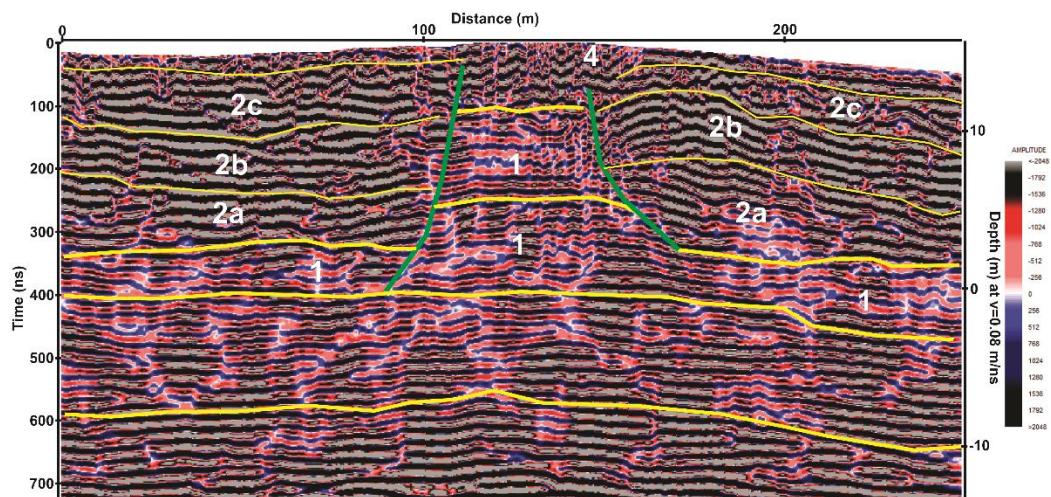


Figure 11 – Radargrams for GPR survey lines in the Quinta subarea (GPR Line 54: limit between BR1 and BR3, Rio Grande Brazil). Legend as in Figure 6.

DISCUSSION ON EVOLUTION OF THE QUINTA – CASSINO STRANDPLAIN

The Quinta erosional cliff (Godolphin, 1985; Long and Paim, 1987) is here shown to be a normal fault escarpment: the Quinta Listric Fault. It began its displacement ~ 7.5 ka, considering the deepest and oldest ^{14}C ages in the Holocene interval (Dillenburg *et al.*, 2017). The upper beach ridges estimated age (~ 6.0 ka: Godolphin, 1985; and Milana *et al.*, 2016) is in accordance with ^{14}C age in the Holocene interval (Dillenburg *et al.*, 2017) in sediments close to fault escarpment.

The Quinta Listric Fault is part of the gravitational tectonic supported by Pelotas Basin since Upper Miocene (Castillo *et al.*, 2009; Santos, 2020). Santos (2020) showed that Pelotas Basin gravitational tectonics started in the continental slope, and upper normal fault branches propagate westward into the platform. Fontoura *et al.* (submitted) analyzed and discussed the kinematic development of the Lagoa do Peixe Growth Fault to the north.

The radargrams presented above show that Quinta Listric Fault is a branching normal fault, displaying synthetic and antithetic faults. The horst structures and the Pleistocene basement rotation in the hanging-wall block were also observed. These indicate that space problem for displacing hanging-wall was accommodated through an imbricate fan of faults and lead to the development of horst and grabens in the mechanically subsiding area.

The superficial OSL ages are in agreement with the beach ridges progradation. Milana *et al.* (2016) sampled the actually exposed edge of the beach ridges (except for RG2). Dillenburg *et al.* (2017), on the other hand, sampled the edges of the TDS. Despite the difference in sampled sedimentary units, and the fact that TDS covers beach ridges, the OSL ages consistently decrease seaward. Additionally, it is to observe that these seaward younging TDS are mostly aligned upon the trace lines dividing beach ridges sets (see figures 3 and 4; Figure 2 of Milana *et al.*, 2016; Figure 9 of Dillenburg *et al.*, 2017).

These results indicate that each trace line separating beach ridges sets is a branching listric normal fault. From Quinta main fault scarp seaward, each

successive beach ridges set is the footwall for the next one. Despite the branching normal fault in the strandplain do not show the same topographic amplitude as Quinta fault escarpment, they are enough for sand blowing from beach to be deposited in the low relief scarps and on the footwall summit.

These results also account for beach ridges truncation along trace line separating sets in the north segment and in the southern segment. Gravity-driven listric normal faults are concave in section and plan view (see Figure 2 to view ridge set limits geometry). Gravity-driven listric normal faults produce blocks with distinctive displacements (and rates) and tilting, despite the overall movement in their extensional sector (Varnes, 1978; Jaboyedoff *et al.*, 2013).

The alternating ridge truncation at trace line separating each ridges set, despite some erosion can be claimed to occur, can be a major result of different displacement rates and amounts for the evolving branching faults. In such a gravity tectonic scenario, ridge truncation can not be attributed completely to coastal erosion as initially suggested by Godolphin (1985) and well detailed by Milana *et al.* (2016). The detailed mapping and numbering of beach ridges presented by Milana *et al.* (2016) and their truncation give support to interpret the fault branching sequence: the older (master) fault is the Quinta Listric Fault, and the younger one is close to the shore.

It is to be observed that these branching listric normal faults represent the extensional zone of a large-scale gravity-driven structure. Its compressional zone structures counterpart was developed in the Atlantic Continental Shelf, as has being reported by Reis *et al.* (2016) and Santos (2020).

CONCLUSION

The Quinta – Cassino strandplain was developed under the influence of an imbricated fan of gravitational listric fault, whose Pleistocene basement was cut by synthetic and antithetic faults. The faulted blocks display different rates and amounts of displacement and rotation.

Gravity tectonics, rather than sea level or climate changes, or longshore currents, is the major controlling mechanism for sedimentation and stratigraphic evolution of the Quinta – Cassino strandplain. This tectonic process does not suppress the operation of other important mechanism, such as: sea level and climate changes, longshore currents, erosion and deposition rates, sediment influx rates. But it controls them. For example: mechanical subsidence overcomes sea level changes; longshore current changes must be evaluated regarded to the differential fault blocks movements.

The Quinta Fault scarp represents the first tectonic barrier for beach ridges development as a closely attached geomorphic feature. The subsequent branching faults also show that beach ridges are closely attached to less expressive fault scarps. These aspects do not suppress, once more, the existence of minor fault-controlled lagoons. However, they were clogged yearly in the development of the Quinta – Cassino strandplain.

This new investigation approach is under development in other areas to evaluate the extent the gravitational tectonic took in the RGS coastal plain. It is clear that more geophysical survey is needed to have a complete scenario for the gravitational tectonic influencing the Holocene sedimentary and stratigraphic features of the RGSCP.

REFERENCES (CAPÍTULO 4)

Barboza, E. G., M. L. C. C. Rosa, S. R. Dillenburg, and, L. J. Tomazelli, 2013, Preservation potential of foredunes in the stratigraphic record: *Journal of Coastal Research*, 165, 1265–1270.

Castillo, L. L. A., T. S. Kazmierczak, and F. Chemale. Jr., 2009, Rio Grande Cone tectono-stratigraphic model - Brazil: seismic sequences: *Earth Sciences Research Journal*, 13(1), 42–53.

Cooper, J. A. G., A. N. Green, R. P. Meireles, A. H. F. Klein, J. Souza, and E. E. Toldo, 2016, Sandy barrier overstepping and preservation linked to rapid sea level rise and geological setting: *Marine Geology*, 382, 80–91.

Cooper, J. A. G., R. P. Meireles, A. N. Green, A. H. F. Klein, and E. E. Toldo, 2018, Late Quaternary stratigraphic evolution of the inner continental shelf in response to sea-level change, Santa Catarina, Brazil: *Marine Geology*, 397, 1–14.

Dillenburg, S. R., E. G. Barboza, M. L. C. C. Rosa, F. Caron, and A. Sawakuchi, 2017, The complex prograded Cassino barrier in southern Brazil: geological and morphological evolution and records of climatic, oceanographic and sea-level changes in the last 7-6 ka: *Marine Geology*, 390, 106–119.

Fonseca, V. P., 2006, Estudos morfotectônicos aplicados à planície costeira do Rio Grande do Sul e adjacências: Doctoral thesis, Universidade Federal do Rio Grande do Sul.

Fontoura, B. S., A. J. Strieder, J. S. Behling, R. S. Wetzel, R. S. S. Duarte, T. C. Silva, P. R. Mendes, A. A. V. Nobrega, and L. J. Calliari, 2015, Structural control of HM placer deposits at RGS (Brazil) Coastal Plain using ground penetrating radar: 8th International Workshop on Advanced Ground Penetrating Radar (IWAGPR), IEEE, P0153.

Godolphim, M. F., 1985, Paleogeografia da Região do Cassino no Município de Rio Grande, Brasil: *Pesquisas*, 17, 233–254.

Jaboyedoff, M., I. Penna, A. Pedrazzini, I. Baroñ, G. B. Crosta, 2013, An introductory review on gravitational-deformation induced structures, fabrics and modeling: *Tectonophysics*, 605, 1–12.

Long, T. and P. S. G. Paim, 1987, Modelo de evolução histórica e holocênica do estuário da Lagoa dos Patos: 2º Congresso da Associação Brasileira de Estudos do Quaternário, Porto Alegre, ABEQUA, 227–248.

Milana, J. P., C. C. F. Guedes, and V. V. Buso, 2016, The coastal ridge sequence at Rio Grande do Sul: A new geoarchive for past climate events of the Atlantic coast of southern Brazil since the mid Holocene: *Quaternary International*, 438, 187–199.

Neal, A., 2004, Ground-penetrating radar and its use in sedimentology: principles, problems and progress: *Earth-Science Reviews*, 66(3–4), 261–330.

Neal, A., and C. L. Roberts, 2001, Internal structure of a trough blowout, determined from migrated ground-penetrating radar profiles: *Sedimentology*, 48, 791–810.

Otvos, E. G., 2012, Coastal barriers – Nomenclature, processes, and classification issues: *Geomorphology*, 139–140, 39–52.

Reis, A. T., C. G. Silva, M. A. Gorini, R. Leão, N. Pinto, R. Perovano, M. V. M. Santos, J. V. Guerra, I.K. Jeck, and A. A. A.Tavares, 2016, The Chuí Megaslides Complex: Regional-Scale Submarine Landslides on the Southern Brazilian Margin. In: G. Lamarche, J. Mountjoy, S. Bull, T. Hubble, S. Krastel, E. Lane, A. Micallef, L. Moscardelli, C. Mueller, I. Pecher, and S. Woelz (Org.). *Advances in Natural and Technological Hazards Research*, 1ed. Springer International Publishing, 41, 115-123.

Santos, A. C. O., 2020, Tectônica Gravitacional no Cone do Rio Grande, Bacia de Pelotas (RS): Doutoral thesis, Universidade Federal do Rio Grande.

Strieder, A. J., B. S. Fontoura, J. S. Behling, R. S. Wetzel, R. S. S. Duarte, T. C. Silva, P. R. Mendes, A. A. V. Nobrega, L. F. H. Niencheski, and L. J. Calliari,

2015, Gravitational tectonics evidences at RGS (Brazil) Coastal Plain using Ground Penetrating radar: 8th International Workshop on Advanced Ground Penetrating Radar (IWAGPR), IEEE, P0151.

Tomazelli, L. J., S. R. Dillenburg, and J. A. Villwock, 2000, Late Quaternary geological history of Rio Grande do Sul coastal plain, southern Brazil: *Revista Brasileira de Geociências*, 30(3), 470–472.

Tomazelli, L. J., and J. A. Villwock, 1996, Quaternary geological evolution of Rio Grande do Sul coastal plain, southern Brazil: *Anais da Academia Brasileira Ciências*, 68(3), 373–382.

Varnes, D. J., 1978, Slope Movement Types and Processes. In: Schuster, R. L. and R. J. Krizek, Eds., *Landslides, Analysis and Control*, Transportation Research Board, Special Report, 176, National Academy of Sciences, 11–33.

Vespremeanu-Stroe, A., L. Preoteasa, F. Zăinescu, S. Rotaru, L. Croitoru, and A. Timar-Gabor, 2016, Formation of Danube delta beach ridge plains and signatures in morphology: *Quaternary International*, 415, 268–285.

Villwock, J. A., 1972, *Contribuição à Geologia do Holoceno da Província Costeira do Rio Grande do Sul*: M.S. thesis, Universidade Federal do Rio Grande do Sul.

Villwock, J. A., L. J. Tomazelli, E. L. Loss, E. A. Dehnhardt, N. O. Horn Filho, F. A. Bachi, and B. A. Dehnhardt, 1986, *Geology of the Rio Grande do Sul Coastal Province*.

CAPÍTULO 5

5. COMPROVANTE DE SUBMISSÃO DO ARTIGO 3:

22/09/2023, 14:50

Gmail - ORGEO-D-23-00621 - Confirming your submission to Ore Geology Reviews



Bruno Silva da Fontoura <fontoura.bs@gmail.com>

ORGEO-D-23-00621 - Confirming your submission to Ore Geology Reviews

1 mensagem

Ore Geology Reviews <em@editorialmanager.com>
 Responder a: Ore Geology Reviews <support@elsevier.com>
 Para: Bruno Silva da Fontoura <fontoura.bs@gmail.com>

21 de setembro de 2023 às 20:53

This is an automated message.

Structural Controls of the Coastal Bujuru and Retiro Heavy Minerals deposits in Southern Brazil

Dear Mr Silva da Fontoura,

We have received the above referenced manuscript you submitted to Ore Geology Reviews. It has been assigned the following manuscript number: ORGEO-D-23-00621.

To track the status of your manuscript, please log in as an author at <https://www.editorialmanager.com/orgeo/>, and navigate to the "Submissions Being Processed" folder.

Thank you for submitting your work to this journal.

Kind regards,
 Ore Geology Reviews

More information and support

You will find information relevant for you as an author on Elsevier's Author Hub: <https://www.elsevier.com/authors>

FAQ: How can I reset a forgotten password?
https://service.elsevier.com/app/answers/detail/a_id/28452/supporthub/publishing/kw/editorial+manager/

For further assistance, please visit our customer service site: <https://service.elsevier.com/app/home/supporthub/publishing/>. Here you can search for solutions on a range of topics, find answers to frequently asked questions, and learn more about Editorial Manager via interactive tutorials. You can also talk 24/7 to our customer support team by phone and 24/7 by live chat and email.

This journal uses the Elsevier Article Transfer Service. This means that if an editor feels your manuscript is more suitable for an alternative journal, then you might be asked to consider transferring the manuscript to such a journal. The recommendation might be provided by a Journal Editor, a dedicated Scientific Managing Editor, a tool assisted recommendation, or a combination. For more details see the journal guide for authors.

At Elsevier, we want to help all our authors to stay safe when publishing. Please be aware of fraudulent messages requesting money in return for the publication of your paper. If you are publishing open access with Elsevier, bear in mind that we will never request payment before the paper has been accepted. We have prepared some guidelines (<https://www.elsevier.com/connect/authors-update/seven-top-tips-on-stopping-apc-scams>) that you may find helpful, including a short video on Identifying fake acceptance letters (<https://www.youtube.com/watch?v=o5I8thD9XIE>). Please remember that you can contact Elsevier's Researcher Support team (<https://service.elsevier.com/app/home/supporthub/publishing/>) at any time if you have questions about your manuscript, and you can log into Editorial Manager to check the status of your manuscript (https://service.elsevier.com/app/answers/detail/a_id/29155/c/10530/supporthub/publishing/kw/status/).#AU_ORGEO#

To ensure this email reaches the intended recipient, please do not delete the above code

In compliance with data protection regulations, you may request that we remove your personal registration details at any time. (Remove my information/details). Please contact the publication office if you have any questions.

STRUCTURAL CONTROLS OF THE COASTAL BUJURU AND RETIRO HEAVY MINERALS DEPOSITS IN SOUTHERN BRAZIL

Bruno Fontoura ^{a,*}, Adelir J. Strieder ^b, Iran S. Correa ^a, Paulo R. Mendes ^c, Aureliano V. Nóbrega ^d

^a Instituto de Geociências, Universidade Federal do Rio Grande do Sul, Avenida Bento Gonçalves, 9500, Bairro Agronomia; 91501-970, Porto Alegre, Rio Grande do Sul, Brazil

^b Centro de Engenharias, Universidade Federal de Pelotas, Praça Domingos Rodrigues, 2, Bairro Centro; 96010-440, Pelotas, Rio Grande do Sul, Brazil

^c HIDROSERV Geophysical Surveys Ltd, Rua Tunísia, 193/401, Bairro Vila Ipiranga; 91370-290, Porto Alegre, Rio Grande do Sul, Brazil

^d Rio Grande Mineração S.A., Rua Borges de Medeiros, 168, Bairro Centro; 96225-000, São José do Norte, Rio Grande do Sul, Brazil

ABSTRACT

This paper brings new results for Bujuru and Retiro HM deposits, located in the Coastal Plain of the Rio Grande do Sul state (Brazil). Ground Penetrating Radar (GPR), drillholes and fieldworks were applied to investigate deformational structures in controlling Holocene sediment deposition and also the HM deposits accumulation. The Bujuru and Retiro HM deposits were developed in consequence to deformational traps. Mechanical subsidence, instead of sea level changes, is the main responsible for structural placers that lead to existing HM deposits. Based on fault displacement and sedimentation rates, it was possible to distinguish three stages of lagoonal deposition, and two main episodes of HM accumulation. The preliminary HM concentration episode is due to sediment reworking from Pleistocene footwall escarpment and from a Pleistocene

structural barrier developed in the hanging-wall oceanward (LFS 6). The second HM concentration episode is characterized by TDS and TD (LFS 5) developing upon a braquianticlinal build due to the progressive deformation of the hanging-wall that includes previous Holocene lagoonal radarfacies. The TDS and TD are a sedimentary barrier and migrates inland due to NE onshore winds, that also accumulate over the structurally controlled lagoons.

Key words: gravity-driven deformation, structural traps, HM placer deposits

INTRODUCTION

Detrital heavy mineral (HM) deposits are significant in several countries, such as Vietnam, Australia, United States and Brazil. Despite ilmenite is largely the most abundant mineral, some others may show a concentration such that it can make this type of ore deposits to be even more economic.

The HM placer deposits in coastal plains tend to have their evolution controlled by sea level changes; weathering, erosion, and reworking of sedimentary rocks and coastal sediments; sediment deposition from offshore to backshore; aeolian erosion and deposition in dunes ridges (e.g. Hou *et al.*, 2017; Nguyen *et al.*, 2018, Dill *et al.*, 2017,2018). In this way, HM deposits along southern Australia and southern Vietnam coast seem to display similar characteristics to Bujuru HM deposits in Rio Grande do Sul Coastal Plain (RGSCP, southern Brazil; Dillenburg *et al.*, 2004).

Along South America Atlantic Coast, there exist a number of HM occurrences hosted in Holocene beach sediments (e.g.: Aguiar Neto, 2015; França, 2013; Souza *et al.*, 2017; Tomazzolli *et al.*, 2007; Villwock *et al.*, 1979; Angelelli & Chaar, 1967; Cávana & Mykietiuik,1999; Isla, 1991; Dill *et al.*, 2017, 2018). However, only two of them showed mean HM concentration up to 4,5% to be mined: i) Guaju Mine in Mataraca (Paraíba state; Ferreira, 2006), and ii) Bujuru and Retiro areas (RGSCP, Munaro, 1994).

Most of studies are focused on transport and deposition of HM (Slingerland, 1977; Komar & Wang, 1984; Patyk-Kara, 2002; Lalomov, 2003) to build up an economic deposit (Roy, 1999; Hou *et al.*, 2017) on coastal plains. The recent advances investigate aeolian landforms that can develop aeolian mineral deposits (Dill & Buzatu, 2022a), and also summarized sedimentological parameters, mineralogical and chemical compositions for different landforms series to be used as a prospective proxy (Dill, 2022b).

The investigations on Brazilian Atlantic coast HM occurrences consider a scenario where coastal units are dynamically homogeneous, at least during upper Holocene (< 8,000 yr BP). However, recent investigations on central RGSCP revealed a large-scale growth fault controlling sedimentation in Bujuru District area (Fontoura *et al.*, submitted).

The aim of this paper is to present the deformational framework that controls the placing of Bujuru to Retiro HM deposits in the RGSCP during the Holocene. 50 MHz RTA Ramac GPR surveys, drillholes and field surveys were carried out to investigate the regional deep structures, as well as recent dunes barrier encompassing HM concentrations. GPR surveying in RGSCP are being conducted by some researchers (e.g. Barboza *et al.*, 2021; Dillenburg *et al.*, 2017), but they are focused on sedimentary features of upper strata, and do not search for deep deformational structures.

GEOLOGICAL SETTING

The Rio Grande do Sul Coastal Plain (RGSCP) is the emerged part of the Pelotas Basin, which started deposition in the Barremian/Aptian (125 Ma approximately), after Gondwana rupture. The coastal plain is up to 100 km in wide and >600 km long. The geomorphic and stratigraphic configuration of RGSCP were formed by deltaic alluvial plains and four lagoons/barrier systems in response to sea level changes between Middle Pleistocene and Holocene eras (Figure 1).

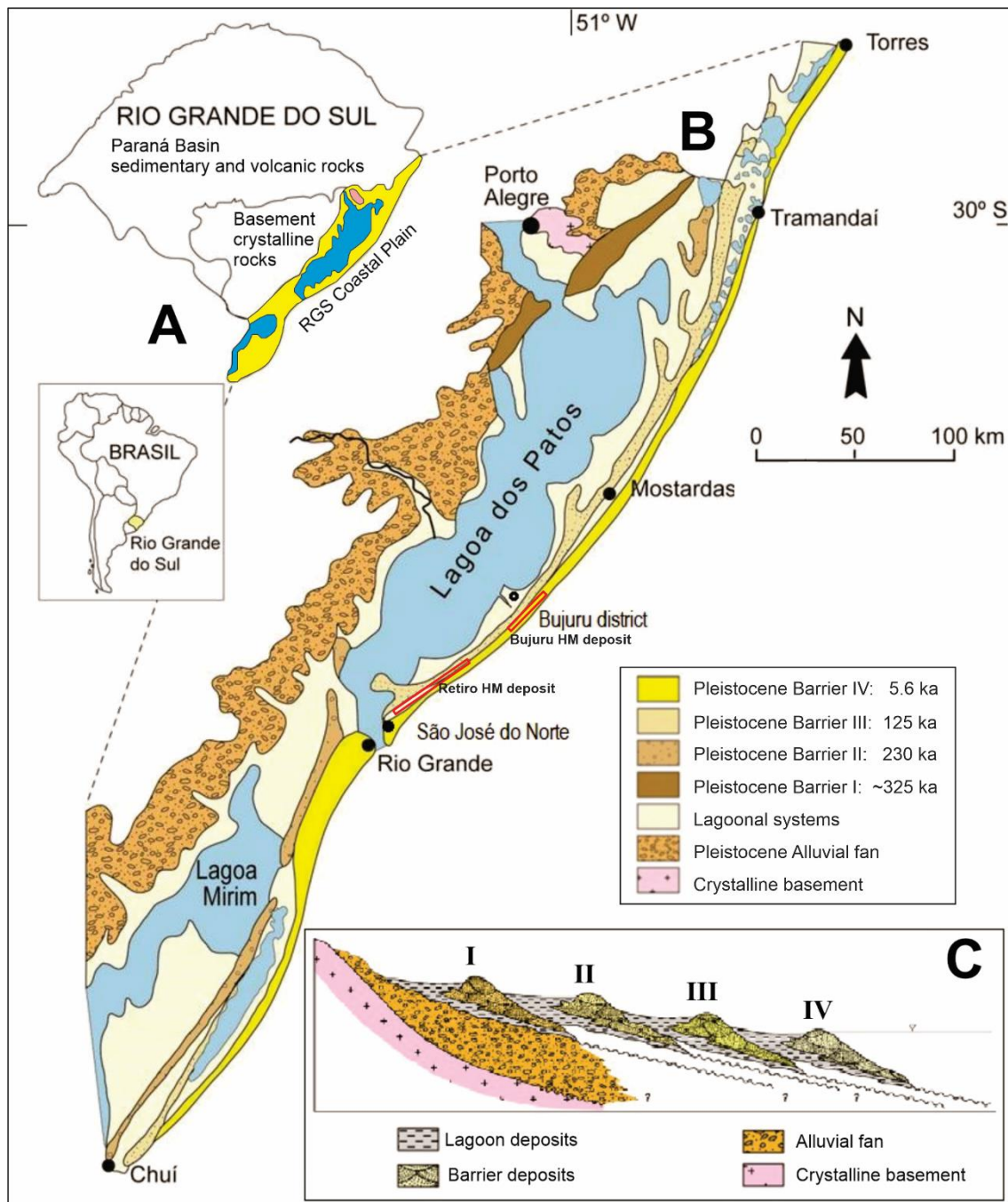


Figure 1 – Rio Grande do Sul Coastal Plain location (A), its regional geological map and HM deposits placement (B), and the model for its depositional systems (C). Modified from Tomazelli & Villwock (1996) and Tomazelli *et al.* (2000). Lagoon/Barrier system ages according to Rosa *et al.* (2017).

São José do Norte County (Brazil) presents two HM placer deposits, which is now under licensing for mining: i) Bujuru and ii) Retiro. Both make up the largest known deposit in Brazil, and display similar structural, sedimentological, mineralogical, and economic grade characteristics (Munaro, 1994; Dillenburg *et al.*, 2004; Takahashi & Hartmann, 2014).

According to Dillenburg *et al.* (2004), the Bujuru deposit is closely related to the sediments deposited by the old Camaquã River course, whose position at 125 ka was geographically close to the present deposit. The same heavy mineral content was identified in surface sediments from the adjacent shield (Tomazelli, 1978; Barros *et al.* 2008,2010).

Dillenburg *et al.* (2004) proposed a three steps scenario for Bujuru HM deposit formation. The first step incorporated HM into the beach and washover facies of a transgressive barrier during the Postglacial Marine Transgression (ends at 5.6 ka). The second step additionally concentrated HM in backshore deposits by eroding and recycling Pleistocene sediments during slow sea-level fall and Holocene barrier retreat. And, the third step eroded backshore deposits and HM were transported by onshore winds into an inter-barrier depression to give rise to transgressive dune deposits.

Fontoura *et al.* (submitted) investigations showed that the inter-barrier depression in the Bujuru area is, in fact, due to a large, gravity-driven listric growth fault, which controls the Lagoa do Peixe escarpment and hanging-wall sedimentation. Fontoura *et al.* (submitted) also showed that the balance of fault displacement and sedimentation rates established three main radarfacies (Figure 2). Table 1 summarizes the main findings related to the Lagoa do Peixe Growth Fault displacement and sedimentation.

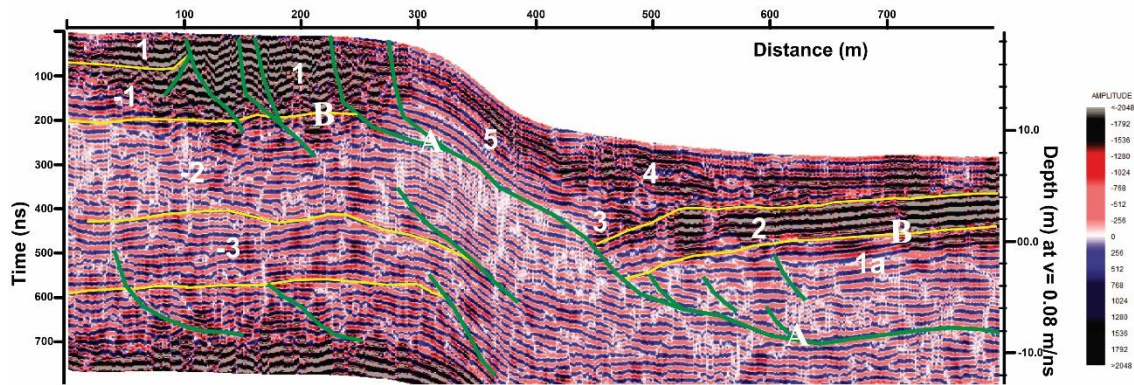


Figure 2 – Radargram in the Talhamar Road (Tavares, Brazil), cutting across Lagoa do Peixe Growth Fault (Tavares GPR line 2). See Table 1 for a description of the geophysical units and surfaces.

Table 1 – Summary of main radar radarfacies and surfaces distinguished for GPR survey lines in the Lagoa do Peixe and Bujuru HM deposit (RGSCP, Brazil). See Fontoura *et al.* (submitted) for a detailed description and analysis.

Radarfacies / Surface	DESCRIPTION
1	Pleistocene sediments cropping out at the footwall top west of fault escarpment (Barrier III)
A	Upward concave geometry surface that truncate Pleistocene sediments (west) and lower lagoonal unit (east): Listric gravitational growth fault.
B	<i>Offlap-toplap</i> for reflectors underlying lower lagoonal unit: an erosional surface developed on the down-throwing hanging-wall before fault controlled lagoonal accumulation
2	Convex upward arcuted lower lagoonal unit, displaying <i>onlap</i> for lowermost reflections in the thickest zones, close to listric surface, and parallel reflections for uppermost strata. The upper sediments of this radarfacies is aged 3.49 ka (Dillenburg <i>et al.</i> 2004)

	First stage: fault displacement rate higher than sedimentation rate
3	Horizontal reflections in a hanging-wall triangular area close to listric surface, showing <i>onlap</i> upon lower lagoonal unit and listric surface. Second stage: equalized fault displacement and sedimentation rates
4	Upward arcuated reflections at both Lagoa do Peixe margins, showing alternating <i>onlap-downlap</i> and <i>toplap-offlap</i> features. The peat layer cropping out at Bujuru District is aged 1.06 ka (Dillenburg <i>et al.</i> 2004) and is defined as the lowermost strata of this radarfacies. Third stage: sedimentation rate higher than fault displacement rate
5	Dipping sinuous reflections in the Lagoa do Peixe escarpment, showing discrete downlap with lagoon sediment reflections. Erosional degradation of the fault escarpment and deposition as interbedded layer of sands and lagoon sediments
C	Irregular surface underlying recent dune sediments. Surface upon which recent dune sediments are laid on with down lapping features (6a).
6	Horizontal and steeply dipping sigmoidal reflections (6a), as also as thin horizontal reflection (6b) near the topographic surface, produced by Holocene transgressive dunes and dune sheets.

GEOLOGICAL AND GEOPHYSICAL SURVEYING METHODS

Satellite images and aerial photographs were applied to investigate local and regional geological and sedimentary features. They enabled to recognize the fault escarpment to the northwest lagoon borders, and to delineate the Holocene transgressive dunes and dune sheets (TD and TDS) due to southwest direct onshore winds. They also enabled to identify the continuity of surficial sedimentary units during field works.

The GPR survey lines were acquired perpendicular to shoreline, to the fault escarpment and to TD direction (Figure 3).

The GPR surveys were produced mainly by a 50 MHz (RTA) antenna, and the acquired using Pro-EX GPR System (MALA-RAMAC). Acquisition parameters were set to high lateral resolution (20 cm trace spacing) and time window to investigate at least 20-23 m depth. The mean vertical resolution was determined through hyperbola analysis on radargrams. The first geophysical campaign used a minor time window, and the velocity was approximated to 0.09 m/ns (vertical resolution close to 0.9 m); the second campaign used a greater time window, and the mean velocity was approximated to 0.08 m/ns (vertical resolution close to 0.8 m).

The GPR survey lines were tracked by DGPS (Emlid, Reach RS+ model, base and rover receptors). The kinematic and post-processed corrections (PPP-IBGE and Leica Geo Office respectively) do permit a high horizontal (7mm + 1ppm) and vertical precisions (14mm +1 ppm) positioning.

Post-processing used Reflex-W software and included the following main steps: dewow filter; bandpass filter (butterworth, but sometimes trapezoidal); migration ($v = 0.297$ m/ns) for removing surface reflections in unshielded antenna; topographic correction; 3D topographic migration (e.g. $v = 0.08$ m/ns) and butterworth filtering.

Three percussion cores were drilled to correlate with GPR survey line (Bujuru01). This GPR survey line extend to the beach, and the drillholes were set in it to follow the peat layer cropping out the beach. Then, it was possible to determine the sand thickness covering the peat layer, and the stratigraphic features of the Pleistocene barrier (III) sediments.

STRUCTURAL AND GEOLOGIC CONTROLS OF HM DEPOSITS

Satellite images and aerial photographs interpretation and fieldworks did permit to distinguish between main geological features and structures. As pointed

out by Fontoura *et al.* (submitted), the northwest margin of the Lagoa do Peixe (lagoon) is controlled by a listric growth fault (Figure 2), whose displacement gave rise to mechanical subsidence for lagoonal sedimentation.

Bujuru HM deposit is located at the southwestern tip of the Lagoa do Peixe Growth Fault. The Bujuru area is also de tip zone for the Retiro – Estreito Fault (Figure 3), which controls the northwest margin of another almost clogged lagoon located to the southwest. This tip zone for both, Lagoa do Peixe and Retiro – Estreito faults (Figure 4A), is a structurally elevated area, where lower sedimentary units are exposed due to the rotation due to listric fault displacement.

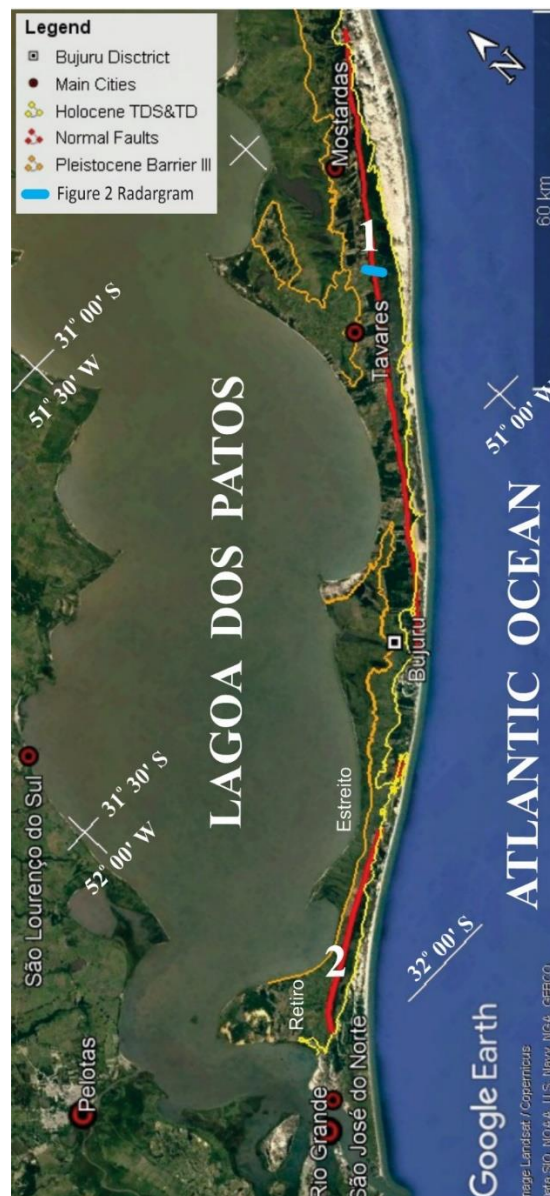


Figure 3 – Simplified geological map of the Retiro and Bujuru HM deposits area, showing the tip zone of the Lagoa do Peixe (1) and Retiro – Estreito (2) faults.

The Bujuru area tip zone is entirely covered by Holocene transgressive dunes (TD) and dune sheets (TDS), which extends well upon Pleistocene sediments (Barrier III). In this area, then, one can not exactly define the fault interactions and fault-controlled sedimentation.

Retiro HM deposit, on the other hand, extends from midway through the southwest tip of the Retiro – Estreito Fault (Figure 4B). The Holocene TD and TDS covers the fault tip zone close to São José do Norte city, so that it also can not be exactly followed.



Figure 4 – Simplified geological map for Bujuru (A) and Retiro (B) HM deposits. Lagoa do Peixe (1) and Retiro – Estreito (2) normal fault traces define the Northwest escarpment against Pleistocene sediments. **Legend GPR radargrams:** a) Figure 9 radargram; b) Figure 10 radargram; c) Figure 11 radargram.

The actual sedimentation process in the fault-controlled lagoons is taken place under very low fault displacement rate (Stage 3, Table 1). Figure 5 and 6 show the geomorphic expression of two sedimentary processes that are actually clogging both lagoons: i) erosion of previous stage lagoonal sediments in fore to backshore, and onshore wind transport (NE to SW) in the hinge zone of the rotating hanging-wall fault block (Figures 5A,C,D,E and 6A,B); ii) fault scarp erosion and gravity- and hydraulic-driven transport into de lagoon (Figures 5B,C and 6A).



Figure 5 – High resolution satellite images in the Lagoa do Peixe area from north (A) to south (E) showing the interplay of two clogging processes, from aeolian dunes construction (A), to gravity- and hydraulic-driven deposition (B), a combination of both (C), and the final fill of the lagoon by aeolian dunes (D,E).

The wind transport of fine-grained sands into the lagoon seems to create a blanket deposit, that when emersed acts as a base for transgressive dune movement (Figure 5A). In the central part of the Lagoa do Peixe (Talhamar road), where the total fault displacement is the highest (Figure 2) and the lagoon is wider, gravity- and hydraulic-driven fault scarp erosion built up small triangular deltas (Figure 5B) in their initial stages of development, and/or due to water level lowering (Feng *et al.*, 2019). Where fault scarp is not cut by drainage incisions, parallel sand bars are observed (Figure 5C). However, as Lagoa do Peixe Growth Fault tip zone is approached, aeolian TDS and TD covers entirely the lagoonal sediments deposited at the fault scarp base (Figure 5D) and also de fault (Figure 5E).

Along the Retiro – Estreito Fault (Figure 6), some of these sedimentary processes can also be observed. But, the TD and TDS covers almost completely the original lagoon. On the other hand, Retiro – Estreito Fault has half the Lagoa do Peixe Growth Fault trace length. Then, it is to be expected that vertical fault displacement should be proportionally lesser. In actual evaluation, it is observed a larger predominance of aeolian process upon this lagoon.

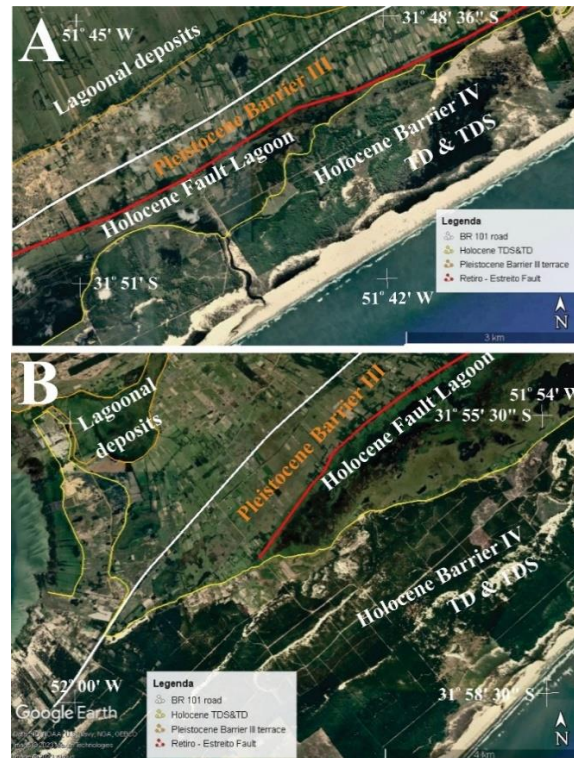


Figure 6 – High resolution satellite images in the Retiro (A) and Estreito (B) showing the predominance of aeolian dunes construction in these areas.

In the structural high developed at the tip zone for both Lagoa do Peixe and Retiro – Estreito faults (Figure 5E), the peat layer defining the base of the upper depositional radarfacies (1.06 ka, Figure 7A) is under wave erosion and dispersion along the beach. The TD and TDS covers discordantly the exposed peat layer (Figure 7B). These fragments are being covered by aeolian sediments and being incorporated into interdune layers (Figure 7C,D).

The base of dunes and interdune space are also the main locus for HM accumulation, where it displays and horizontal stratification (Figure 7E,F).

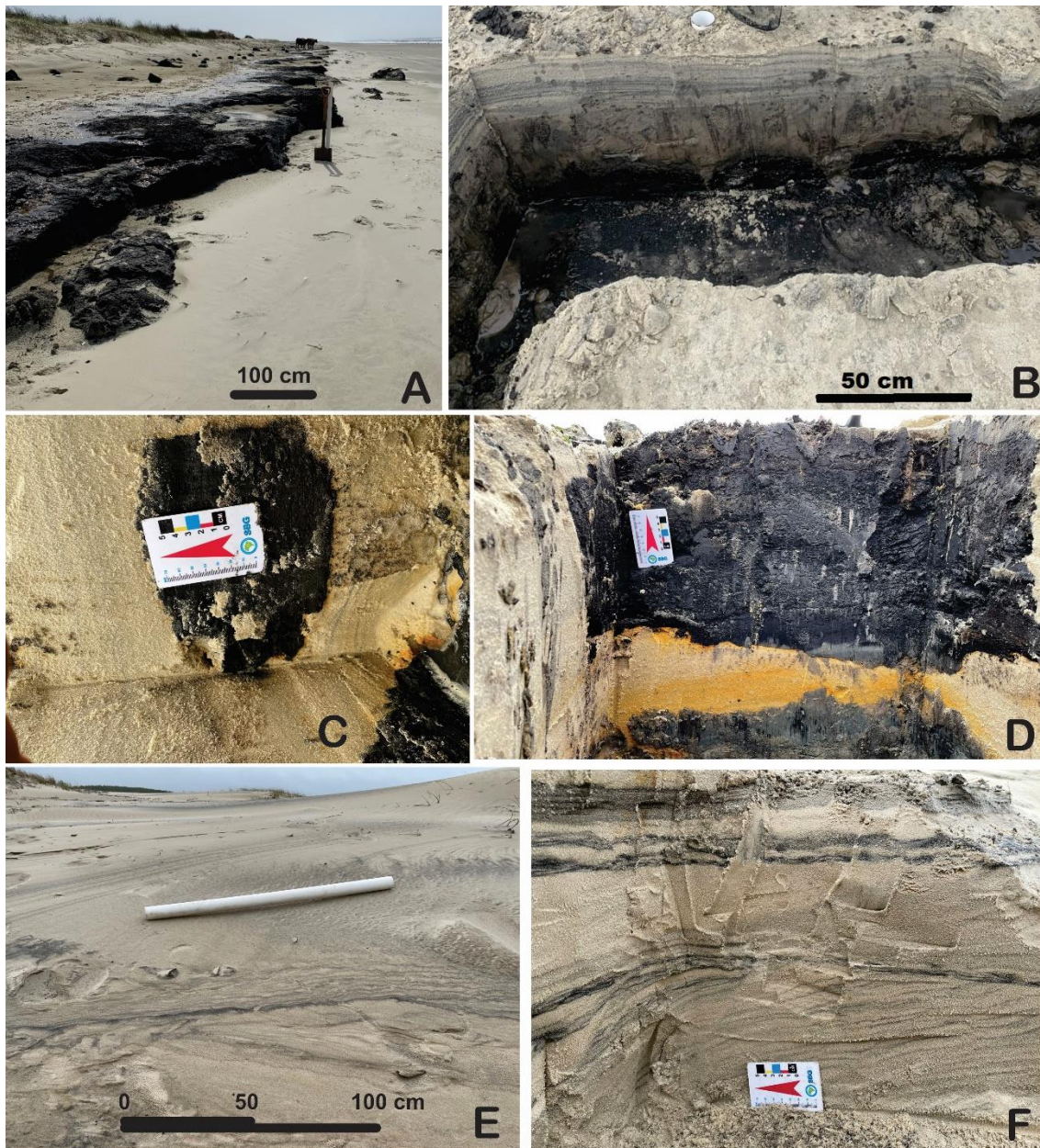


Figure 7 – Stratigraphic relationships between peat layer and TD hosting HM in the structural high at Bujuru District. A) Peat layer cropping out at Bujuru beach under erosional fragmentation. B) Undulated contact between peat and dune sediments. C) Vertical peat fragment identified in an excavated trench. D) Horizontal peat fragment in an excavated trench. E) Natural vertical cut of HM layering close to interdune area. F) Orthogonal trench cut showing HM lamination; note higher HM concentration in the horizontal layering.

GEOPHYSICAL STRUCTURES CONTROLLING HM DEPOSITS

GPR lines were surveyed in the NW-SE direction in order to investigate the NW dipping peat layer (Radarfacies 3) and the underlying lagoonal sediments (Radarfacies 1). This direction is also perpendicular to gravitational faults. Then, GPR surveying was conducted to emphasize the deformational structures and their relationships with TD deposition. In this direction, it is to be noted that TD stratification will appear as two different geophysical signatures: i) dipping sigmoidal reflections for the lateral segment (6a), and ii) thin horizontal reflection (6b) for the frontal segment (see Table 1).

The geological control of upper radarfacies was carried out based on surface geologic surveying and also based on three percussion drills located midway between GPR lines Bujuru-2 and PB-13 (a and b in Figure 4). The drillhole logs is presented in figure 8, and shows the Pleistocene sediments (radarfacies 1), the peat layer cropping out in Bujuru beach (base of the radarfacies 4), and Holocene TD and TDS (radarfacies 6a and 6b).

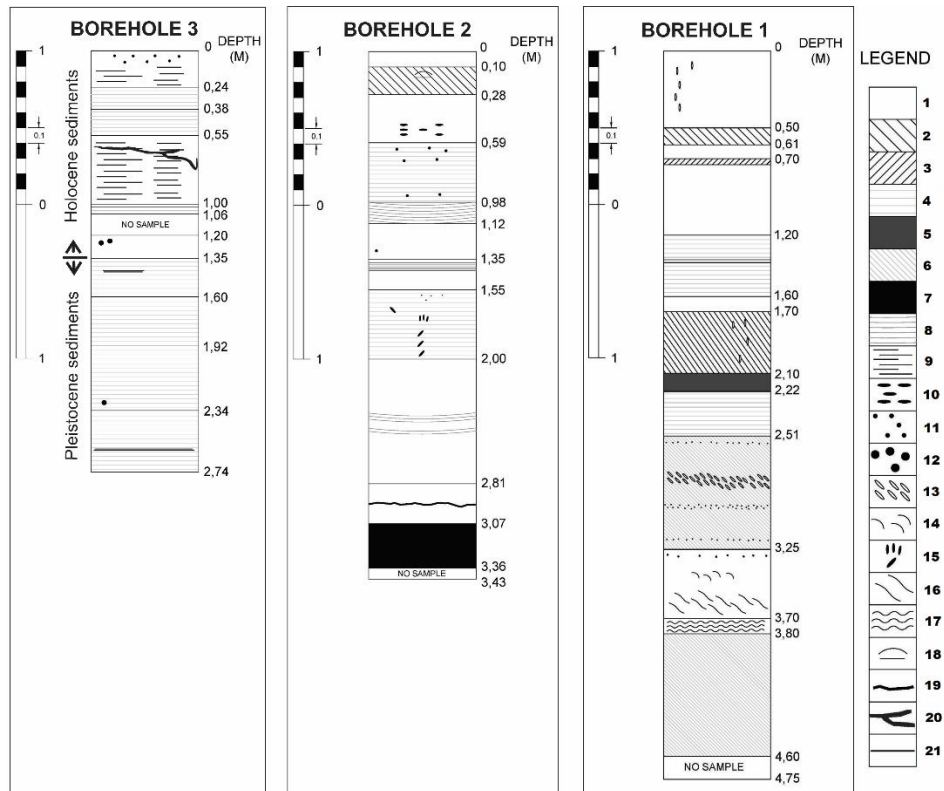


Figure 8 – Description of the percussion Drillholes Logs in the Bujuru area.

Borehole logs legend: 1) Light yellow sand; 2) Light yellow sand with coarse lamination (1-5 mm thick); 3) light yellow sand with gently inclined lamination (1-2 mm thick) and disseminated heavy minerals; 4) light yellow sand with thin horizontal lamination (1 mm) and disseminated heavy minerals; 5) Massive, dark gray sand with high quantity of heavy minerals; 6) Massive light yellow sand and disseminated heavy minerals; 7) Peat; 8) light yellow sand with gently arched lamination (1 mm); 9) isolated thin horizontal laminas of heavy minerals; 10) up to 2 cm recent root fragments; 11) small recent root fragments; 12) small disseminated shell fragments; 13) up to 1 cm shell fragments; 14) oxidized material; 15) oxidized (orange) dark gray sand; 16) heavy minerals concentration; 17) light yellow sand with fragmentary structure; 18) dispersed organic matter; 19) relicts of organic matter; 20) local breccia structure; 21) dark yellow sand lamination.

Figure 9 shows a radargram surveyed for deepest structural relationships in the Bujuru HM deposit area. It emphasizes the normal fault truncation of the Pleistocene units (1) and also the first (2) and third (4) lagoonal radarfacies. The transgressive nature of the Holocene dunes (6) can be recognized by their both lateral and frontal geophysical signatures.

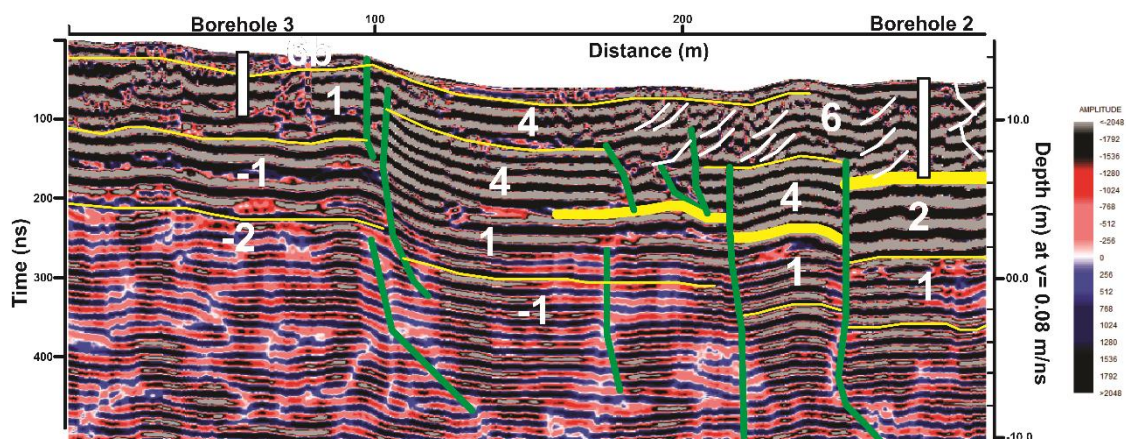


Figure 9 – Radargram depicting deep structural relationships in the Bujuru area. **Radargram legend:** i) white numbers: radarfacies as presented in Table 1; ii) green lines: normal faults; iii) thick yellow lines: ~1.0 m peat layer cropping out at Bujuru beach; thin yellow lines: geophysical units/radarfacies; white lines: lateral stratification of dunes (6a in Table 1). Boreholes position is projected into the radargram.

Two other GPR lines were selected to illustrate the deformational structures, and also the sedimentary relationships between each radarfacies. Such GPR lines were located close to Bujuru Project drillhole sections, to better correlate direct data with geophysical results (PB-01 and PB-13). In this way, a re-interpreted profile is presented with each of the radargrams.

Figure 10A shows the radargram close to PB-13 drillhole section, and is parallel and close to radargram present in Figure 9 (~500 m to the NE). The most striking geological feature is the presence of two normal faults dipping towards the SE. The peat layer overlying the first lagoonal radarfacies (2b) is interrupted in the hanging-wall block, as already noticed in figure 2.

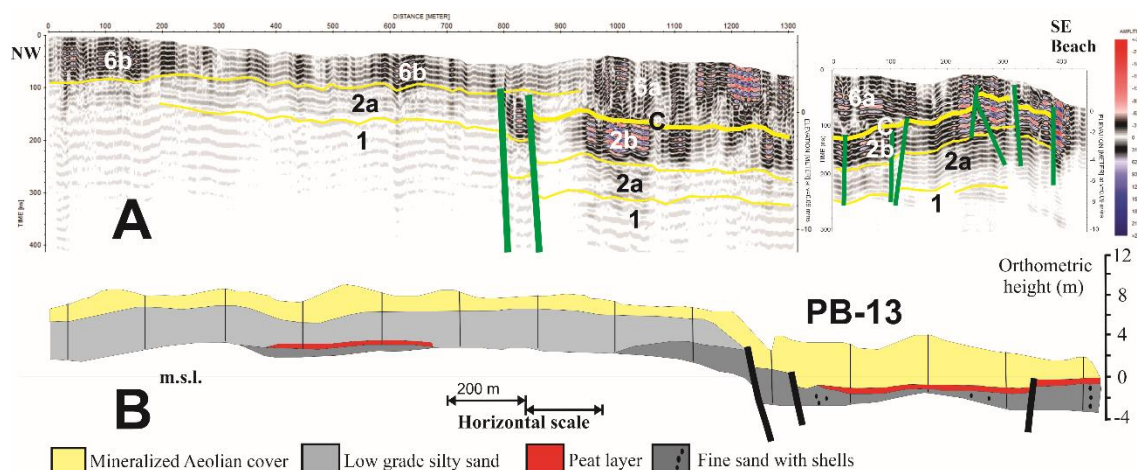


Figure 10 – PB-13 section structural features. **A)** Radargram close to **B)** PB-13 drillhole section. Drillhole section under permission of RGM S.A. Radargram legend as shown in Figure 9.

The first lagoonal radarfacies (2), then, is folded to a gentle sinclinal and an anticlinal in the hanging-wall block (Figure 10A), as a consequence of normal, listric faulting. It can be recognized that thickest TD is deposited in the sinclinal, where the lateral geophysical signature of TD (6a) shows its best down lap expression over the exposed peat layer (C). Fieldwork has also observed that gentle folds are, in fact, braquianticlinal and braquisynclinal, since their hinge zone dips NE and SW parallel to the master listric normal faults.

The PB-13 radargram (Figure 10A) also enable to distinguish two different first lagoonal radarfacies (2a and 2b) overlying the Pleistocene sediments (1). They correspond well to PB-13 Drillhole Section description (Figure 10B). The Drillhole Section can be re-interpreted based on radargram by including fault displacement of some key sedimentary strata.

Figure 11A is a radargram surveyed to the southwest (~11 km SW of PB-13), near to PB-01 Drillhole Section. It shows mainly the gentle anticlinal close to the beach, and the first half of the synclinal. PB-01 radargram presents quite the same radarfacies as described for Figure 10A. However, an additional radarfacies was distinguished: the third lagoonal one (4, as described in Table 1), onlapping the first lagoonal one (2). It is to be noticed that peat layer cropping out at Bujuru beach is one of the basal strata of the third lagoonal radarfacies (4).

Figure 11B shows the complete PB-01 Drillhole Section re-interpreted, now including normal listric faults displacing the key layers. The corresponding GPR line was placed some distance to the north due to access facilities and represents just the ~600 m of its southeastern segment. In any way, the correlation between radargram and drillhole section is quite good.

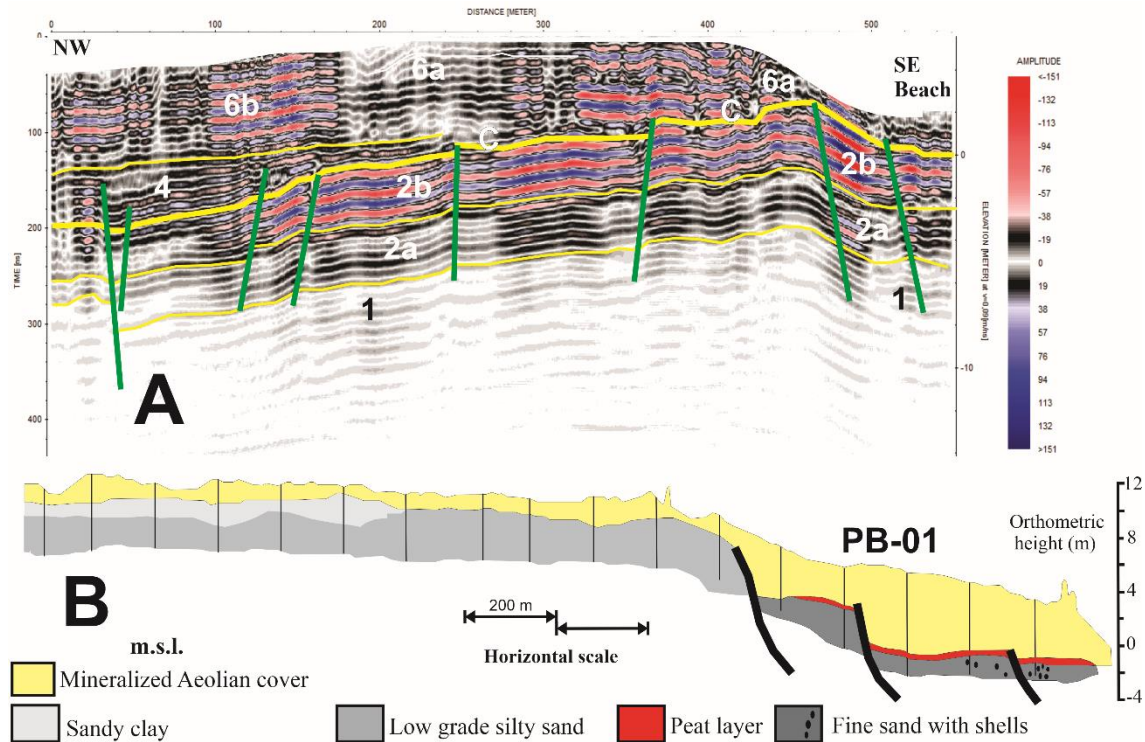


Figure 11 – PB-13 section structural features. **A)** Radargram close to **B)** PB-01 drillhole section. Drillhole section under permission of RGM S.A. Radargram legend as shown in Figure 9.

DISCUSSION

Deep GPR surveys in the Bujuru and Retiro HM deposits brought in evidence a series of deformational structures that were not yet described for the RGSCP: listric normal faults related to gravitational tectonic supported by the Pelotas Basin.

Radargrams presented in figures 2, 9, 10 and 11 show the main deformational structures controlling the erosional and depositional conditions supported by the RGSCP from the on. The onset of gravitational tectonics in the Bujuru District is estimated to be 9-8 ka taken the geological records for lagoonal sediments (see Weschenfelder *et al.*, 2008; Fontoura *et al.*, submitted).

The main listric normal faults related to gravitational tectonics promotes the hanging-wall block rotation and gentle folding of the stratigraphic units, as

also as minor interconnected faults, even synthetic or antithetic ones (Jaboyedoff *et al.*, 2013).

The Bujuru HM deposit is placed upon the tip zone of the Lagoa do Peixe and Retiro – Estreito faults (Figure 4). Radargrams in this area (Figures 10 and 11) show a gentle anticlinal close to the Bujuru beach, which gave rise to the hinge zone of the rotating hanging-wall block. That radargrams also show that the thickest Holocene mineralized TD and TDS are placed in the synclinal area. The Retiro HM deposit, on the other hand, is placed mainly upon the depocenter of the fault controlled Retiro Lagoon (hanging-wall), and upon the southwestern Pleistocene footwall bulkhead block.

The intersection of two master fault systems at Bujuru District area introduces additional structural complexity in erosion and sedimentary deposition of Holocene radarfacies. Additional investigation is being conducted in this area, since the deformational structures are covered by mineralized Holocene TD and TDS. The extent the down warping block open space for Holocene deposition and erosion of the Pleistocene sediments on the footwall and in the hanging-wall is still under concern. The presence of some different radarfacies shown in figures 9, 10 and 11 is a clear consequence of the diachronous development of regional master and local faults of each interconnecting system.

The HMs are still being transported by onshore winds and deposited in TD (Figure 7). It is interesting to observe, however, that HMs are present in the TD overlying exposed peat layer (base of the radarfacies 4) and de underlying radarfacies 2. From the northeastern tip zone of Lagoa do Peixe Growth Fault to southwestern exposed tip of the Retiro – Estreito Fault, it is noticed that TD and TDS have not HMs, or have very low HM concentration when peat layer is not still exposed due to folding and/or faulting along the beach.

The deformational structures along the fault direction seem to control not only the lagoonal sedimentation (radarfaceis 2 and 4, mainly), but also their erosion to give rise the economic HM deposits. The source for HMs transport by onshore winds and their deposits in Holocene TD is to be considered.

Dill & Buzatu (2022a) analyzed a series Quaternary aeolian landforms and the particular physical, chemical and sedimentological conditions that make possible the development of aeolian mineral deposits of economic grade. Dill (2022b) reviewed a number of aeolian landforms with emphasis on their textural, compositional, and geodynamic maturity of the sedimentary deposits, to propose a kind of “hybrid manual” for practical field studies of aeolian mineral deposits. On this basis and on additional research papers, it is possible to evaluate the source and concentration processes that led to Bujuru and Retiro HM deposits.

The HM occurrences in the RGSCP were first reported by Villwock *et al.* (1979) and Da Silva (1979). Both papers sampled HM in the foreshore and backshore of actual beaches, and suggested the HM were transported by SW to NE swell action. Da Silva (1979) suggested HMs were concentrated by swash and backwash action in the foreshore and backshore, water sheet flows by berm-top spillover and eolian winnowing action. Da Silva (1979) investigation was restricted to southern RGSCP segment (Cassino to Chuí beaches) and found that the north part has a slight non-opaque minerals predominance, while the south part (Chuí) has opaque minerals predominance.

The proportion of different HMs along RGSCP Holocene beach zones and continental shelf varies. Corrêa *et al.* (2008) sampled a large area in the continental shelf from north Rio Grande do Sul (Brazil) to north Argentina, to discuss the regional and local sources of HMs based on opaque HMs concentration, and on mineralogical index and multivariate data analysis (non-opaque HMs). They showed the higher opaque minerals (ilmenite, limonite, leucosene e pyrite) concentration in front of Rio de la Plata Estuary, and suggested it represent a regional source due Rio de la Plata draining mainly Paraná Basin sedimentary and volcanic rocks. Local sources are put in evidence non-opaque minerals (hypersthene, hornblende, tourmaline, staurolite, apatite and zircon). Martins (2011) showed a large variation on HMs composition from Chuí area to Lagoa da Ave (SC state, to the north) sampled on swash zone, and pointed out some proximal source correlation.

Barros *et al.* (2008) made a series of microprobe analysis in non-opaque HMs along the northern RGSCP and compared their chemical composition with

composition of same minerals from different stratigraphic units: continental plateau basalts (Serra Geral Fm., Paraná Basin) and Rio Grande do Sul Precambrian Shield (granite-gnaisses and metamorphosed vulcanosedimentary rocks). Barros *et al.* (2008) found that non-opaque HMs are mainly derived from RGS Precambrian Shield. Additionally, Barros *et al.* (2010) analysed zircon composition and found that zircon grains mainly derived from an association of subalkaline to alkaline granitic rocks of nearby Pelotas Batholith (RGS Precambrian Shield). These results corroborate Corrêa *et al.* (2008) results for HM sampled in the continental shelf.

The sediment reworking in the RGSCP is usually mentioned as a mechanism for HMs differentiation and concentration. Anoni (2015) sampled different barrier/lagoon system near Chuí area (southmost area of RGSCP) and showed some different HMs concentrations in each barrier/lagoon system. Additionally, Anoni (2015) reported an increase in total concentration of HMs from Barrier/Lagoon II to Barrier/Lagoon IV (0.042%; 1.89%; up to 4.66%). Carassai *et al.* (2018) sampled the aeolian and the upper shoreface - foreshore facies for all four Barrier/Lagoon systems and could define some trends for HMs differentiation from older to younger barrier/lagoon systems. However, Anoni (2015) and Carassai *et al.* (2018) investigations have limited sampling locus distribution in the RGSCP for a complete discussion about HMs differentiation along barrier/lagoon systems.

Table 2 lists HMs compositional differentiation and concentration determined in some of previous investigations to compare them with Bujuru and Retiro HM deposits. It is noteworthy that ilmenite+magnetite is the most abundant HM specie in each barrier/lagoon system, and sampling site. It is also interesting to observe the expressive epidote+zircon+amphibole+pyroxene increasing from older to younger barrier/lagoon system. This non-opaque HMs increase can imply the advance of Rio Grande Arc denudation processes toward the NNW, where metavolcanic rocks (epidote+amphibole), alkaline granites (zircon) and stratiform mafic-ultramafic complexes (pyroxenes) predominates in the exposed RGS Precambrian Shield.

Bujuru and Retiro HM deposits, in this way, as also Da Silva (1979) and Corrêa *et al.* (2008) results for backshore-foreshore and shoreface-offshore zones, do reflect these conditions. Corrêa *et al.* (2008) identified an opaque HM and ZTR anomalous area offshore the Bujuru and Retiro HM deposits.

The composition and concentration of HMs, however, are not sufficient conditions to give rise to a mineral deposit. An economic mineral deposit depends on the existence of high-grade HMs concentration in a large volume of material; other way, one has an uneconomic HM occurrence. Then, it is to be discussed what kind of conditions led to the development of the Bujuru and Retiro HM deposits.

Table 2 – HMs compositional differentiation and concentration as recorded in some investigations to compare with Bujuru and Retiro HM deposits. SKA = sillimanite+kyanite+andalusite.

Barrier/Lagoon System (age)	Da Silva (1979) Hermenegildo - Chuí (southern RGSCP)	Corrêa <i>et al.</i> (2008)	Carassai <i>et al.</i> (2018) HMs listed in order of abundance	Munaro (1994), Dillenburg <i>et al.</i> (2004) Bujuru HM deposit	Takahashi & Hartmann (2014) Retiro HM deposit
B/L system IV (8 a 0 ka)	Ilmenite (46.6%), magnetite (3.2%), epidote (10.8%), pyroxene (12.5%), tourmaline (2.6%), staurolite (4.4%), zircon (2.9%), rutile (1.8%), garnet (3.0%), kyanite (1.7%), andalusite (0.3%) and others (9.9%)	Opaque minerals (31.6%): ilmenite, limonite, leucosene and pyrite. Non-opaque minerals: tourmaline (11,5%), hornblende (9,3%), staurolite (9,3%), augite (8,9%), epidote (7,4%), hypersthene (6,3%), zircon	Ilmenite+magnetite, epidote, zircon, rutile, tourmaline, staurolite, garnet, SKA, amphibole, pyroxene, chromite+pinels	Ilmenite (58.6%), zircon (8.4%), epidote (8%), tourmaline (6.3%), magnetite (5.3%), staurolite (5%), rutile (2.5%), kyanite (2.1%), leucosene (2.1%), garnet (0.7%), perovskite (0.5%), chromite (0.3%) and others (0.2%)	Ilmenite (62.3%), zirconite (7.5%), Ti-magnetite (6.2%), quartz (5.9%), epidote (5.2%), staurolite (4.8%), Rutile (2.2%), Turmaline (2.2%), Garnet (1.7%), kyanite (1.1%), leucosene (0.7%)

		(4,5%), garnet (4,4%), kyanite (3,9%), apatite (3,6%), sillimanite (1,1%) and rutile (0,8%)			
B/L system III (125 ka)	No samples	No samples	Ilmenite+magnetite, tourmaline, epidote, staurolite, rutile, zircon, SKA, garnet, chromite+spinels	No samples	No samples
B/L system II (230 ka)	No samples	No samples	Ilmenite+magnetite, tourmaline, staurolite, rutile, zircon, SKA, garnet, chromite+spinels	No samples	No samples
B/L system I (325 ka)	No samples	No samples	Ilmenite+magnetite, zircon, staurolite, tourmaline, rutile,	No samples	No samples

		SKA, chromite, garnet, spinels		
--	--	-----------------------------------	--	--

The deformational structures and the associated mechanical subsidence presented here must have played an important role HM concentration and purification processes. Figure 12 shows a simplified geologic-structural sketch depicting the stratigraphic units distinguished by Fontoura *et al.* (submitted) and detailed in this work. Figure 13 present a synthesis of HM concentration, purification, and accumulation in different stages of structural development.

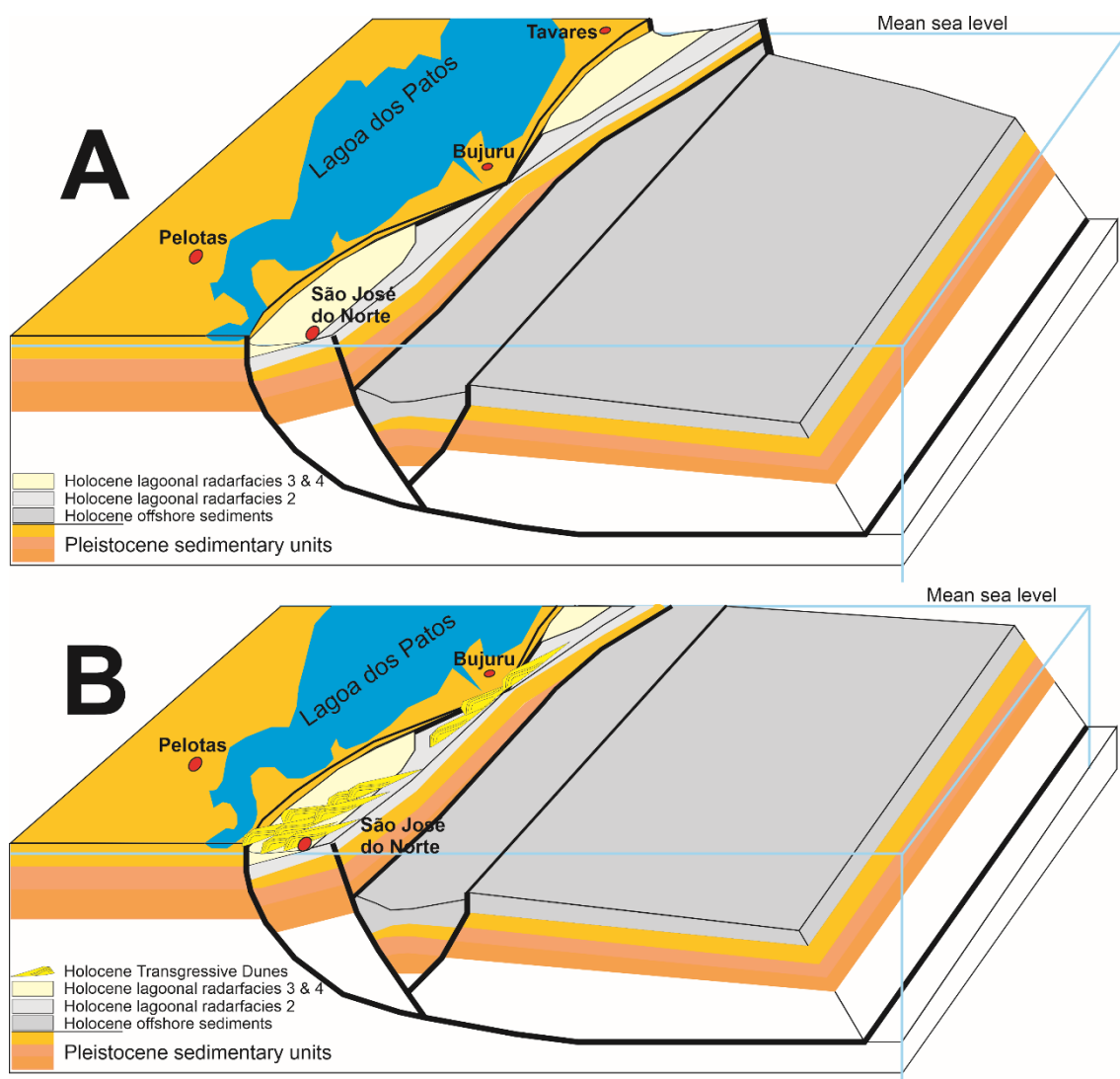


Figure 12 – Geologic-structural model for placer Bujuru and Retiro HM deposits (RGSCP, Brazil). A) The development of the structural trap (placer) for

first stage of HM concentration. B) The third stage HM concentration and purification on Transgressive Dunes.

The first stage is characterized by a fault displacement rate higher than sedimentation rate and the development of a structural basin to constitute the trap (placer) for preliminary HM concentration. The rotation of the Pleistocene sedimentary units in the hanging-wall by listric normal fault developed a structural barrier oceanward, whose remnants are still observed in actual beach line (e.g. Dillenburg *et al.*, 2004). Erosion of this structural barrier was responsible for sediment reworking and deposition in the rapidly subsiding, fault-controlled lagoon (Lagoa do Peixe and Retiro-Estreito lagoons). Swash and backwash by waves and tides may have acted to erode Pleistocene units and to concentrate the HM in the First Lagoonal radarfacies (Figure 12A). The erosional process supported by the structural barrier was certainly facilitated by transfer faults, which open channels to ocean water sheets spreading on lagoons. These processes additionally contributed to HM concentration in the First Lagoonal radarfacies.

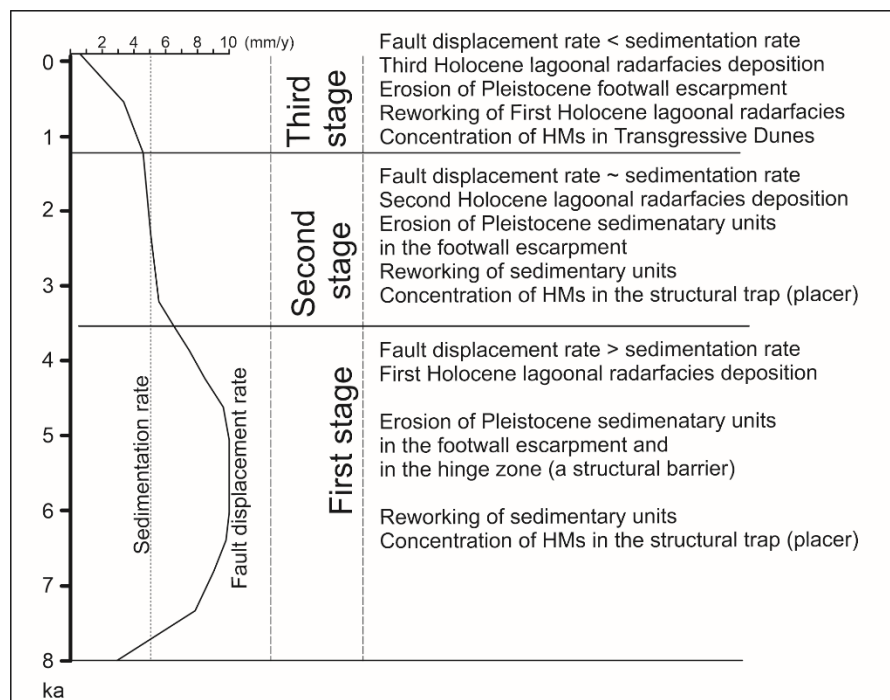


Figure 13 – Cartoon showing the development stages for structurally controlled lagoons, and the formation of Bujuru and Retiro HM deposits. Rate scale is only for illustration.

The second stage began in the period when fault displacement rate equals sedimentation rate (~3.46 ka upper age for the first lagoonal radarfacies). The corresponding radarfacies is not actually exposed, since it was deposited as a triangular unit (Figure 12A) in the asymmetric lagoon depocenter close to the fault escarpment (Fontoura *et al.*, submitted). This triangular zone was progressively developed during the high fault displacement, and filled with sediments chiefly derived from Pleistocene footwall block (bulkhead structure west of fault). It also constitutes a structural trap for HMs. The continuity of fault displacement and hanging-wall block rotation (high to medium rates) began the folding of the first lagoonal radarfacies into braquisynclinals and braquianticlinals. The sedimentation gap (3.46 to 1.06 ka) identified close to Bujuru beach is the time interval for the second lagoonal radarfacies deposition (Fontoura *et al.*, submitted).

The third stage is characterized by a sedimentation rate higher than fault displacement rate, and imply lagoon clogging due to sediments derived from Pleistocene bulkhead (footwall structural high) to the west and from braquianticlinal that was exposed near the beach. The peat layer (~1.06 ka) now exposed by folding in the beach is the lowermost strata of this radarfacies. At this stage, the initial Pleistocene structural barrier at the beach was completely eroded, and a new structural barrier is present: the braquianticlinal. Tides and waves erosion on the previous lagoonal radarfacies exposed in the beach zones, HM hydraulic sorting in the offshore to backshore zones, onshore winds transport, and winnowing are the processes responsible for the Bujuru and Retiro HM deposits. The braquianticlinal erosion and sediment transport by onshore winds are the main mechanisms building up the TDS and TD that are actually clogging the Lagoa do Peixe and Retiro-Estreito lagoons, and giving rise to HM deposits (Figure 12B).

CONCLUSIONS

The RGSCP was developed close to a super-mature crustal section (RGS Precambrian Shield). The Bujuru and Retiro HM deposits were developed in consequence to deformational traps. Mechanical subsidence, instead of sea level changes, is the main responsible for structural placers that lead to existing HM deposits.

A three stages evolutionary model is suggested based on fault displacement and sedimentation rates. A preliminary HM concentration episode was promoted by reworking sediments of the Pleistocene footwall escarpment and from a Pleistocene structural barrier developed in the hanging-wall oceanward. A second HM concentration episode is still in operation: TDS and TD developing upon another structural barrier (braquianticlinal), that was build due to the progressive deformation of the hanging-wall upon the previous Holocene lagoonal radarfacies. The actual sedimentary barrier (TDS and TD) developed upon a braquianticlinal barrier and migrates inland due to NE onshore winds, also accumulating over structurally controlled lagoons to clog them.

The results of this investigation seem to show a double evolution when classifying the aeolian landforms for Mostardas to Retiro-Estreito area in the RGSCP, following Dill (2022). The structurally controlled Lagoa do Peixe and Retiro-Estreito lagoons, in the first and second stages of development, evolved as coastal lagoons (LFS 6), perennial lacustrine environment. The fine-grained sediments and organic matter define this depositional environment, as discussed in Fontoura *et al.* (submitted). However, the third stage (actual) stage of development is actually occurring as typical coastal-marine (LFS 5) in warm temperate climate and in microtidal-wave-dominated coastal-marine environments (Dill and Buzatu, 2022).

HM sources for this placer deposits seems to be regarded to Pleistocene sediments reworking induced by deformational structures. However, new HM input could have played an important role, chiefly due longshore Atlantic currents as pointed out by Corrêa *et al.* (2008).

HM transport and accumulation differ from first to second episodes. But, erosion of previous Holocene lagoonal deposit, HM longshore transport, hydraulic sorting in the offshore to backshore zones, onshore winds transport, and winnowing are the envisaged processes as sedimentary structures show. Purification and diagenetic processes may have played another important role in the relative concentration and composition of the HM deposits, as demonstrated by Dill and Skoda (2017) and Dill *et al.* (2017, 2018). However, this subject was not under the scope of this paper, and may be addressed in future investigations.

ACKNOWLEDGEMENTS

Dr. Harald G. Dill is acknowledged for the suggestions to improve the paper presented in the first version submitted. Rio Grande Mineração is acknowledged for access to the area and overall support, including drill-cores. HIDROSERV (Hidrogeologia e Geofísica Ltda) allowed use of GPR lines. Support was also given by the Geological Engineering course, Universidade Federal de Pelotas. This article is part of the doctoral thesis of the first author at Programa de Pós-Graduação em Geociências, Universidade Federal do Rio Grande do Sul.

REFERENCES (CAPÍTULO 5)

- Abreu, J.G.N., Langella, R.F., Horn Filho, N.O., Calliari, L.J., Sant'ana, R., 2020. Minerais pesados da plataforma continental interna adjacente à ilha de Santa Catarina, SC, Brasil. *Quat. Environ. Geosci.* 11, 25–39.
- Aguiar Neto, A.B., 2015. Ocorrência de minerais pesados na plataforma continental interna/média oeste do Ceará. (PhD Thesis), Universidade Federal do Ceará, Fortaleza, Brazil (116 pp.).
- Angelelli, V., Chaar, E. 1967. Los depósitos de titanomagnetita, ilmenita y circon de la Bahía San Blas (Tramo Baliza La Ballena-Faro Segunda Barranca).

Partido Carmen de Patagones, Provincia de Buenos Aires. Comisión Nacional de Energía Atómica. Informe 210.

- Angulo, R.J., Giannini, P.C.F., Suguio, K., Pessenda, L.C.R., 1999. Relative sea-level changes in the last 5500 years in southern Brazil (Laguna-Imbituba region, Santa Catarina State) based on vermetid ^{14}C ages. *Mar. Geol.* 159, 323–339.
- Anoni, R.A.O., 2015. Estudo comparativo da assembleia de minerais detríticos pesados não-opacos dos depósitos praias nos três sistemas laguna-barreira da porção extremossul da Planície Costeira do Rio Grande do Sul. Curso de Graduação em Geologia. Universidade Federal do Rio Grande do Sul, Porto Alegre, Brazil (52 pp.)
- Barboza, E.G., Dillenburg, S.R., Ritter, M.N., Angulo, R.J.; Silva, A.B., Rosa, M.L.C.C., Caron, F., Souza, M.C., 2021. Holocene Sea-Level Changes in Southern Brazil Based on High Resolution Radar Stratigraphy. *Geosci.* 11, 326.
- Barros, C.E., Nardi, L.V.S., Dillenburg, S.R., Baitelli, R., Dehnhardt, B.A., 2008. Distribuição e origem dos minerais detríticos pesados das areias praias holocênicas do litoral norte do Rio Grande do Sul. *Rev. Bras. Geoc.* 38(2), 319–335.
- Barros, C.E., Nardi, L.V.S., Dillenburg, S.R., Ayup, R., Jarvis, K., Baitelli, R., 2010. Detrital minerals of modern beach sediments in Southern Brazil: a provenance study based on the chemistry of zircon. *J. Coast. Res.* 26(1), 80–93.
- Cábana, M.C., Mykietiuik, K. 1999. Arenas ferrotitaníferas y circoníferas del litoral de la provincia de Buenos Aires. En: Recursos Minerales de la Republica Argentina (Ed. E.O. Zappetini), Instituto de Geología y Recursos Minerales SEGEMAR, Anales 35, 1899–1903, Buenos Aires.

- Carassai, J.J., Lavina, E.L.C., Chemale Jr., F., Girelli, T.J., 2018. Provenance of heavy minerals for the Quaternary coastal plain of southernmost Brazil (Rio Grande do Sul State). *J. Coast. Res.* 00(0), 000–000.
- Corrêa, I.C.S., 1990. Analyse morphostructurale et evolution paleogeographique de la plata-forme continentale atlantique sud-bresilienne (Rio Grande do Sul - Bresile). Universite de Bordeaux I (PhD Thesis), 314 pp.
- Corrêa, I.C.S., 1995. Les variations du niveau de la mer durant les derniers 17.500 ans BP: l'exemple de la plate-forme continentale du Rio Grande do Sul-Brésil. *Mar. Geol.* 130, 163–178.
- Corrêa, I.C.S., Zouain, R.N.A., Weschenfelder, J., Tomazelli, L.J., 2008. Áreas Fontes dos Minerais Pesados e sua Distribuição sobre a Plataforma Continental Sul-brasileira, Uruguia e Norte argentina. *Rev. Pesq. Geoci.* 35 (1), 137-150.
- Da Silva, M.A., 1979. Provenance of heavy minerals in beach sands southeastern Brazil from Rio Grande to Chui. *Sediment. Geol.* 24, 133–148.
- Dill, H.G., 2022b. Trends and Composition—A Sedimentological-Chemical-Mineralogical Approach to Constrain the Origin of Quaternary Deposits and Landforms—From a Review to a Manual. *Geosciences.* 12(1), 24.
- Dill, H.G., Buzatu, A., 2022a. From the aeolian landform to the aeolian mineral deposit in the present and its use as an ore guide in the past. Constraints from mineralogy, chemistry and sediment petrography. *Ore Geol. Rev.* 144, 104490.
- Dill, H. G., Goldmann, S., & Cravero, F., 2018. Zr-Ti-Fe placers along the coast of NE Argentina: Provenance analysis and ore guide for the metallogenesis in the South Atlantic Ocean. *Ore Geol. Rev.* 95, 131–160.
- Dill, H. G., Kus, J., Kaufhold, S., Rammlmair, D., & Techmer, A., 2017. Oligo-Miocene coal in a microtidal environment reworked under Quaternary periglacial conditions (Western Falkland Islands/Isla Gran Malvina) –

- Coal formation and natural sand processing. *Int. J. Coal Geol.* 174, 8–22.
- Dill, H. G., Skoda, R., 2017. Provenance analysis of heavy minerals in beach sands (Falkland Islands/Islas Malvinas) – A view to mineral deposits and the geodynamics of the South Atlantic Ocean. *J. South Am. Earth Sci.* 78, 17–37
- Dillenburg, S.R., Barboza, E.G., Rosa, M.L.C.C., Caron, F., Sawakuchi, A.O., 2017. The complex prograded Cassino barrier in southern Brazil: Geological and morphological evolution and records of climatic, oceanographic and sea-level changes in the last 7-6 ka. *Mar. Geol.* 390, 106–119.
- Dillenburg, S.R., Tomazelli, L.J., Barboza, E.G., 2004. Barrier evolution and placer formation at Bujuru southern Brazil. *Mar. Geol.* 203, 43–56.
- Els, G., Eriksson, P., 2006. Placer formation and placer minerals. *Ore Geol. Rev.* 28, 373–375.
- Ferreira, K.R.S., 2006. Caracterização do Concentrado de Ilmenita produzido na Mina do Guaju, Paraíba, visando identificar Inclusões de Monazita e outros Contaminantes (Master Degree), Universidade Federal do Rio Grande do Sul, Porto Alegre, Brazil.
- Fonseca, V.P. 2006. Estudos morfotectônicos aplicados à planície costeira do Rio Grande do Sul e adjacências. (PhD Thesis), Universidade Federal do Rio Grande do Sul, Porto Alegre, Brazil, (306 pp.) (unpublished).
- França, P.P., 2013. Caracterização de minerais pesados e avaliação da radioatividade natural “*in situ*” em sedimentos praias de Acaú, Carne de Vaca e Ponta de Pedras do estuário do rio Goiana. (Master Degree), Universidade Federal de Pernambuco, Recife, Brazil (76 pp.).

- Hou, B., Keeling, J., Van Gosen, B.S., 2017. Geological and Exploration Models of Beach Placer Deposits, Integrated from Case-Studies of Southern Australia. *Ore Geol. Rev.* 80, 437–459.
- Isla, F. I., Vilas, F.E., Bujalesky, G., Ferrero, M., Bonorino, G.G., Miralles, A.A., 1991. Gravel drift and wind effects over the macrotidal San Sebastián Bay, Tierra del Fuego. *Mar. Geol.* 97, 211–224.
- Jaboyedoff, M., Penna, I., Pedrazzini, A., Baroň, I., Crosta, G.B., 2013. An introductory review on gravitational-deformation induced structures, fabrics and modeling. *Tectonophysics*, 605, 1–12.
- Komar, P.D. & Wang, C., 1984. Processes of Selective Grain Transport and the Formation of Placers on Beaches. *J. Geol.* 92, 637–655.
- Lalomov, A.V., 2003. Differentiation of Heavy Minerals in the Alongshore Debris Flow and Modeling of Processes of Coastal-Marine Placer Formation. *Lithology and Mineral Resources.* 38(4), 306–313.
- Lima, E.S., 2011. Avaliação do potencial de formação de placeres diamantíferos na região do delta do Rio Jequitinhonha e plataforma continental adjacente no sul da Bahia. (Master Degree), Universidade Federal da Bahia, Salvador, Brazil (unpublished).
- Martins, L.P., 2011. Estudo e avaliação das assembléias de minerais pesados detríticos das areias holocênicas praias da margem emersa da Bacia de Pelotas. (Master Degree), Universidade Federal do Rio Grande do Sul, Porto Alegre, Brazil (46 pp.).
- Minter, W.E.L., Craw, D., 1999. A special issue on placer deposits. *Econ. Geol.* 94, 603–604.
- Munaro, P., 1991. Relatório de avaliação das reservas geológicas de minerais pesados. Paranapanema Mineração. São Paulo, 12 pp.

- Munaro, P., 1994. Geologia e Mineralogia do depósito de minerais pesados de Bujuru-RS. (Master Degree), Universidade Federal do Rio Grande do Sul, Porto Alegre, Brazil (96 pp.).
- Nguyen, H.H., Carter, A., Hoang, L.V., Vu, S.T., 2018. Provenance, routing, and weathering history of heavy minerals from costal placer deposits of southern Vietnam. *Sediment. Geol.* 373, 228–238.
- Patyk-Kara, N.G., 2002. Placers in the System of Sedimentogenesis. *Lithol. Miner. Resour.* 37, 429–441.
- Rosa, M.L.C.C., Barboza, E.G., Abreu, V.S., Tomazelli, L.J., Dillenburg, S.R., 2017. High-frequency sequences in the Quaternary of Pelotas Basin (coastal plain): a record of degradational stacking as a function of longer-term base level fall. *Braz. J. Geol.* 47(2), 183–207.
- Roy, P.S., 1999. Heavy mineral beach placers in Southeastern Australia: their nature and genesis. *Econ. Geol.* 94, 567–588.
- Silva, C.G., 2000. Placeres marinhos. *Revista Brasileira de Geofísica.* 18(3), 327–336.
- Slingerland, R.L., 1977. The effects of entrainment on the hydraulic equivalence relationships of light and heavy minerals in sand. *J. Sediment. Petrol.* 47, 753–770.
- Sousa, S.S.C.G., Castro, J.W.A., Guedes, E., 2017. Variações Granulométricas e Minerais Pesados das Praias do Norte do Estado do Rio de Janeiro, SE, Brasil: Condições de distribuição e Deposição dos Sedimentos. *Geoci.* 36, 365–380.
- Strieder, A.J., 2004. Georradar e suas aplicações em investigações de sub-solo. Departamento de Engenharia de Minas. Escola de Engenharia. Universidade Federal do Rio Grande do Sul, 43–56.
- Takahasi X.Y., Hartmann, F.Z., Coordenadores, 2014. Relatório de impacto Ambiental Projeto Retiro. São José do Norte, RS, Brazil, 71. Available

online: <http://imagenature.com.br/wp-content/uploads/2014/07/RIMA-Projeto-Retiro.pdf>

- Tomazelli, L.J., 1977. Minerais pesados da plataforma continental do Rio Grande do Sul. (Master Degree), Universidade Federal do Rio Grande do Sul, Porto Alegre, Brazil (81 pp.).
- Tomazelli, L.J., 1978. Minerais pesados da plataforma continental do Rio Grande do Sul. *Acta Geol. Leopold.* 3, 103–159.
- Tomazelli, L.J. & Villwock, J.A., 1996. Quaternary Geological Evolution of Rio Grande do Sul Coastal Plain, Southern Brazil. *An. Acad. bras. Ci.* 68(3), 373–382.
- Tomazelli, L.J., Dillenburg, S.R., Villwock, J.A., 2000. Late quaternary geological history of RGS Coastal plain, southern Brazil. *Rev. Bras. Geoc.* 30(3), 474–476
- Tomazelli, L.J., Villwock, J.A., 2005. Mapeamento geológico de planícies costeiras: o exemplo da costa do Rio Grande do Sul. *Gravel*, Porto Alegre, 3, 109–115.
- Tomazelli, L.J., Villwock, J.A., Dillenburg, S.R., Bachi, F.A., Dehnhardt, B.A., 1998. Significance of present-day coastal erosion and marine transgression, Rio Grande do Sul, Southern Brazil. *Anais Acad. Bras. Ciênc.* 70, 221–229.
- Tomazzoli, E.R., Oliveira, U.R., Horn Filho, N.O., 2007. Proveniência dos minerais de óxidos de fe-ti nas areias da praia do pântano do Sul, ilha de Santa Catarina (SC), Sul do Brasil. *Rev. Bras. Geof.* 25(1), 49–64.
- U.S.G.S, 2023. Mineral commodity summaries 2023. U.S. Geological Survey, 210.
- Villwock, J.A., 1972. Contribuição a Geologia do Holoceno da Província Costeira do Rio Grande do Sul, Brasil. (Master Degree), Universidade Federal do Rio Grande do Sul, Porto Alegre, Brazil (113 pp.).

- Villwock, J.A., Dehnhardt, E.A., Loss, E.L., Tomazelli, L.J., Hofmeister, T., 1979. Concentraciones de arenas negras a lo largo de la costa de Rio Grande do Sul, Brasil. Memorias, Seminario Sobre Ecologia Bentonica y Sedimentacion de la Plataforma Continental del Atlantico Sur, Montevideo, UNESCO, 405-414.
- Villwock, J.A., Tomazelli, L.J., Loss, E.L., Dehnhardt, E.A, Horn Filho, N.O., Bachi, F.A, Dehnhardt, B.A., 1986. Geology of the Rio Grande do Sul Coastal Province. Quatern. South Am. and Antarctic Peninsula. 4, 79–97.
- Weschenfelder, J., Medeanic, S., Corrêa, I.C.S., Aliotta, S., 2008. Holocene Paleoinlet of the Bojuru Region, Lagoa dos Patos, Southern Brazil. J. Coast. Res. 24, 99.

CAPÍTULO 6

6. CONSIDERAÇÕES FINAIS

A presente Tese de Doutorado teve como principal objetivo trazer uma nova abordagem para a formação de uma parte da Planície Costeira do Rio Grande do Sul, através do processo de subsidência mecânica que ocorre na Barreira Pleistocênica III. Com isso, foram apresentados dados a partir de levantamentos geofísicos (GPR) e geológicos (análise de fotografias aéreas e sondagem à percussão) que evidenciam a presença de estruturas deformacionais gravitacionais nessa região.

Para tal propósito, o capítulo 2 da Tese traz uma síntese dos conceitos de neotectônica e tudo relacionado a esse tema, elucidando a respeito da dinâmica dessas estruturas e, principalmente das condições de seu desenvolvimento em ambiente subaquoso. Por fim, resume os trabalhos publicados sobre o tema na Bacia de Pelotas, tais como: Delaney (1965), Müller Fo. (1970), Cecarelli (1996), Saadi et al. (2002), Fonseca (2006), Castillo et al. (2009) e Santos (2020).

O capítulo 3 da Tese, aborda presença de uma falha de crescimento lítrica e o controle da sedimentação na PCRS. Por meio de levantamentos geológicos e por GPR, mostra-se que o controle estrutural presente na região. O deslocamento da falha controlou diferentes estágios de sedimentação na Lagoa do Peixe, que afunda tectonicamente, e na verdade está em processo de entupimento devido a erosão da escarpa da falha e migração das dunas eólicas do Holoceno (Barreira IV).

O artigo mostra que a falha de crescimento da Lagoa do Peixe, pelo menos nesta área, deve aflorar uma nova discussão sobre o sistema laguna/barreira com a presença do tectonismo. Falha de crescimento, controle gravitacional sobre geometria e sedimentação no PCRS introduz novos tópicos ao assunto barreira/laguna.

Deste modo, o artigo traz uma recomendação para trabalhos futuros. A fim de avaliar a extensão que a tectônica gravitacional pode ter na planície costeira do RS, novas abordagens devem ser realizadas em outras áreas, bem como em outros sistemas lagunares da PCRS.

No capítulo 4 da Tese, o enfoque é dado na gênese e morfologia dos cordões litorâneos da Quinta – Cassino (RS). Foi demonstrado que a planície costeira Quinta – Cassino foi desenvolvida sob a influência de um leque imbricado de falha lístrica gravitacional, cujo embasamento do Pleistoceno foi cortado por falhas sintéticas e antitéticas. Os blocos falhados exibem diferentes taxas e quantidades de deslocamento e rotação.

A tectônica de gravidade, em vez das alterações do nível do mar, mudanças climáticas, ou correntes longitudinais, é o principal mecanismo de controle da sedimentação e evolução estratigráfica. Além disso, salienta que este processo tectônico não suprime a operação de outros importantes mecanismo, tais como: nível do mar e mudanças climáticas, correntes litorâneas, taxas de deposição e erosão, taxas de entrada de sedimentos, porém não os controla. Deixando claro que mais levantamentos geofísicos são necessários para corroborar o desenvolvimento do processo de subsidência mecânica na formação da PCRS.

Ademais, no capítulo 5 a Tese discute processo de formação dos minerais pesados de Bujuru (RS). Os levantamentos geofísicos (GPR) com baixa frequência realizados na área foram confrontados com as amostras obtidas através do método de sondagem à percussão. Logo, entende-se que os depósitos de minerais pesados (MP) de Bujuru e do Retiro foram desenvolvidos em consequência de armadilhas deformacionais. A subsidência mecânica, em vez das mudanças no nível do mar, é a principal responsável pelos placers estruturais.

Um modelo evolutivo de três estágios é sugerido baseado no deslocamento de falhas e nas taxas de sedimentação. Um episódio preliminar de concentração de MP foi promovido pelo retrabalhamento de sedimentos da escarpa *footwall* do Pleistoceno e de uma barreira estrutural do Pleistoceno desenvolvida a *hangingwall* em direção ao oceano. Um segundo episódio de concentração de MP ainda está em operação e camadas de dunas transgressivas e dunas transgressivas desenvolvem-se sobre outra barreira estrutural (braquianticlinal), que foi construída devido à deformação progressiva da *hangingwall* sobre os radarfácies lagunares holocênicos anteriores. Por fim,

a barreira sedimentar atual (TDS e TD) desenvolveu-se sobre uma barreira braquianticlinal e migra para o interior devido aos ventos de NE, acumulando-se também sobre lagoas estruturalmente controladas para obstruí-las.

As fontes de MP para estes depósitos de placeres parecem ser consideradas como retrabalhamento de sedimentos do Pleistoceno induzido por estruturas deformacionais. No entanto, novas contribuições de MP poderiam ter desempenhado um papel importante, principalmente devido às correntes longitudinais do Atlântico, como apontado por Corrêa et al. (2008).

A mineração de MP na região de Bujuru e Retiro é uma realidade. Para tanto, o planejamento da extração desses minérios do ponto de vista da otimização do processo pode ser melhorado com a execução de levantamentos geofísicos em frente de lavra.

Por fim, conclui-se que a hipótese apresentada foi confirmada: há a presença de falhas normais sintéticas e antitéticas controlando a formação dos depósitos sedimentares holocênicos e o processo de subsidência mecânica teve influência na origem dos minerais pesados encontrados na PCRS.

REFERÊNCIAS (CAPÍTULOS 1, 2 E 6)

- BUENO, G.V., ZACHARIAS, A.A., OREIRO, S.G., CUPERTINO, J.A., FALKENHEIN, F.U.H., NETO, M.A.M. 2007. **Bacia de Pelotas**. Boletim de Geociências da Petrobrás, v. 15, nº 2, p. 551–559.
- BARBOZA, E.G. & TOMAZELLI, L.J., 2003. **Erosional features of the eastern margin of the Patos Lagoon, southern Brazil: significance for Holocene history**. Journal of Coastal Research, SI 35, p. 260–264.
- BARBOZA, E. G., ROSA, M.L.C.C., DILLENBURG, S.R., WATANABE, D.S.Z., ESTEVES, T., MARTINS, E.M., GRUBER, N.L.S. 2018. **Diachronic Condition Between Maximum Transgressive and Maximum Eustatic Sea-Level in Holocene: Subsidies for Coastal Management**. Journal of Coastal Research, v. 85, p. 446–450.
- BARBOZA, E.G., ROSA, M.L.C.C., HESP, P.A., DILLENBURG, S.R., TOMAZELLI, L.J., AYUP-ZOUAIN, R.N. 2011. **Evolution of the Holocene coastal barrier of Pelotas Basin (southern Brazil) – a new approach with GPR data**. Journal of Coastal Research, Special Issue, 64:646–650.
- BUCHMANN, F.S.C., CARON, F., LOPES, R.P., UGRI, A., LIMA, L.G. 2009. **Panorama geológico da Planície Costeira do Rio Grande do Sul**. In: RIBEIRO, A.M., BAUERMANN, S.G., SCHERER, C.S. (Org.) Quaternário do Rio Grande do Sul. Porto Alegre: Grafica Palloti, v., p. 35–56.
- CARDOZO, T. 2011. **Caracterização do Arcabouço Estrutural da Bacia de Pelotas e da área emersa adjacente**. Dissertação de Mestrado, Universidade Estadual Paulista Júlia de Mesquita Filho, 112 pp.
- CARON, F. 2014. **Estratigrafia e evolução da barreira holocênica na região costeira de Santa Vitória do Palmar, Planície Costeira do Rio Grande do Sul, Brasil**. Tese de Doutorado, Programa de Pós-Graduação em Geociências, Universidade Federal do Rio Grande do Sul, 167 pp.

- CASTILLO, L.L.A., KAZMIERCZAK, T.S., CHEMALE Jr., F. 2009. **Rio Grande Cone tectonostratigraphic model Brazil: seismic sequences**. Earth Sciences Research Journal 13 (1), 40–53.
- CATUNEANU, O. 2006. **Principles of Sequence Stratigraphy**. Elsevier. 375 pp.
- CECARELLI, I.C.F., 1996. **Evidências de feições neotectônicas na Província Costeira do Rio Grande do Sul, identificadas em imagens Landsat**. in Congresso Brasileiro de Geologia, 39. Anais Sociedade Brasileira de Geologia, Salvador-BA, v. 5, p. 467–470.
- CONTRERAS, J., ZÜHLKE, R., BOWMAN, S., BECHSTÄDT, T. 2010. **Seismic stratigraphy and subsidence analysis of the southern Brazilian margin (Campos, Santos and Pelotas basins)**. Marine and Petroleum Geology, v. 27, P. 1952–1980.
- COOPER, W.S., 1958. **Coastal sand dunes of Oregon and Washington**. Geol. Soc. Am. Mem. 72, 169 pp.
- CORRÊA, I.C.S., 1990. **Analyse Morphostructurale et Evolution Paleogeographique de la Plata-Forme Continentale Atlantique Sud-Bresilienne (Rio Grande do Sul - Bresile)**. Universite de Bordeaux I, Talence-France. Tese de Doutorado, 314p (Inédito).
- CORRÊA, I.C.S. 1994. **Interpretação morfoestrutural da plataforma continental do Rio Grande do Sul através da análise cartográfica**. In: XXXVIII CONGR. BRAS. GEOLOGIA, Balneário Camboriú, 1994. Anais... Balneário Camboriú, 1994. p. 372–374.
- CORRÊA, I.C.S. 1995. **Les variations du niveau de la mer durant les derniers 17.500 ans BP: l'exemple de la plate-forme continentale du Rio Grande do Sul-Brésil**. Mar Geol 130:163–178.
- COSTA, K.B., TOLEDO, F.A.L., SANTOS JUNIOR, E.C., QUADROS, J.P. 2005. **Inferências sobre taxas de sedimentação através do estudo de**

- isótopos de oxigênio em Foraminíferos bentônicos.** In: X Congresso da ABEQUA, 2005, Guarapari, ES. Anais do X Congresso da ABEQUA, 2005. v. 1.
- COWELL, P.J. & THOM, B.G. 1994. **Morphodynamics of coastal evolution.** In: R. W. G. Carter, & C. D. Woodroffe, (Eds), Coastal evolution, late quaternary shoreline morphodynamics. Cambridge University Press, Cambridge, pp. 33–86.
- CURRAY, J.R. 1964. **Transgressions and Regressions.** In: Miller, R. L. (ed.) Papers in Marine Geology. Shepard Commemorative Volume. MacMillan Co., New York, pp. 175–203.
- DALRYMPLE R.W., ZAITLIN B.A. & BOYD, R. 1992. **Estuarine facies models: conceptual basis and stratigraphic implications.** J Sediment Petrol, 62, pp. 130–146.
- DELANEY, P.J.V. 1965. **Fisiografia e Geologia da superfície da Planície Costeira do Rio Grande do Sul.** Publ. Esp. da Esc. Geologia UFRGS, n. 6: 1–195.
- DILLENBURG, S.R., ROY, P.S., COWELL, P.J., TOMAZELLI, L.J. 2000. **Influence of antecedent topography on coastal evolution as tested by the Shoreface Translation-Barrier Model (STM).** J. Coast. Res, v. 16, p. 71–81.
- DILLENBURG, S.R., TOMAZELLI, L.J., BARBOZA, E.G., 2004. **Barrier evolution and placer formation at Bujuru southern Brazil.** Mar. Geol. v. 203, p. 43–56.
- DILLENBURG, S.R., BARBOZA, E.G., TOMAZELLI, L.J., HESP, P.A., CLEROT, L.C.P., AYUP-ZOUAIN, R.N. 2009. **The Holocene Coastal Barriers of Rio Grande do Sul.** In: DILLENBURG, S.R. and HESP, P.A. (eds). Geology and Geomorphology of Holocene Coastal Barriers of Brazil. Springer, pp. 53–91.

- DILLENBURG, S.R., BARBOZA E.G., ROSA, M.L.C.C., CARON, F. SAWAKUCHI, A.O. 2017. **The complex prograded Cassino barrier in the southern Brazil: Geological and morphological evolution and records of climatic, oceanographic and sea-level changes in the last 7-6 ka.** *Marine Geology*, v. 390. p. 106–119.
- DINGLE, R.V. 1977. **The anatomy of a large submarine slump on a sheared continental margin (SE Africa).** *Journal of Geological Society of London* 134: 293–310.
- DOS REIS, A.T., SILVA, C.G., GORINI, M.A., LEÃO, R., PINTO, N., PEROVANO, R., SANTOS, M.V.M., GUERRA, J.V., JECK, I.K., TAVARES, A.A.A. 2016. **The Chuí Megaslides Complex: Regional-Scale Submarine Landslides on the Southern Brazilian Margin.** In: LAMARCHE, G., MOUNTJOY, J., BULL, S., HUBBLE, T., KRASSTEL, S., LANE, E., MICALLEF, A., MOSCARDELLI, L., MUELLER, C., PECHER, I., WOELZ, S. (Org.). *Advances in Natural and Technological Hazards Research*. 1ed.: Springer International Publishing, v. 41, p. 115–123.
- DOTT Jr, R.H. 1963. **Dynamics of subaqueous gravity depositional processes.** *American Association of Petroleum Geologists Bulletin* 47: 104–128.
- EARNEY, F.C.F. 1990. **Mineral Marine Resources.** Routledge (pubs.) London & New York, 325 pp.
- ELS, G., ERIKSSON, P. 2006. **Placer formation and placer minerals.** *Ore Geology Reviews*, v. 28, p. 373–375.
- FERNANDEZ, B.M., MOHRIAK, W.U., MENEZES, P.T.L. 2003. **Structural and stratigraphic aspects of salt tectonics in the Eastern Brazilian margin: evolution model and seismic restoration.** In: 8th International Congress of SBGf and 5th Latin American Geophysical Conference, 2003, Rio de Janeiro. CDROM-8th International Congress of SBGf and 5th Latin American Geophysical Conference. v. 1. p. 1–6.

- FONSECA, V.P., 2006. **Estudos morfotectônicos aplicados à planície costeira do Rio Grande do Sul e adjacências**. Tese de doutorado, Programa de Pós-Graduação em Geociências, Universidade Federal do Rio Grande do Sul, 306 pp.
- FONTANA, R.L. 1990. **Investigações geofísicas preliminares sobre o Cone de Rio Grande, Bacia de Pelotas - Brasil**. Acta Geol. Leopold, v. 13, p. 161–170.
- FONTANA R.L. 1996. **Geotectônica e sismoestratigrafia da Bacia de Pelotas e Plataforma de Florianópolis**. Tese de doutorado, Programa de Pós-Graduação em Geociências, Universidade Federal do Rio Grande do Sul, Porto Alegre, 2 v, 214 p.
- FONTOURA, B.S. 2015. **Controle geológico-estrutural do depósito placer de Bujuru (São José do Norte, RS)**. Trabalho de Graduação, Curso de Engenharia Geológica, Universidade Federal de Pelotas, 65 pp.
- FONTOURA, B.S., STRIEDER, A.J, BEHLING, J.S., WETZEL, R.S., DUARTE Jr, R.S.S., SILVA, T.C., MENDES, P., NÓBREGA, A.V.V., CALLIARI, L.J. 2015. **Structural control of HM placer deposits at RGS (Brazil) Coastal Plain using Ground Penetrating Radar**. Advanced Ground Penetrating Radar (IWAGPR). 8th International Workshop on, p. 1–4.
- FONTOURA, B.S., STRIEDER, A.J, BEHLING, J.S., WETZEL, R.S., DUARTE Jr, R.S.S., SILVA, T.C., MENDES, P., NÓBREGA, A.V.V., CALLIARI, L.J. 2017. **Controle estrutural do depósito placer de minerais pesados na região praial ao norte da desembocadura da lagoa dos patos (Bujuru, Brasil)**. Revista de Engenharia e Tecnologia, v. 9, nº 2, p. 177–185.
- HAMPTON, M.A., LEE, H.J. & LOCAT, J. 1996. **Submarine landslides**. Reviews of Geophysics, 34: 33–59.

- HIGHLAND, L.M. & BOBROWSKY, P. 2008. **The landslide handbook – a guide to understanding landslides**. Reston, Virginia, U.S. Geological Survey Circular 1325, 129 p.
- JABOYEDOFF, M., PENNA, I., PEDRAZZINI, A., BAROŇ, I., CROSTA, G.B. 2013. **An introductory review on gravitational-deformation induced structures, fabrics and modeling**. *Tectonophysics*, v. 605, pp. 1–12.
- LIMA, L. G., DILLENBURG, S. R., MEDEANIC, S., BARBOZA, E. G., ROSA, M. C. C., TOMAZELLI, L. J., DEHNHARDT, B.A., CARON, F. 2013. **Sea-level rise and sediment budget controlling the evolution of a transgressive barrier in southern Brazil**. *Journal of South American Earth Sciences*, 42, 27–38.
- LOCAT, J. & LEE, H.J. 2002. **Submarine landslides: advances and challenges**. *Canadian Geotechnical Journal*, 39(1): 193–212.
- LOPES R.P., KINOSHITA, A., BAFFA O., FIGUEIREDO, A.M.G., DILLENBURG, S.R., SCHULTZ, C.L., PEREIRA, J.C. 2014. **ESR dating of Pleistocene mammals & marine shells from the coastal plain of Rio Grande do Sul state, southern Brazil**. *Quaternary International*, 352:124–134.
- LÓPEZ, L. A. C. 2009. **Interpretação Sismoestratigráfica e Geomorfologia Sísmica do Cone de Rio Grande, Bacia de Pelotas**. Tese de Doutorado, Programa de Pós-Graduação em Geociências, Universidade Federal do Rio Grande do Sul, 159 pp.
- MARTINS, I.R. 1984. **Modelo Sedimentar do Cone do Rio Grande**. *REVISTA PESQUISAS*, v. 16, n.4, p. 91–189.
- MARTINS, L.R., URIEN, C.M., BUTLER, L.W. 1972. **Províncias fisiográficas e sedimentos da margem continental atlântica**. In: SBG, Congresso Brasileiro de Geologia, 26, Belém. Anais, 105–114.

- MUNARO, P. 1994. **Geologia e Mineralogia do depósito de minerais pesados de Bujuru-RS**. Dissertação de Mestrado, Programa de Pós-Graduação em Geociências, Universidade Federal do Rio Grande do Sul, 96 pp.
- MÜLLER Fo., L. 1970. **Notas para o estudo da Geomorfologia do Rio Grande do Sul, Brasil**. Publ. Esp., UFSM/Depto. Geociências, Santa Maria. n.1, 34 p.
- NEUENDORF, K.K.E., MEHL Jr, J.P., JACKSON, J.A. 2011. **Glossary of geology**, 5ª ed., Virginia (USA), American Geoscience Institute. 3132 p.
- ROSA, M.L.C.C. 2009. **Análise Gravimétrica e Magnetométrica da região sul da província costeira do Rio Grande do Sul, setor sudoeste da Bacia de Pelotas**. Porto Alegre. Dissertação de Mestrado, Universidade Federal do Rio Grande do Sul, 79 pp.
- ROSA, M.L.C.C., TOMAZELLI, L.J., COSTA, A.F.U., BARBOZA, E.G. 2009. **Integração dos métodos potenciais (Gravimetria e Magnetometria) na caracterização do embasamento da região sudoeste da Bacia de Pelotas, sul do Brasil**. Revista Brasileira de Geofísica, v. 27, nº 4, p. 641–657.
- ROSA, M.L.C.C., BARBOZA, E.G., DILLENBURG, S.R., TOMAZELLI, L.J., AYUP-ZOUAIN, R.N. 2011. The Rio Grande do Sul (Southern Brazil) shoreline behavior during the Quaternary: a cyclostratigraphic analysis. *Journal of Coastal Research*, Special Issue, 64, 686–690.
- ROSA, M.L.C.C., BARBOZA, E.G., ABREU, V.S., TOMAZELLI, L.J., DILLENBURG, S.R., 2017. **High-frequency sequences in the Quaternary of Pelotas Basin (coastal plain): a record of degradational stacking as a function of longer-term base level fall**. *Brazilian Journal of Geology*, 47(2), 183–207.
- ROY, P.S., COWELL, M.A., FERLAND, M.A. & THOM, B.G. 1994. **Wave-dominated coasts**. In: CARTER, R.W.G. & WOODROFFE, C.D. (Ed.).

Coastal Evolution – Late Quaternary Shoreline Morphodynamics. Cambridge, Cambridge University Press, pp. 121–186.

SANTOS, A.C.O. 2020. **Tectônica gravitacional no Cone do Rio Grande, Bacia de Pelotas (RS)**. Tese de Doutorado, Universidade Federal do Rio Grande. 157 pp.

SAVAGE, W.Z. & VARNES, D.J. 1987. **Mechanics of gravitational spreading of steep-sides ridges (sackung)**. International Association for Engineering Geology Bulletin, 35, 31–36

SEMENIUK, V., MEAGHER, T.D., 1981. **The geomorphology and surface processes of the Australind-Leschenault inlet coastal area**. J. R. Soc. West Austr. 64, 33–51.

SHANMUGAM, G. 2013. **Slides, Slumps, Debris Flows, and Turbidity Currents**. In: Elias, S. A. (ed). Reference Module in Earth Systems and Environmental Science. Elsevier Online.

SHANMUGAM, G. 2018. **Slides, Slumps, Debris Flows, Turbidity Currents, Hyperpycnal Flows, and Bottom Currents**. In: Elias, S. A. (ed). Reference Module in Earth Systems and Environmental Science. Elsevier Online.

SIEGLE, E. 1996. **Distribuição sedimentar ao longo do litoral Sul Riograndense (trecho: F. da Conceição a Arroio Chuí) e fatores condicionantes**. Trabalho de Graduação, Curso de Oceanologia, Universidade Federal do Rio Grande, 91 pp.

STRIEDER, A.J. 2004. **Georradar e suas aplicações em investigações de subsolo**. Departamento de Engenharia de Minas, Universidade Federal do Rio Grande do Sul, p. 43–56.

STRIEDER, A.J, FONTOURA, B.S., BEHLING, J.S., WETZEL, R.S., DUARTE Jr, R.S.S., SILVA, T.C., MENDES, P., NÓBREGA, A.V.V., NIENCHESKI, L.F.H., CALLIARI, L.J. 2015. **Gravitational tectonics evidences at**

- RGS (Brazil) Coastal Plain using Ground Penetrating Radar.** Advanced Ground Penetrating Radar (IWAGPR). 8th International Workshop on, p. 1–4.
- TOMAZELLI, L.J. 1978. **Minerais pesados da plataforma continental do Rio Grande do Sul.** Acta Geol. Leopold, v. 3, p. 103–159.
- TOMAZELLI, L.J. & VILLWOCK, J.A. 1996. **Quaternary Geological Evolution of Rio Grande do Sul Coastal Plain, Southern Brazil.** Anais da Academia Brasileira de Ciências, 68(3), pp.373–382.
- TOMAZELLI, L.J. & VILLWOCK, J.A. 2000. **O Cenozóico Costeiro do Rio Grande do Sul.** In: HOLZ, M & DE ROS, L. F. (eds.). Geologia do Rio Grande do Sul. P. 375–406.
- TOMAZELLI, L.J., DILLENBURG, S.R. 2007. **Sedimentary facies & stratigraphy of a last interglacial coastal barrier in south Brazil.** Marine Geology, 244:33–45.
- VARNES, D.J. 1958. **Landslide types and processes.** In: Eckel ED (ed.) Landslide and engineering practice, pp. 20–47. Washington, D.C: Highway Research Board Special Report 29.
- VARNES, D.J. 1978. **Slope movements types and processes.** IN: SCHUSTER R.L., KRIZEK R.J. (Eds.), Landslides: Analysis and Control. Special Report 176, Transportation Research Board, Washington D.C. (USA), pp. 11–35.
- VELLOZO, T.G. & ALVES, A.R. 2006. **Características gerais do fenômeno da maré no Brasil. Anais Hidrográficos da Diretoria de Hidrografia e Navegação.** Tomo LXI.
- VILLWOCK, J. A. 1972. **Contribuição à Geologia do Holoceno da Província Costeira do Rio Grande do Sul.** Dissertação (MSc). UFRGS / Curso de Pós-Graduação em Geociências. Porto Alegre. 113p + anexos.

VILLWOCK, J.A. & TOMAZELLI, L.J. 1995. **Geologia costeira do Rio Grande do Sul**. Notas Técnicas, 8:1–45.

VILLWOCK, J.A. & TOMAZELLI, L.J. 2007. Planície Costeira do Rio Grande do Sul: gênese e paisagem atual. IN: BECKER, F.G., RAMOS, R.A., MOURA, L.A. (ed.). **Biodiversidade: Regiões da Lagoa do Casamento e dos Butiazais de Tapes, Planície Costeira do Rio Grande do Sul**. Ministério do Meio Ambiente e Fundação Zoobotânica do Rio Grande do Sul. Brasília (DF). p. 20–33.

ANEXO I
Título da Tese:
“NEOTECTÔNICA E CONTROLE DA SEDIMENTAÇÃO NA PLANÍCIE COSTEIRA DO RS”
Área de Concentração: Geologia Marinha
Autor: Bruno Silva da Fontoura
Orientador: Prof. Dr. Iran Carlos Stalliviere Corrêa (URFGS/PPGGEO) Coorientador: Prof. Dr. Adelir José Strieder (UFPeI)
Examinador: Prof. Dr. Nelson Luiz Sambaqui Gruber
Data: 10/10/2023
Conceito: B
PARECER:
<p>O presente trabalho é relevante e traz novas e inéditas considerações sobre comportamento da neotectônica na PCRS, onde embora, em sua gênese não tenha sido evidenciados movimentos tectônicos em estruturas de grande escala na região, por outro lado a pesquisa revela a existência de falhas de crescimento que controlam a sedimentação e a formação do sistema lagunar holocênico da Barreira IV, indicando a ocorrência daqueles movimentos.</p> <p>O trabalho é bem estruturado, na forma de 3 artigos estrutura é clara com objetivos bem definidos e que foram atingidos, integrando técnicas de geofísica GPR e sensoriamento remoto, estudos geológicos (furos de sondagem) e geomorfológicos. Na metodologia os novos dados sísmicos correlacionados á sondagem, são esclarecedores e revelam nos mapeamentos com SIG, a origem de muitos comportamentos atribuídos as linhas fixadoras das barreiras costeiras da PCRS.</p> <ol style="list-style-type: none"> 1. Artigo GEOPHYSICS trata da falha da Lagoa do Peixe através dos radargrama/radarfácies GPR e furos de sondagem com os perfis são muito elucidativa revelando relações estruturais e traz novas evidências com apoio de precisos registros de GPR para os modelos evolutivos da região da Lagoa do Peixe; 2. O Artigo 2 GEOPHYSICS trata do Quinta CASSINO e apresenta os lineamentos dos cordões litorâneos truncando paredes de falha e radargramas da Quitéria e 3. Artigo 3 (em avaliação) na Revista ORE GEOLOGY REVIEW: <i>Structural Controls of the Coastal Bujuru and Retiro Heavy Minerals deposits in Southern Brazil.</i> Bojuru deformações e retrabalhamento sedimentar em Bojuru.

Os resultados são relevantes e trazem nova luz aos comportamentos das Morfologias da PCRS sobretudo com uso do GPR atrelado a outras técnicas de geológica furos de sondagem e uso de SIG.

Trabalho mostra condições plenas de requisito parcial para Doutorado.

Assinatura:



Documento assinado digitalmente
NELSON LUIZ SAMBAQUI GRUBER
Data: 10/10/2023 17:06:42-0300
Verifique em <https://validar.iti.gov.br>

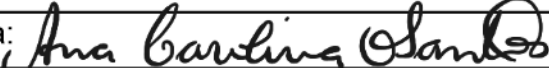
Data: 10/10/2023

Ciente do Orientador:



Documento assinado digitalmente
IRAN CARLOS STALLIVIERE CORREA
Data: 17/10/2023 13:50:58-0300
Verifique em <https://validar.iti.gov.br>

Ciente do Aluno:

ANEXO I	
Título da Tese:	
“NEOTECTÔNICA E CONTROLE DA SEDIMENTAÇÃO NA PLANÍCIE COSTEIRA DO RS”	
Área de Concentração: Geologia Marinha	
Autor: Bruno Silva da Fontoura	
Orientador: Prof. Dr. Iran Carlos Stalliviere Corrêa (URFGS/PPGGEO) Coorientador: Prof. Dr. Adelir José Strieder (UFPeI)	
Examinadora: Profa. Dra. Ana Carolina Oliveira dos Santos	
Data: 10/10/2023	
Conceito: B	
PARECER:	
<p>O trabalho apresentado traz um novo e importante viés, a neotectônica, para o conhecimento da evolução da Planície Costeira do RS, o qual pode ter grande relação com outros eventos tectônicos já conhecidos na Plataforma e Talude Continental da Bacia de Pelotas, na região que abrange o Cone do Rio Grande.</p> <p>Com base na Tese enviada para análise da banca examinadora e na apresentação do doutorando, deixo as seguintes observações/sugestões:</p> <ol style="list-style-type: none"> 1) Os objetivos específicos serão melhor apresentados se estiverem alinhados com os objetivos dos 3 artigos da Tese; 2) Verificar se o número de sessões georradar citadas no texto correspondem às apresentadas (não há necessidade de citar no texto e apresentar nas figuras dos artigos as linhas de GPR não usadas); 3) Os parâmetros e métodos de aquisição e processamento devem ser apresentados em todos os artigos, a exemplo do terceiro artigo; 4) Mapas: nomear todas as linhas e furos de sondagem e marcá-los nos mapas geológicos para permitir a interpretação adequada; quando existirem linhas de GPR muito próximas (Bujuru) mostrar em detalhe na figura e apenas marcar a região na figura principal; 5) Sessões georradar: marcar furos de sondagem nas sessões para permitir a interpretação adequada; verificar algumas escalas; 6) Verificar nas tabelas das radarfácies se constam todas aquelas apresentadas nas sessões georradar; 7) Na apresentação, poderia ter abordado/exemplificado como foram definidas as radarfácies; 8) Formatação do trabalho: eliminar grandes espaços em branco e evitar a divisão em folhas separadas da legenda e entre título e texto subsequente; colocar a figura o mais próximo possível de onde foi citada pela primeira vez, porém, sem deixar espaços em branco; 9) Todas as referências citadas no texto devem estar na lista de referências e vice-versa. Sugiro revisar, pois algumas não constam na lista; 10) Redação: evitar citar o autor no início da frase e evitar números iniciando a frase. Ex.: Fulano (2020) afirma que... substituir por: Conforme Fulano (2020)... 11) Figuras: marcar letra A e B nas figuras que contém; As legendas devem ser autoexplicativas: todos os elementos das figuras devem constar na legenda; traduzir integralmente as figuras. 	
Assinatura: 	Data: 10/10/2023
Ciente do Orientador:	<p style="text-align: center;"><small>Documento assinado digitalmente</small></p> <p style="text-align: center;">gov.br IRAN CARLOS STALLIVIERE CORREA Data: 17/10/2023 16:41:26-0300 Verifique em https://validar.iti.gov.br</p>
Ciente do Aluno:	

ANEXO I	
Título da Tese:	
“NEOTECTÔNICA E CONTROLE DA SEDIMENTAÇÃO NA PLANÍCIE COSTEIRA DO RS”	
Área de Concentração: Geologia Marinha	
Autor: BRUNO SILVA DA FONTOURA	
Orientador: Prof. Dr. Iran Carlos Stalliviere Corrêa Coorientador: Prof. Dr. Adelar José Strieder	
Examinador: Prof. Dr. Jair Weschenfelder	
Data: 10/10/2023	
Conceito: B (BOM)	
PARECER:	
<p>A Tese de Doutorado apresentada pelo aluno do Programa de Pós-Graduação em Geociências (PPGGEO) da UFRGS, BRUNO SILVA DA FONTOURA, trata de um tema a longo tempo debatido e controverso no estudo da evolução geológica da planície costeira do Rio Grande do Sul e, conseqüentemente, da margem continental sul brasileira – ‘a ocorrência de eventos neotectônicos’.</p> <p>A estrutura da tese segue os requisitos e normativas de ‘tese por artigo’, requeridas pelo PPGGEO/UFRGS, com três artigos submetidos à publicação em revistas científicas nos estratos Qualis-CAPES indicados, os quais seguem um formato/estrutura padrão em publicações científicas conhecidas.</p> <p>Os três artigos científicos submetidos à publicação em importantes revistas relacionadas à temática da tese são bem ilustrados e apresentam e discutem diversos registros de radargramas e radarfacies da área de estudo, em áreas alvos, de forma a atingir os objetivos gerais e específicos elencados na preliminar e a demonstrar e confirmar a hipótese do trabalho de tese.</p> <p>A apresentação da Tese de Doutorado foi feita de forma satisfatória, com o candidato esclarecendo, tb de forma satisfatória, os questionamentos feitos pelos integrantes da Banca Examinadora. -----</p>	
Assinatura:	Data: 10/10/2023
Ciente do Orientador:	
Ciente do Aluno:	